学位論文

Morphological and genetic studies on neuroendocrine regulation of reproduction in teleosts

(真骨魚類における生殖の中枢制御機構に関する形態学的・遺伝学的研究)

平成 26 年 12 月博士(理学)　申請

東京大学理学系研究科

生物科学専攻

高橋　晶子

Abstract

Regulatory mechanisms of life that are conserved among species are generally considered to be the ones crucial for the organism, although each component of such conserved biological regulatory mechanisms, i.e., genes, metabolites, and morphology, are not necessarily conserved among species. In mammals, the hypothalamic-pituitary-gonadal (HPG) axis regulation is considered to be the essential regulatory mechanism of reproduction. The hypothalamic gonadotropin releasing hormone (GnRH) neurons induce release of luteinizing hormone (LH) and follicle stimulating hormone (FSH) in the pituitary, and LH and FSH thus secreted promote the growth of ovarian follicles. Estrogen signaling from developed follicles mediates negative and positive feedback of GnRH secretion. Recently, it has been widely accepted that a new player, kisspeptin neuron, is pivotal for the HPG axis regulation by receiving estrogen feedback signals and modulating GnRH neuron firing activities. However, it is unclear whether each component of the HPG axis regulation is essential for reproduction throughout vertebrates.

In the present thesis, I aimed to clarify what is important for the HPG axis regulation in vertebrates, by focusing on the key components of the HPG axis regulation known in mammals, i.e. GnRH, LH, FSH, and kisspeptin, with special reference to the functional conservation of its mechanisms. I chose to use a teleost, medaka, a model animal, because teleosts are one of the most distinctly evolved species from mammals, and they often show interesting commonality and specificity.

First, in Chapter 1, I identified hypophysiotropic GnRH1 neurons localized in the ventral POA and several non-hypophysiotropic subpopulations of GnRH neurons in medaka by analyses of two newly generated transgenic medaka, *gnrh1*:EGFP and

gnrh3:EGFP using segmentation analysis of 3-D images. I also clearly demonstrated hypophysiotropic innervation of GnRH1 neurons as early as 10 days post-hatching, which is much earlier than they are supposed to function. In Chapter 2, I generated knockout (KO) medaka lines for each gene, *gnrh1*, and *b* subunit genes of gonadotropin, *lhb* and *fshb*, and scrutinized their phenotypes, to examine essentiality of the components for the HPG axis regulation using a genome editing technique, TALEN. By histological, expression, and behavioral analyses, I clearly demonstrated that LH release, which is strongly suggested to be triggered by GnRH1, is essential for ovulation in female medaka, while FSH, release, which do not necessarily require GnRH regulation, is essential for the folliculogenesis (growth of ovarian follicles). On the other hand, I unexpectedly found that males of all KO medaka were fertile, meaning that lack of either one of the gonadotropins is dispensable for reproduction in male medaka. In Chapter 3, I demonstrated by using genome editing techniques, TALEN and CRISPR/Cas9, that *kiss1*/*kiss2*/*gpr54-1*/*gpr54-2* KO, as well as double KO of *kiss1* and *kiss2* medaka, show normal expression level of *lhb*/*fshb*, gonadal development, and fertility. These results clearly indicate that the HPG axis regulation in teleost is not dependent on kisspeptin signaling, unlike that in mammals. In conclusion, I demonstrated that FSH, LH, and GnRH functions are roughly similar between mammals and teleosts, with newly found significant differences. I here describe the commonalities and specificities of the HPG axis regulation I have shown in this study. In addition, I propose from the kisspeptin KO study that non-mammalian species like medaka may have an estrogen feedback loop not dependent on kisspeptin neurons.

Table of contents

List of Abbreviations

DM	dorsomedial thalamus
dPOA	dorsal preoptic area
FB	forebrain
FSH	follicle stimulating hormone
GnRH	Gonadotropin releasing hormone
HPG axis	hypothalamic-pituitary-gonadal axis
LH	luteinizing hormone
OP	olfactory placode
OT	optic tectum
PMSG	pregnant mare serum gonadotropin
POA	preoptic area
rLH	recombinant medaka LH
tel	telencephalon
TN	terminal nerve
VM	ventromedial thalamus
vPOA	ventral preoptic area

General Introduction

Regulatory mechanisms of life that are conserved among species are generally considered to be the ones crucial for the organism. However, each component of such conserved biological regulatory mechanisms, i.e., genes, proteins, and metabolite, are not necessarily conserved among species. For instance, animal behaviors, such as sex or social behaviors, are often mediated by a mechanism in which pheromonal signals activate certain neural circuits in the brain. However, the key component of these behaviors, e.g. pheromones, are species-specific, so that the animals can discriminate pheromones of the same species from those of the other species (Cummins and Bowie 2012). Such robustness of the regulatory mechanisms per se in spite of the variations in the regulatory component may be explained by two different ways of compensations; one is the functional compensation in the same pathway by other genes, and the other is that by a novel or alternative metabolic pathways, which has been proposed in the study of *Arabidopsis thaliana* (Hanada et al. 2011). Needless to say, for the elucidation of the conserved mechanisms in the brain, in which numerous different neurons are functionally connected as neural networks, we have to analyze their morphological interactions in addition to the gene functions of particular neurons in the network. Interestingly, several neuronal circuits are reported to be conserved even though the overall organization of the whole brain is totally different among species. For example, although the cerebral neocortex of mammals and the telencephalon of teleosts appear quite different at first glance, the neuronal circuit of visual information processing is common between them are functionally equivalent: the mammalian visual pathway, retina- superior colliculus -pulvinar-visual cortex of the cerebral neocortex, and the teleost one retina-optic tectum-prethalamus-lateral part of the dorsal telencephalon

(Yoshimoto and Itoh., 2002). Thus, for the analysis of the morphological conservation, we have to know the functional connections of the neural components very carefully.

In mammals, the hypothalamic-pituitary-gonadal (HPG) axis is considered to be essential for the regulation of reproduction. The hypothalamic gonadotropin releasing hormone (GnRH) neurons are believed to induce the release of luteinizing hormone (LH) and follicle stimulating hormone (FSH) by stimulating gonadotrophs in the pituitary, and LH and FSH thus secreted promote the growth of ovarian follicles (Sisk and Foster 2004). Before ovulation, estrogen secreted from the developed follicles exerts an inhibitory effect on GnRH release (negative feedback), while during the preovulatory period, increase in the estrogen level triggers GnRH surge and subsequent LH surge to induce ovulation in the ovary (positive feedback) (Couse et al. 2003, Glidewell-Kenney et al. 2007, Ohkura et al. 2009, Smith 2013). Until recently, however, there has been a missing link to explain the mechanisms of negative/positive steroid feedback; it has been unclear how the GnRH neurons, which lack estrogen receptor α (*ERα*), essential for the estrogen feedback (Couse et al. 2003, Glidewell-Kenney et al. 2007), are regulated by estrogen feedback signaling. Recently, it is widely accepted that a new player, kisspeptin neuron, is pivotal in the HPG axis regulation by receiving estrogen feedback signals and modulating GnRH neuron firing activities (Ohkura et al. 2009, Smith 2013).

On the other hand, in non-mammalian vertebrates, there is no clear evidence how and to what extent GnRH, FSH, and LH play important roles in the regulation of reproduction, although there are not a few lines of pharmacological evidence that these hormones stimulate gonadal functions. There are several reports that GnRH peptides

increase release and/or synthesis of LH and FSH in various species including amphibians and teleosts (Daniels and Licht 1980, Breton et al. 1998, Mananos et al. 1999, Weil et al. 1999, Dickey and Swanson 2000, Karigo et al. 2012a, Karigo et al. 2014). By using recombinant LH and FSH glycoproteins or human chorionic gonadotropin, *in vivo* and *in vitro* studies showed that gonadotropins promote growth of ovary and cause induction of ovulation (Reynhout et al. 1975, Kazeto et al. 2008, Hagiwara et al. 2014). However, there has been no conclusive evidence for the essentiality of GnRH, LH and FSH for reproduction. Furthermore, there are conflicting reports of effect of kisspeptin on serum LH level, one reported increase (Chang et al. 2012), and the other reported no significant effect (Karigo et al., 2012a). Therefore, I think that the critical examination of the commonality and specificity of the HPG axis regulation mechanisms in teleosts in comparison with that in mammals should give us insights into the understanding of the evolutionary process of one of the most essential regulatory mechanisms of life, reproduction.

In the present thesis, I chose to use a teleost, medaka, because teleosts are one of the evolutionarily most distantly related species from mammals, and they often show interesting commonality and specificity. I focused on the key components of the HPG axis regulation, GnRH, LH, FSH, and kisspeptin, and analyzed what is important for the HPG axis regulation. The schematic illustration in Figure 0-1 shows the aims of the present thesis. Medaka is an especially useful and advantageous animal model for the study of reproductive neuroendocrinology using multidisciplinary techniques, because it is amenable to various state-of-the-art genetic manipulations and to experimental

manipulation of reproductive status by alteration of day length and rearing water temperature.

First, I generated GFP-labeled GnRH transgenic medaka to scrutinize the morphology of GnRH neurons, especially of larval fish. Here, I identified hypophysiotropic GnRH neurons that project their axons to the pituitary gland, the neural functions and regulation, which are believed to be conserved between medaka and mammals (Chapter 1). Next, I analyzed functions of GnRH, LH and FSH by generating and analyzing gene knockout (KO) medaka (Chapter 2). Finally, I generated and analyzed the phenotypes of kisspeptin KO and kisspeptin-receptor KO medaka (Chapter 3).

Figure legend

Figure 0-1

A schematic illustration showing the aims of the present thesis. The circled numbers in the figure correspond to the Chapters in this thesis.

Figure 0-1

What are the functions of the HPG axis regulation of reproduction in medaka (teleosts)?

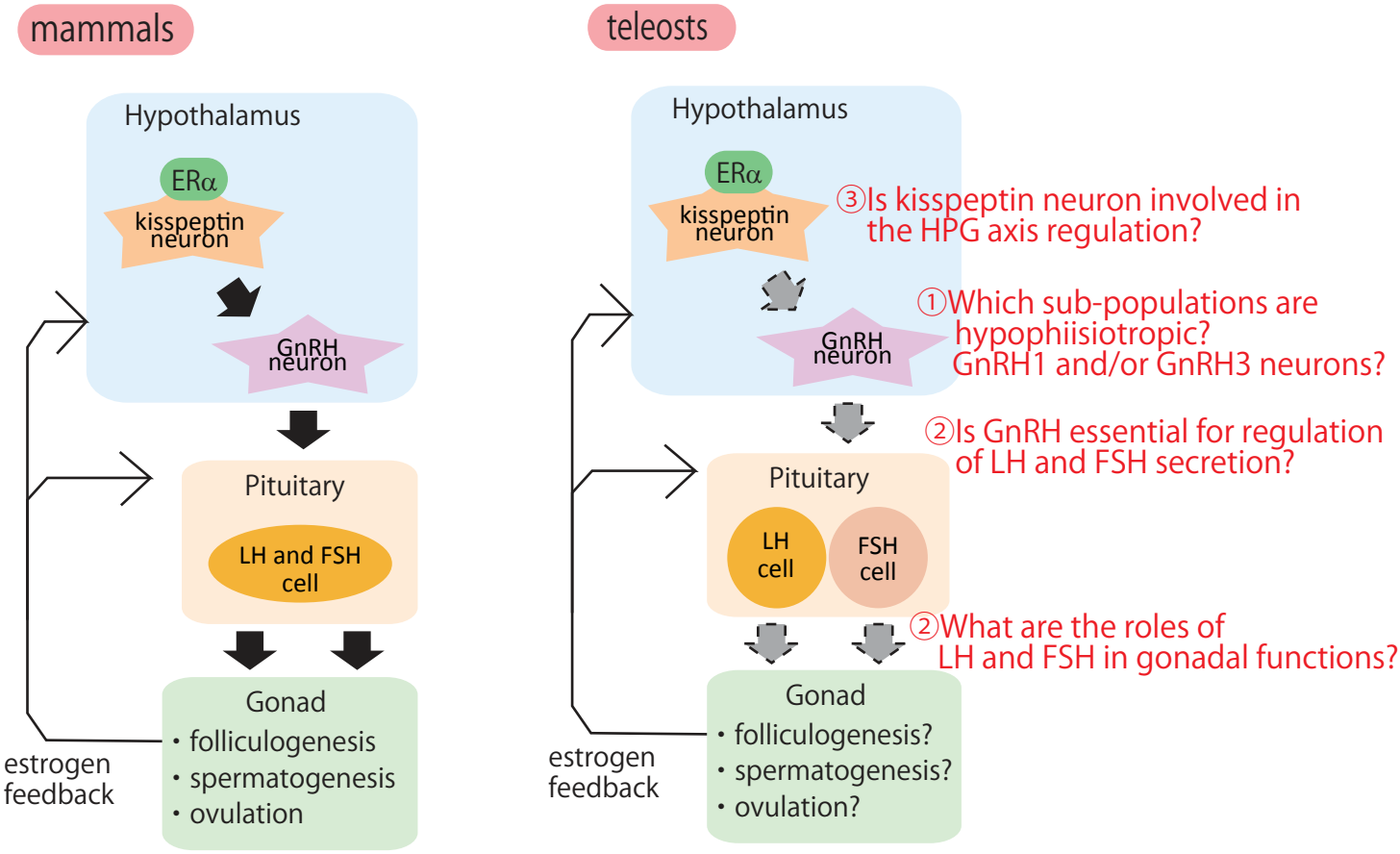

Chapter 1

Morphological analysis of the early development of telencephalic and diencephalic gonadotropin-releasing hormone neuronal systems in the EGFP-expressing transgenic medaka

Introduction

In mammals, gonadotropin releasing hormone (GnRH) neurons are considered to be crucial for reproduction (Clayton 1985). GnRH peptides, released from GnRH neurons in the hypothalamus (hypothalamic GnRH neurons), delivered through hypophyseal portal vessel and act on pituitary gonadotropes and stimulate the secretion of luteinizing hormone (LH) and follicle stimulating hormone (FSH) in mammal (Sisk and Foster 2004). On the other hands, the direct projection to the pituitary of GnRH neurons were detected in teleosts (Ishizaki and Oka 2001, Yaron et al. 2003). In addition to these hypothalamic neurons, there are also extra-hypothalamic, neuromodulatory GnRH neurons. These neuromodulatory GnRH neurons reside in the ventral part of telencephalic area and midbrain (Yamamoto et al. 1995). In all the vertebrates studied to date, fibers from these neuromodulatory neurons do not project to the pituitary but project to a wide variety of brain regions (Oka and Matsushima 1993, Yamamoto et al. 1995, Karigo and Oka 2013). In addition, terminal nerve (TN) GnRH neuronal innervation has been detected in the retina (Behrens and Wagner 2004), and TN GnRH neurons have been shown to regulate olfaction (Eisthen et al. 2000, Kawai et al. 2010) and some reproductive behaviors (Yamamoto et al. 1997, Okuyama et al. 2014).

It is generally accepted that, in most vertebrates, the majority of hypothalamic and TN GnRH neurons originate from the olfactory placode and migrate to the brain during development (Schwanzel-Fukuda and Pfaff 1989, Wray et al. 1989, Daikoku-Ishido et al. 1990, Murakami et al. 1991, Okubo et al. 2006, Palevitch et al. 2007). The somata of these neurons appear in the olfactory placode and migrate along the fibers of the olfactory tracts until they reach their destination (Wray 2010). In addition, it has been

suggested that the GnRH neurons can also originate from neural crest cells (Whitlock et al. 2003, Forni et al. 2011).

Three *gnrh* paralogous genes, *gnrh1*, *gnrh2* and *gnrh3*, have been identified in vertebrates, although *gnrh3* has only been found in teleosts. Expression of each paralog shows characteristic distribution throughout the brain. Some teleost species lack *gnrh1* or *gnrh3*, while *gnrh2* is evolutionary conserved (Okubo and Nagahama 2008). In vertebrates studied to date, both hypothalamic and TN GnRH neurons express one of the two paralogous genes, *gnrh1* or *gnrh3* (Okubo and Nagahama 2008). In teleosts that possess both *gnrh1* and *gnrh3* genes, all hypophysiotropic GnRH neurons, generally called preoptic area (POA) GnRH neurons in non-mammalian vertebrates, express *gnrh1*. On the other hand, teleosts that have lost either *gnrh1* or *gnrh3* gene, the remaining *gnrh* gene are expressed in both hypophysiotropic and TN GnRH neurons. On the other hand, midbrain GnRH neurons express *gnrh2*; these midbrain GnRH2 neurons are considered to play neuromodulatory roles (Kanda et al. 2010).

Developmental analyses of GnRH neurons have been performed previously in several teleost species using immunohistochemistry (Francis et al. 1994, White and Fernald 1998, Dubois et al. 2001). The developmental features of POA and TN GnRH neurons in teleosts were studied using enhanced green fluorescent protein (EGFP) transgenic zebrafish (*gnrh3*:EGFP) (Palevitch et al. 2007). However, it is difficult to distinguish hypophysiotrophic GnRH neuronal populations from telencephalic populations in zebrafish, because the both populations express *gnrh3*. Medaka (*Oryzias latipes*), a commonly used model teleost fish, possesses all three paralogous *gnrh* genes and synthesizes GnRH1 in POA GnRH neurons and GnRH3 in the TN and trigeminal

ganglion (TG) (Okubo et al. 2006). These characteristics mean that medaka is useful for developmental analyses of each GnRH neuronal population, utilizing genetic engineering. Importantly, the peptide sequence of GnRH1 shows diversity among species, while the peptide sequence of GnRH3 is strongly conserved (Okubo and Aida 2001). In fact, the medaka GnRH1 peptide shows 1–3 amino acid replacements compared to those in other teleosts, and thus, immunohistochemical detection of medaka GnRH1 using antibodies raised against GnRH1 from other animals has been unsuccessful. Because a specific antibody raised against medaka GnRH1 demonstrated relatively weak labeling of fibers, and anti-GnRH3 antibodies have low specificity (cross-reaction with GnRH2), GnRH1 and GnRH3 neuronal morphology has been studied using transgenic medaka expressing humanized-renilla (hr) GFP under the control of *gnrh1*/*gnrh3* gene promoters (Okubo et al. 2006); (Wayne et al. 2005). However, the fluorescence intensity of the hrGFP has often been too weak for detailed observation of fine dendritic morphology and axonal projections. In addition, there are no specific antibodies for immunohistochemical tissue detection of hrGFP. Therefore, I here established *gnrh1*:EGFP and *gnrh3*:EGFP transgenic medaka lines in order to conduct a detailed morphological analysis of the development of GnRH1 and GnRH3 neuronal systems. I selected EGFP as a reporter gene because a highly specific antibody with very high affinity is available (Tamamaki et al. 2000). Furthermore, EGFP fluorescence is much brighter than that of hrGFP. The morphological characteristics and cellular migratory pathways of GnRH1 and GnRH3 neurons during early development were analyzed using EGFP fluorescence in combination with EGFP immunohistochemistry and confocal microscopy. In addition, segmentation analysis of

three dimensional (3-D) images using FluoRender enabled us to trace the intertwined GnRH1 and GnRH3 neuronal fibers and accurately detail their projections. This led us to clearly identify the hypophysiotropic innervation of GnRH1 neurons residing in the ventral preoptic area (vPOA) from as early as 10 days post hatching. Furthermore, these analyses also revealed projections of non-hypophysiotropic GnRH1 neurons in vPOA to the retina or the optic tectum, and of GnRH3 neurons in the dorsal diencephalon.

Materials & Methods

Animals

Wild type strain (d-rR strain) medaka (*Oryzias latipes*) were used for generation of our transgenic lines. All fish and embryos were maintained under a 14 hour light/10 hour dark photoperiod cycle at 28 °C. Animals were maintained and used in accordance with the guidelines of the University of Tokyo's Use and Care of Experimental Animals.

Generation of transgenic medaka lines

The transgene constructs used for generation of *gnrh1*/*gnrh3*:EGFP medaka are schematically illustrated in Figure 1-1. For generation of DNA constructs, I replaced hrGFP reporter gene of *gnrh*1/*gnrh3*:hrGFP construct (Okubo et al. 2006); (Wayne et al. 2005) with EGFP sequence. The constructs for *gnrh1*/*gnrh3*:hrGFP were digested with BamHI, and dephosphorylated. For EGFP cDNA fragment, BamHI recognition sites were introduced in the both ends by PCR using a set of primers (Fw (CGCAAATGGGCGGTAGGCGTG); Rv (GGATCCTGGAACAACACTCAACCCTATCTCG)) and a template (pEGFP-N1;

TaKaRa, Otu, Japan), and digested by BamHI. The dephosphorylated backbone fragments were ligated with the digested EGFP fragment. To facilitate screening in the early developmental stages, the 5' -flanking region (1 kb) of *cardiac myosin light chain 2* (*cmlc2*; accession number: AB458318) was inserted in the 3'-region of the *gnrh1*:EGFP construct. A recognition site of I-SceI, a type of meganuclease that increases the efficiency of transgenesis in medaka when injected with the construct (Thermes et al. 2002), was inserted in the 5'-end of the 5'-flanking region of *gnrh1*.

DNA constructs (10-30 ng/μL) were injected into the cytoplasm of one- cell stage fertilized eggs with intact chorion. Before injection, the *gnrh1*:EGFP construct was digested by I-SceI (New England Biolabs, Ipswich, MA, USA) for 1 h at 37 °C. Fluorescence was monitored at 3 days post-fertilization (dpf), and only embryos displaying fluorescence in the heart were grown to adulthood. I crossed candidates of transgenic medaka with wild type fish to identify germline transmission. Bright field fluorescence microscopy was conducted using a fluorescence stereomicroscope (MVX10; Olympus, Tokyo, Japan) with GFP filter (U-MGFPHQ; Olympus). Pairs of sibling adults from F1 fish were intercrossed. I selected fish with homozygous transgenes from F2 fish.

Antibody Characterization

All the antibodies used in the present study are listed in Table 1. The specificity of rabbit anti-EGFP antibody (Tamamaki et al. 2000) is shown using immunohistochemistry according to the method as stated below (Figure 1-2C, 2D). Although immunoreactivity was not detected in the section of wild type brain (Figure 1-2C), immunoreactive neurons were detected in the section of *gnrh1*:EGFP medaka brain

(Figure 1-2D).The sensitivity and specificity of rabbit anti-salmon GnRH antibody ((Okuzawa et al. 1990); reactive with medaka GnRH3 peptide (Parhar et al. 1998)); generous gift of Dr. Okuzawa, National Fisheries Research Agency) was shown by radioimmunoassays in (Okuzawa et al. 1990); (Senthilkumaran et al. 1999).

Immunohistochemistry

Cryosections of adult brain from fish were prepared and immersed in 0.05 M phosphate-buffered saline with 0.5 % Triton X-100 (PBST) and incubated for 8 hours at RT with rabbit anti-EGFP antibody (1: 1000) or rabbit anti-salmon GnRH (sGnRH) antibody (1:10,000) diluted with PBST containing 10% normal goat serum. After washout with PBST, the sections were incubated with biotinylated goat anti-rabbit IgG antibody (1:200; Vector Laboratories, Burlingame, CA, USA) diluted in PBST for 2 hours at RT. They were then incubated with Vectastain Elite ABC (Vector Laboratories) for 1 hour at RT, washed in PBST, and then incubated with 3,3'-diaminobenzidine.

Whole mount immunohistochemistry

I labeled embryonic GnRH1 neurons expressing EGFP using whole mount immunohistochemistry with anti-EGFP antibody, because the EGFP expression of *gnrh1*:EGFP medaka during the embryonic stage was not strong enough for observation of neurite morphology using EGFP fluorescence by itself. Embryos (2-6 dpf) and newly hatched fry from *gnrh1*:EGFP fish were fixed with 4% paraformaldehyde (PFA) in 0.05 M phosphate-buffered saline (PBS) for 1 hour at 4 °C. The embryos were washed with PBST and incubated for 8 hours with rabbit anti-EGFP antibody (1:1000) diluted with PBST containing 10% goat serum. After washout of first antibody with PBST, the

embryos were incubated for 2 hours at RT with Alexa Fluor 488-conjugated goat anti-rabbit IgG (1:200; Invitrogen) and Rhodamine-Phalloidin diluted with PBST (2dpf, Figure 1-3A2, 1:200; life technologies, CA, USA) for labeling F-actin (Tsuda et al., 2009). After washout of the excessive antibody with PBS, the embryos were gradually transferred to 50% glycerol in 0.05 M PBS and mounted on slides. The brains of fry at 10 days post hatching were fixed with 4% PFA for 1 hour, dissected, and treated in the same way as for embryos. The 2.5 dpf embryos of *gnrh3*:EGFP fish were incubated with Rhodamine-Phalloidin (Figure 1-4B2, 1:200). The embryos and fry of *gnrh3*:EGFP fish were gradually transferred to 50% glycerol for mounting on slides after fixation and PBS wash. Specimens were mounted with 10% polyvinyl alcohol in 2.5 mM Tris-HCl (pH 8.7) containing 2.5% 1,4-diazabicyclo[2,2,2]octane and 5% glycerol. Fluorescence of Alexa Fluor 488 (*gnrh1*:EGFP) or EGFP (*gnrh3*:EGFP) were observed under a confocal laser-scanning microscope LSM-710 (Carl Zeiss, Oberkochen, Germany). Z-stacks were acquired using a 40x/1.1 NA water immersion objective at a step size of 0.52 μm.

Image analysis

Images were analyzed and processed into 3-D configurations using Fiji (Schindelin et al. 2012) for stitching multiple z-stacks, and FluoRender (https://github.com/SCIInstitute/fluorender, Wan et al., 2009; Wan et al., 2012) for 3D reconstructions and visualization of positional relation of fibers and somata. FluoRender is an open-source interactive rendering tool for confocal microscopy data visualization. 3D volume rendering data were generated, and consecutive fibers and somata in volume rendered data were semi-automatically labeled with pseudo-colors to visually

discriminate the different population of neurons by FluoRender. (Figure 1-5A2, 5A3, 7A2, 7B2, 8B2-4; see figure legends in detail). Merging and trimming of images were performed by using Photoshop (Adobe Systems Inc, San Jose, CA).

***In situ* hybridization**

Three-month-old wild type and transgenic medaka were deeply anesthetized with MS-222 (Sigma, St. Louis, MO). Brains were fixed in 4% PFA in 0.05 M PBS for 6 hours at 4 °C. Fixed specimens were immersed in diethyl pyrocarbonate-treated PBS with 30 % sucrose for 3–6 hours, embedded in 5% agarose (type IX-A; Sigma) containing 20% sucrose in PBS, then frozen in *n*-hexane at −80 °C. Serial frontal sections were cut at 20 μm thickness using a cryostat (Leica CM3050S, Leica Microsystem Inc., IL).

To detect *gnrh3* mRNA, I prepared a *gnrh3*-specific digoxigenin (DIG)-labeled RNA probe and performed *in situ* hybridization, as previously described (Okubo et al. 2006). Briefly, every section from the olfactory bulb to the spinal cord was washed with PBS, fixed with 4 % PFA, neutralized with 0.2 % glycine in PBS, and then incubated with 0.25 % acetic anhydride in 0.1 M triethanolamine for 10 min. Finally, the sections were hybridized with 1 μg/mL DIG-labeled antisense RNA probes synthesized from medaka brain cDNA using DIG RNA Labeling Kit (T7, Roche Diagnostics Corp, Mannheim, Germany) diluted with hybridization buffer (50 % formamide, 3x saline sodium citrate (SSC), 0.12 M phosphate buffer (pH 7.4), 1x Denhardt's solution, 125 g/ml tRNA, 0.1 mg/ml herring sperm DNA, and 10 % dextran sulfate) overnight at 58 °C. After hybridization, they were washed twice with 2xSSC containing 50 % formamide for 15 min at 58 °C. They were immersed sequentially, twice each, with 2x SSC and 0.5x SSC for 15 min at 58 °C, and washed with DIG-1 buffer (100 mM Tris-HCl (pH 7.5), 150

mM NaCl, and 0.1 % Tween 20) for 5 min at room temperature (RT). They were immersed in 1.5 % blocking reagent (Roche) in DIG-1 buffer for 30 min at RT and incubated with alkaline phosphatase-conjugated anti-DIG antibody (1:3000; Roche) for 2 hour at RT. They were then washed with DIG-1 buffer and treated with DIG-3 buffer (100 mM Tris-HCl (pH 9.5), 100 mM NaCl, and 50 mM $MgCl_2$). They were then treated with a chromogen solution (337 mg/mL 4-nitroblue tetrazolium chloride, 175 mg/mL 5-bromo-4-chloro-3-indoyl-phosphate in DIG-3 buffer) for 3–4 hours. The reaction was stopped by adding reaction stop solution (10 mM Tris-HCl (pH 7.6) and 1 mM EDTA (pH 8.0)). The sections were observed under a light microscope. For a more detailed examination of brain morphology, they were counter-stained with neutral red. I followed the Medaka Histological Atlas (Ishikawa et al.) to determine nomenclature of medaka brain nuclei.

Double labeling by *in situ* hybridization & immunohistochemistry

Cryosections were prepared as described above. The sections were immersed in PBS (RNase free) and incubated for 8 hour with rabbit anti-EGFP antibody (1: 1000) diluted in PBS containing 10% goat serum. After washout with PBS, they were incubated with biotinylated goat anti-rabbit IgG antibody (1:200; Vector Laboratories) diluted in PBS for 2 hours. After PBS wash, they were fixed with 4% PFA. Neutralization and acetylation were performed as mentioned above. They were hybridized at 58 °C with 1 μg/mL DIG-labeled antisense RNA probes (*gnrh1* or *gnrh3* (Okubo et al. 2006)) diluted with hybridization buffer. After hybridization, they were washed twice with 50% formamide and 2× SSC for 15 min each at 58 °C and immersed in TNE (10 mm Tris-HCl, pH 7.5; 500 mm NaCl; and 1 mm EDTA, pH 8.0) for 10 min at 37 °C. They were

incubated with 20 μg/ml ribonuclease A (Sigma) in TNE for 30 min at 37 °C, and then washed with TNE for 10 min at 37 °C to remove the ribonuclease A. They were then washed with 2× SSC twice, followed by 0.5× SSC twice for 15 min each at 58 °C. They were then incubated with Vectastain Elite ABC (Vector Laboratories) for 1 hour and washed in PBST. They were incubated with Alexa Fluor 488 conjugated streptavidin (1:500; Invitrogen) and alkaline phosphatase-conjugated anti-DIG antibody (1:1000; Roche Diagnostics Corp) for 2 hours at RT. After washing with PBST, they were incubated with HNPP Fluorescent Detection Set (Roche Diagnostics) according to the manufacturer's instructions. The incubation continued until visible signals were detected (up to overnight) and was stopped by washing in PBS containing 0.5 mM EDTA. After washing with PBS, they were incubated with Hoechst 33342 (1:1000; life technology) for 5min at RT for nuclear counter-staining. They were coverslipped with CC/Mount (Diagnostic BioSystems, Pleasanton, CA, USA). Fluorescence was observed using a confocal laser-scanning microscope LSM-710 (Carl Zeiss) or a light microscope (BX53; OLYMPUS) with CCD camera (DXM 1200C; Nicon, Tokyo, Japan). The data are presented as the mean ± standard error of the mean.

Results

Generation of transgenic medaka lines and assessment of specificity of expression

I generated two transgenic medaka lines, *gnrh1*:EGFP and *gnrh3*:EGFP expressing EGFP under the control of *gnrh1* and *gnrh3* promoters, respectively. I assessed the specificity of EGFP expression using double labeling of *in situ* hybridization for *gnrh1* or *gnrh3* and immunohistochemistry using an anti-EGFP antibody. In vPOA of the adult

brain of *gnrh1:*EGFP medaka, expression of *gnrh1* mRNA was detected in 96.1 ± 3.3 % (24.2 ± 2.6 GnRH1 neurons/25.8 ± 2.9 GFP-positive neurons from 10 fish) of EGFP-immunoreactive (ir) cells in the ventrolateral part (Figure 1-2B6). A small number of cells were also found in the ventral telencephalon and ventral hypothalamus. Here, I counted the cells with diameter 7-10μm. On the other hand, the expression level of *gnrh1* in the medial part of vPOA was not high enough to be detected by double labeling *in situ* hybridization & immunohistochemistry. In dorsal POA (dPOA), EGFP expression was detected in GnRH1 neurons by EGFP immunohistochemistry, although the EGFP fluorescence was faint. Expression of *gnrh1* mRNA was detected in 82.6 ± 7 % (21 ± 4.2 GnRH1 neurons/24.2 ± 3.5 GFP-positive neurons from 10 fish) of EGFP-ir cells in dPOA of the adult brain of *gnrh1:*EGFP medaka. Here, I counted the cells with diameter of 3-6 μm. Although I could detect two or three GnRH1 neurons in the adult optic tectum (OT) using *in situ* hybridization, greater numbers of ectopic EGFP-ir cells were detected in the OT from early developmental stage (Figure 1-4D, Figure 1-5A1, orange arrowheads). Expression of *gnrh3* mRNA was detected in 88.6 ± 1.2% (54.5 ± 8.4 GnRH3 neurons/58.5 ± 10.4 EGFP-ir neurons from 8 fish) of EGFP-ir cells in the TN ganglia (Figure 1-3B) and ventral region of the rostralmost portion of the dorsal thalamus of adult *gnrh3*:EGFP medaka (Figure 1-3C). Here, I counted the cell having diameter of 8-22 μm (in the TN) or 3-10 μm (in the thalamus) as one cell. EGFP expression was also detected in retinal ganglion and photoreceptor cells of *gnrh3*:EGFP medaka. Expression of *gnrh3* in the retina was detected using both *in situ* hybridization and real time PCR (data not shown). The visual intensity and immunoreactivity of EGFP did not necessarily correlate with expression levels of *gnrh3* mRNA.

Characteristics of GnRH1 neurons (*gnrh1*:EGFP)

Using *gnrh1*:EGFP transgenic medaka, I analyzed the developmental characteristics of GnRH1 neurons. I collected embryos at 2.5, 3.5, 4.5, 7.5 dpf, and 10 days post-hatching (dph) fry of *gnrh1*:EGFP medaka. The developmental stages (st.) of the embryos were determined according to Iwamatsu (Iwamatsu et al. 2003). I analyzed EGFP immunoreactivity in the brains of *gnrh1*:EGFP medaka using confocal microscopy. Somata of EGFP-ir neurons appeared at 2.5 dpf (st. 26–27) in the olfactory placode (Figure 1-4A1 and 2 white arrowheads). At 3.5 dpf (st. 29–30), somata of GFP-expressing neurons began to migrate to the forebrain along their extended fibers (Figure 1-4B). At 4.5 dpf (st. 32–33), somata were located at the caudoventral forebrain (Figure 1-4C). There are two subgroups of GnRH1 neurons in the adult brain; one is located dorsally, and the other is located in the vPOA and projects to the pituitary (Karigo et al. 2012a). During the embryonic period, however, the dorsal population could not be definitely identified in this transgenic line. At 7.5 dpf, fibers from GnRH1 neurons extended to the optic nerve and the caudal part of diencephalon (Figure 1-4D, cyan arrowhead), and formed part of the anterior commissure (Figure 1-1-4D, magenta arrowhead). At the same stage, a small, scattered distribution of EGFP-ir neurons was observed in the midbrain, which remained visible in subsequent stages (Figure 1-4D, 5A1, orange arrowheads). At 10 dph, I detected projection of EGFP-ir fibers to the pituitary (Figure 1-5A1). When compared with the brain of an adult medaka (Figure 1-5B), it appeared that the morphological characteristics of GnRH1 neurons projecting to the pituitary are already evident at this early stage. The fibers from EGFP-ir neurons extended caudally through the ventrolateral midbrain (Figure 1-5A1, white arrowhead)

and entered the pituitary from the caudal region of the hypothalamus. A few EGFP-expressing neurons were located along the fibers of future vPOA neurons, and they projected to the pituitary at 10 dph and adulthood (Figure 1-5A1, B). The EGFP-ir neuronal population in the future vPOA could be divided into at least three subgroups. One subpopulation possessed round somata and sent their fibers to the pituitary (Figure 1-5A2, 5A3, shown in white using FluoRender). Direct projection of individual EGFP-ir neurons to the pituitary was also clearly visible. Additionally, some neurons appeared to be on their way to the future vPOA during or after cessation of migration; they were spindle-shaped (Figure 1-5A2, 5A3, shown in green using FluoRender). A separate subgroup of EGFP-ir neurons that projected to the ipsilateral region of midbrain and mainly to the contralateral optic nerve (and not to the pituitary) is shown in cyan using FluoRender (retinopetal GnRH1 neurons: Figure 1-5A2, 5A3). Some of their fibers extended to the caudal part of diencephalon and the ventrolateral region of diencephalon (Figure 1-5A2, 5A3). These neurons were distributed along the medio-lateral axis to the other type of GnRH1 neurons in the future POA at 10 dph (Figure 1-5A1, cyan arrowheads). At adult stage, the retinopetal GnRH1 neurons became inconspicuous.

Characteristics of GnRH3 neurons *(gnrh3*:EGFP)

Using *gnrh3:*EGFP transgenic medaka, I could analyze the developmental characteristics of GnRH3 neurons, owing to its strong EGFP fluorescence. EGFP fluorescence was first detected at 1.5 dpf (st. 21–22) in the trigeminal nerve ganglion (TG, Figure 1-6A, cyan arrowheads). At 2 dpf (st. 24–25), GnRH3 neurons appeared in the olfactory placode (Figure 1-6B1, 6B2, white arrowheads). These GnRH neurons appeared to migrate to the brain at later stages. At 2.5 dpf (st. 27–28), the somata of

GnRH3 neurons located in the olfactory placode extended their fibers to the forebrain (Figure 1-7A). At this stage, fibers of GnRH3 neurons in the olfactory placode (Figure 1-7A2, white) could be distinguished from fibers of the optic nerves, which also contained EGFP-expressing neuronal fibers (Figure 1-7A2, green). There were two other subgroups of non-migratory EGFP- expressing neurons derived from the area outside of the olfactory placode. One subgroup was detected in the thalamus, caudal to the optic chiasm (Figure 1-7A1, 7A2 yellow arrowheads; Figure 1-7A2, yellow). The fibers of these neurons extended caudal to the ipsilateral spinal cord and disappeared at 3.5 dpf (st. 30, Figure 1-7B1, 7B2). The other subgroup was located medio-caudal to the above mentioned population in the forebrain at 2.5 dpf (Figure 1-7A2, cyan) and 3.5 dpf (Figure 1-7B2, cyan). I could not detect EGFP-expressing neuronal fibers from these neurons. The both subgroups of neurons intermingled with the olfactory place-derived neurons at later stages.

The GnRH3 neurons, which first appeared in the olfactory placode, migrated to the forebrain along their extended fibers between 3–4.5 dpf (Figure 1-7B1, 8A). The EGFP-expressing neurites were incorporated in the optic nerves. Some EGFP-expressing cells were distributed to the ventral olfactory bulb, including the TN ganglion, and others migrated more caudally to the thalamus. Just after hatching, three major populations of GnRH3 neurons could be identified in the TN ganglia, the thalamus, and the TG ganglia (Figure 1-8B1). Some EGFP-expressing neurons were located between the TN ganglion and thalamus during migration. Around this stage, EGFP- expressing cells in the retina (probably representing ectopic EGFP expressions; see below) became visible and extended fibers to the OT to form reticulated fibers (Figure 1-8A, B1). The GFP signal

of these reticulated fibers was too strong to analyze the morphology of the GnRH3 neurons in the TN and thalamus. Therefore, I divided the z-stack dataset from Figure 1-8B1 into two sub-stacks, for detailed 3-D reconstruction analysis. The first sub-stack was made by removing image planes from the dorsal region that contained the reticulated fibers of the OT and part of the optic nerve. The 3-D reconstructed image of the sub-stack suggested pathways for fibers from EGFP-expressing neurons in the TN ganglion and thalamus (Figure 1-8B2). EGFP-containing fibers of TN GnRH3 neurons extended caudally and joined the anterior commissure (Figure 1-8B2, magenta arrowhead). GnRH3 neurons in the thalamus (Figure 1-8B2, cyan arrowhead) extended their fibers broadly to the caudal region. It was difficult to distinguish fibers of GnRH3 neurons in the TN from those in the thalamus. Using the FluoRender 3-D reconstruction analysis, I could trace the optic nerve and TN/thalamic GnRH3 neuronal fibers separately (Figure 1-8B3, optic nerve fibers, white; GnRH3 neurons in TN ganglion and thalamus, magenta). Fasciculi of the optic nerves entered the brain and branched into two bundles (Figure 1-8B3; white arrowheads), while the reticulated fibers spread into the dorsal (superficial) layers of the OT (Figure 1-8B3, 8B4). On the other hand, fibers from TN and thalamic GnRH3 neurons (magenta) spread caudally and laterally in the deeper layer of the OT, beneath the reticulated EGFP-expressing optic nerve fibers (white) (Figure 1-8B3, 8B4). To examine whether the EGFP positive retinal cells and their optic fibers express GnRH or not, I performed GnRH immunohistochemistry and compared with GFP immunohistochemistry in the adult brain. Anti-EGFP immunohistochemistry (Figure 1-8C1) labeled fibers in both the deep (stratum album centrale, SAC; red arrowhead) and the superficial (stratum fibrosum et griseum

superficiale, SFGS; blue arrowhead) layers, while anti-GnRH immunohistochemistry (Figure 1-8C2) only labeled the deeper one (red arrowhead). Therefore, the EGFP fibers in the SFGS is considered to be projections from ectopically GFP-expressing retinal cells (Figure 1-8C1).

Figure 1-9 shows a schematic drawing of the developmental pattern of GnRH1 and GnRH3 neurons. Both POA GnRH1 neurons and TN GnRH3 neurons appeared in the olfactory placode and migrated to the brain. GnRH1 neurons migrated to the brain along their fibers, and could be divided into two subgroups upon reaching the presumptive vPOA. One subgroup was composed of neurons projecting to the pituitary (hypophysiotropic), while the other was composed of neurons projecting to the lateral region of OT and optic nerves (non-hypophysiotropic) (see below). Meanwhile, GnRH3 neurons originating in the olfactory placode migrated to the brain, reaching the TN and thalamus.

Discussion

I generated two new transgenic medaka lines, *gnrh1*:EGFP and *gnrh3*:EGFP. In 2006, Okubo et al. described GnRH1 and GnRH3 neuronal development in medaka by analyzing transgenic medaka that expressed hrGFP under the control of *gnrh1* and *gnrh3* promoters (Okubo et al. 2006; Wayne et al. 2005). In the present study, I generated *gnrh1*:EGFP and *gnrh3*:EGFP medaka by replacing the hrGFP used by Okubo with EGFP, for which a specific antibody is available. During early developmental stages, the expression of EGFP could be detected by immunohistochemistry in *gnrh1*:EGFP line, although EGFP fluorescence was not bright enough to be detected by itself. In the adult brain of *gnrh1*:EGFP, GnRH1 neurons

expressing EGFP could be detected by its fluorescence without immunohistochemistry. In accordance with this, the expression level of *gnrh1* was not high enough to be detected by *in situ* hybridization during early developmental stages as stated in Okubo et al., 2006. Although the expression level of reporter protein may not necessarily reflect endogenous gene expression, the changes in the level of EGFP fluorescence in *gnrh1*:EGFP line during development in the present study may parallel with endogenous changes in the expression level of *gnrh1*. Using these transgenic medaka, I performed EGFP immunohistochemical examinations to analyze ontogeny and projections of GnRH1 and GnRH3 neurons in more detail than ever.

By using confocal laser scanning microscopy I reconstructed 3-D images of GnRH1 and GnRH3 neurons including their axonal projections throughout the brain during early development. Furthermore, I performed segmentation analysis of 3-D images by using FluoRender, which enabled us to trace the intertwined GnRH1 and GnRH3 neuronal fibers and accurately assess their projections. I could also eliminate ectopically GFP-expressing retinal neurons (Figures 1-8 and 1-9). Thus, I newly found that GnRH1 and GnRH3 nervous systems consist of several neuronal populations, respectively. Based on the axonal projections, the GnRH1 neurons could be mainly divided into two populations, those with hypophysiotropic projections, and those with retinopetal projections and minor tectal projections. On the other hand, based on the origin and migratory pathway, the GnRH3 neurons could be divided into three populations, TN population originating from the olfactory placode (OP), thalamic population originating from OP or thalamus, and TG population originating from TG. The results of the present study about the population and the morphological characteristics of GnRH

neurons should provide important information towards our further understanding of the functional diversities of the GnRH neuronal system.

Migration of GnRH neurons

In the present study, analysis of the EGFP fluorescence detailed the migration and projection of GnRH1 and GnRH3 neurons during early development (1–7 dpf, 10 dph). The migratory pathway of GnRH neurons has been well studied in several species. GnRH neurons located in the TN and vPOA have been reported to originate from the olfactory placode and migrate to the brain in mouse (Tiong et al. 2004), chicken (Murakami et al. 1991), zebrafish (Abraham et al. 2008), and medaka (Okubo et al. 2006). It has been suggested that neural crest cells are the other source of forebrain and diencephalic GnRH neurons (Whitlock et al. 2006, Forni et al. 2011). In the present study, on 2 dpf, EGFP-expressing cells appeared in the thalamic area of *gnrh3*:EGFP medaka. In *gnrh1*:EGFP medaka, non-olfactory placodal EGFP- expressing neurons appeared at 4–7 dpf in the caudodorsal midbrain. These non-olfactory placodal GnRH1 and GnRH3 neurons remained in the region where they first appeared, and did not seem to migrate to the vPOA. There has been evidence of extra-olfactory placodal origins of POA GnRH neuronal progenitors in several animal species (Forni et al. 2011, Zhao et al. 2013). However, in the present study, the extra placodal GFP positive cells in *gnrh1*/*gnrh3*:GFP medaka never migrated into the POA.

In adult medaka, it has been reported that there are two subgroups of GnRH1 neurons; dPOA and vPOA GnRH1 neurons (Okubo et al. 2006). However, during embryonic and juvenile stages, no GFP positive cells was detected in the dPOA of *gnrh1*:EGFP medaka. Accordingly, the ontogenetic origin of dPOA GnRH1 neurons is unclear.

Projections and possible functions of GnRH1 neurons

In the present study, our results suggest that vPOA GnRH1 neurons can be divided into at least two subgroups according to their projections; hypophysiotropic and non-hypophysiotropic (Figure 1-9). The former is considered to form the HPG axis in the adulthood. Namely, in adult medaka, vPOA GnRH1 neurons have been shown to project directly to the pituitary (Karigo et al. 2012a). Surprisingly, I found that EGFP signal of some hypophysiotropic GnRH1 neurons can be detected in juveniles as early as 10 dph, and these neurons possessed similar morphological characteristics to those of the adult vPOA GnRH1 neurons. It has been suggested that GnRH at fetal stages plays roles in development and/or maturation of gonadotropes in rats (Kudo et al. 1994). Therefore, vPOA GnRH1 neurons that send projections to the pituitary in medaka are possibly involved in development and/or maturation of gonadotropes during juvenile stages.

I clearly showed that a population of vPOA GnRH1 neurons project to the pituitary (hypophysiotropic GnRH1 neuron; see also (Karigo et al. 2012a)), and that this projection emerges as early as 10 dph.

On the other hand, the non-hypophysiotropic vPOA GnRH1 neurons projected to the optic nerves and OT. These projections may indicate a possible role for the subpopulation of GnRH1 neurons in the modulation of visual information processing (also see below). In medaka, neurons projecting to the retina, or retinopetal neurons, have been previously identified in six brain nuclei (Deguchi et al. 2005): the TN ganglion, so called preoptic retinopetal nucleus, dorsolateral thalamus, dorsal and ventral portions of the pretectal area, and the nucleus of the posterior commissure. However, the identity of these neurons has not been clarified yet. It may be suggested that the vPOA

GnRH1 neurons with retinopetal projections, which was first identified in the present study, may at least partly comprise the preoptic retinopetal nucleus.

Projections and possible functions of GnRH3 neurons

TN GnRH3 neurons project widely and are involved in neuromodulation including visual information processing

In the present study, I demonstrated a wide projection of TN GnRH3 neurons in the deep layer of OT. The TN GnRH3 neurons have also been shown by GnRH immunohistochemistry to project to the optic nerves and to the OT (Oka and Ichikawa 1990), which was suggested to be involved in modulation of visual information processing. Furthermore, an electrophysiological study in the OT of rainbow trout (Kinoshita et al. 2007) have shown that GnRH2/GnRH3 application facilitated excitatory postsynaptic currents in the deep layer OT neurons, which were evoked by stimulation of retinal fibers, thus showing possible neuromodulation of tectal visual inputs. On the other hand, it has been reported that TN GnRH3 neurons also project to the retina (Oka and Ichikawa 1990), and GnRH receptors are expressed in some types of retinal cells (Grens et al. 2005) of several teleosts. In addition, it was shown that GnRH peptide modulate light responses of horizontal cells in the retina via dopamine release from interplexiform cells (Umino and Dowling 1991). Taken together, in the medaka, TN GnRH3 neurons are suggested to modulate visual information processing similar to some other teleosts.

TN GnRH3 neurons of medaka also projected to the regions involved in sensory information processing other than visual, from the olfactory bulb to more caudal regions. It has been suggested that TN GnRH neurons modulate olfactory information processing

in the olfaction bulb (goldfish, (Kawai et al. 2010)) and the olfactory epithelium (salamander, (Eisthen et al. 2000)). The OT, which was shown to have robust projections from TN GnRH3 neurons, is also known to be involved in somatosensory information processing in vertebrates in general (Drager and Hubel 1975, Tsurudome et al. 2005). Thus, TN GnRH3 neurons are suggested to modulate various sensory information processing by these wide projections.

Possible functions of thalamic GnRH3 neurons

I detected other subpopulation of GnRH3 neurons in the ventral region of the rostralmost portion of the dorsal thalamus. The thalamus is generally considered to relay a wide variety of sensory information. In holocentridae, it has been reported that retinofugal fibers run through and tectal efferent axons terminate in the dorsolateral thalamus (Ito and Vanegas 1983, 1984), which appears to be close to the thalamic GnRH3 neurons in the present study. I also found that thalamic GnRH3 neurons widely project to the caudodorsal region of brain. It is therefore possible that thalamic GnRH3 neurons relay various sensory information.

In summary, I detected several subpopulations of GnRH1 and GnRH3 neurons classified by their projection and distribution patterns using *gnrh1*:EGFP medaka and *gnrh3*:EGFP medaka. Also, I clearly identified the source of hypophysiotropic GnRH neurons as the vPOA GnRH1 neurons. These findings should serve as a strong anatomical basis for the future functional analysis of the GnRH neuronal system.

Figure legends

Figure 1-1

Constructs used to generate the transgenic medaka lines, *gnrh1*:EGFP (A) and *gnrh3*:EGFP (B). EGFP-coding sequence and polyadenylation signal of the SV40 T antigen gene (SV40 polyA) was fused to the 5' flanking region of *gnrh1*/*gnrh3* (5.5 kbp/5.8 kbp) along with the first exon of *gnrh1*/*gnrh3*. An ISce-I recognition site was added into the 5'-end of the 5'-flanking region of *gnrh1* and the 5'-flanking region of *cmlc2* was inserted into the 3'-end of the *gnrh1*: EGFP construct.

Figure 1-2

Specificity of EGFP expression in the adult brain of *gnrh1:*EGFP medaka. Section levels are indicated in panel A (lateral view of the brain; anterior is to the left). A schematic illustration of the frontal section, including the preoptic area (POA) (B2-6). The red box in B1 indicates the region shown in B2-6. Although no signal is detected by rabbit anti-EGFP antibody in wild type brain (B2), immunoreactive somata or fibers are labeled in *gnrh1*:EGFP (B3). Co-localization of EGFP-immunoreactivity (B4, green) and *gnrh1* mRNA expression (B5, magenta) with nuclear counter-staining by Hoechst 33342 (B5, blue) was detected in the brain of *gnrh1*:EGFP medaka (B6, white in overlaid image). Scale bars indicate 20 μm. POA: preoptic area.

Figure 1-3

Specificity of EGFP expression in the adult brain of *gnrh3:*EGFP medaka. Section levels are indicated in panel A (lateral view of the brain; anterior is to the left). Light

photomicrographs of *gnrh3* mRNA signals from *in situ* hybridization in the medaka brain, with counter staining using neutral red (B1,C1). GnRH3 neurons are located in the TN (B1) and ventral region of the rostralmost portion of the dorsal thalamus (C1). The red box in B1/C1 indicates the region shown in B2-4/C2-4. GFP fluorescence in the TN/thalamus is shown in B2/C2 (green), *gnrh3* expression detected by *in situ* hybridization is shown in B3/C3 (magenta) with counter-staining by hoechst (blue), and the overlaid image of B2/C2 and B3/C3 is shown in B4/C4. Scale bars indicate 100 μm (B1, C1), 20 μm (B2–4, C2–4). DM: dorsomedial thalamus, OT: optic tectum, tel: telencephalon, VM: ventromedial thalamus.

Figure 1-4

EGFP expression in the *gnrh1*:EGFP transgenic medaka from 2.5 to 7.5 dpf. Immunohistochemical detection of EGFP (A–D). These photos were processed by merging the sum of confocal microscopy data using Fiji and Photoshop (A1, B-D). 2.5 dpf (A). White arrowhead indicates GnRH1 neuron (A1). F-actin was labeled by Rhodamine-Phalloidin to detect the boundary of the structure of the olfactory placode and the forebrain and is shown in magenta (A2). A2 is an overlay image of one slice of EGFP fluorescence and of Rhodamine-Phalloidin labeling in the same region as A1. 3.5 dpf (B). 4.5dpf (C). 7.5 dpf (D). Cyan arrowhead indicates EGFP positive neurons extending to the optic nerve, the caudal part of diencephalon, and the dorsolateral region of diencephalons (D). The commissural fibers of GnRH1 neurons was observed (magenta arrowhead, D) at 7.5 dpf. Scale bars = 50 μm (A–D). OP: olfactory placode,

FB: forebrain, POA: preoptic area. White broken lines indicate the outlines of the eye, olfactory placode, left hemisphere of the brain, and pituitary (A-D).

Figure 1-5

EGFP expression in the *gnrh1*:EGFP transgenic medaka 10 dph fry (A) and adult brain (B). These photos were processed by merging the maximum intensity projection of confocal microscopy data using Fiji and Photoshop (A1). Cyan arrowhead indicates EGFP positive neurons extending to the optic nerve, the caudal part of diencephalon, and the ventrolateral region of diencephalons (A1). White arrowhead indicates EGFP positive neurons projecting to the pituitary. Orange arrowheads indicate EGFP-expressing neurons in the midbrain at 4–7 dpf (Figure 1-4C, D). The area corresponding to panels A2 (ventral view) and A3 (lateral view) is boxed in panel A1. Subpopulations of neurons are shown in pseudo-color in accordance with the axonal projections determined by FluoRender (A2, 3). White: EGFP-expressing neurons projecting to the pituitary. Cyan: EGFP-expressing neurons projecting to the ipsilateral dorsolateral region of OT and mainly to the contralateral optic nerve. Green: spindle-shaped somata, which appear to be in the process of migration or have stopped migration. Ventral view of adult brain from *gnrh1*: EGFP medaka (B). OT: optic tectum, m: medial, l: lateral, d: dorsal, v: ventral, Scale bars = 50 μm (A), 100 μm (B). White broken lines indicate the outlines of the brain, and pituitary (A, B).

Figure 1-6

GFP fluorescence of *gnrh3*:EGFP medaka at 1.5 dpf (A), 2 dpf (B). These photos were processed by merging the maximum intensity projection of slices of confocal microscopy data using Fiji and Photoshop (A, B). Cyan arrowheads indicates trigeminal ganglion neurons expressing EGFP (A). The area corresponding to panels A2 is boxed in panel A1. White arrowheads indicate EGFP positive neurons in the olfactory placode (B). F-actin was labeled by Rhodamine-Phalloidin to detect the boundary of the structure of the olfactory placode and the forebrain and is shown in magenta (B2). B2 is an overlay image of one slice of EGFP fluorescence and of Rhodamine-Phalloidin labeling in the same region as B1. OP: olfactory placode, FB: forebrain, MB: midbrain, TG: trigeminal ganglion. Scale bar = 50 μm (A, B, C1) White broken lines in A and B1 indicate the shape of eyes, olfactory placode, and brain.

Figure 1-7

GFP fluorescence of *gnrh3*:EGFP medaka at 2.5 dpf (A), 3.5 dpf (B). These photos were processed by merging the maximum intensity projection of slices of confocal microscopy data using Fiji and Photoshop (A, B). The areas corresponding to the panel A2/B2 (dorsal view) are boxed in panel A1/B1. Yellow arrowheads (A) and neurons (pseudo-color, A2) indicate GnRH3 neurons located just beside the eyes and caudal regions of the optic nerves. Cyan arrowheads (A, B) and neurons (pseudo-color, A2, B2) indicate GnRH3 neurons derived from non-olfactory placodal origins (A, B). Fibers of EGFP positive neurons originating from the olfactory placode are shown in white (pseudo-color, A2, B2). EGFP positive neurons of TG ganglion and ectopic EGFP positive fibers from optic nervs are shown in green (A2, B2). OP: olfactory placode,

FB: forebrain, MB: midbrain, TG: trigeminal ganglion, m: medial, l: lateral. Scale bar = 50 μm (A1, B1), 10 μm (A2, B2). White broken lines indicate the shape of eyes and brain.

Figure 1-8

GFP expression of *gnrh3*:EGFP medaka at 4.5 dpf (A), just after hatching (B), and adult (C). B2 represents the data processed from B1; the dorsal region containing reticulated fibers of the OT and part of the optic nerve were removed from the stack. B3 represents the data processed from B1 without removal of slices; fibers from optic nerves are shown in white, and GnRH3 neurons in the TN ganglion and thalamus are shown in magenta (pseudo-color, B3, B4). The area corresponding to panel B4 is boxed in panel B3. Magenta arrowhead (B2) indicates commissural fibers of EGFP positive neurons of TN ganglia. Cyan arrowhead (B2) indicates EGFP positive neurons in the thalamus. EGFP- expressing fibers (C1) or GnRH3-positive fibers (C2) in the OT were detected by immunohistochemistry (C1/C2). Red arrowheads indicate the stratum album centrale, blue arrowheads indicate stratum fibrosum et griseum superficiale (C1, C2). FB: forebrain, MB: midbrain, TG: trigeminal ganglion, OT: optic tectum, d: dorsal, v: ventral. Scale bar = 50 μm (A, B), 100 μm (C). White broken lines in A and B1 indicate the shape of eyes, brain and pituitary.

Figure 1-9

Schematic diagram of the development of EGFP- expressing neurons from *gnrh1*:EGFP (A) and *gnrh3*:EGFP (B) medaka. (A) Magenta, neurons projecting to the

pituitary; cyan, neurons in the POA projecting to the optic nerves and diencephalon. (B) Red, GnRH3 neurons in TN and the thalamus originating from the olfactory placode, migrating to the brain, and projecting broadly in the brain; blue, GnRH3 neurons in the thalamus originating in the brain; green, GnRH3 neurons in the trigeminal ganglion; gray, retinal neurons expressing EGFP ectopically. Because these ectopic retinal fiber projections interfere with the illustration of GnRH3 neuron projections (red), we only indicated these fibers (gray) in the right half of the brain. During the late stages of development, red and blue neurons appeared to be intermingled.

Antigen	Description of Immunogen	Source, Host Species, Cat. #, Clone or Lot#, RRID	Concentration Used
EGFP	Glutathione S-transferase - GFP fusion protein synthesized by *E. coli*	Drs. Kaneko and Hioki [Kyoto University], rabbit polyclonal, described in Tamamaki et al.,2000	0.3 μg/mL
GnRH3	Synthetic salmon GnRH (Peninsula Lab., Inc., Belmont, CA) bound to bovine serum albumin	Dr. Okuzawa, [National Fisheries Research Agency], rabbit polyclonal, described in Okuzawa et al., 1990	Antiserum was diluted in PBST (1:10000)

Table 1-1. Table of Primary Antibodies Used

Figure 1-1

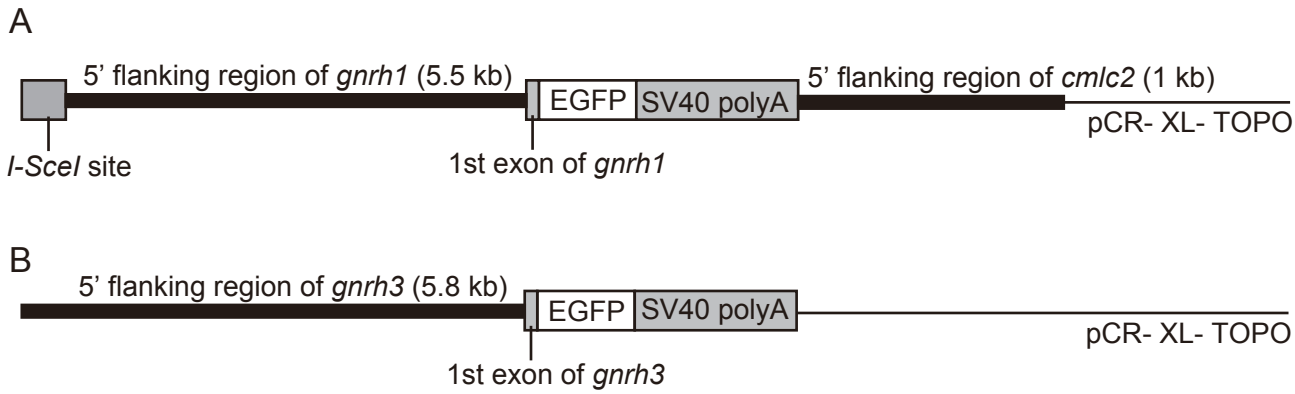
A
5’ flanking region of *gnrh1* (5.5 kb)
EGFP
SV40 polyA
5’ flanking region of *cmlc2* (1 kb)
pCR- XL- TOPO
I-SceI site
1st exon of *gnrh1*
B
5’ flanking region of *gnrh3* (5.8 kb)
EGFP
SV40 polyA
pCR- XL- TOPO
1st exon of *gnrh3*

Figure 1-2

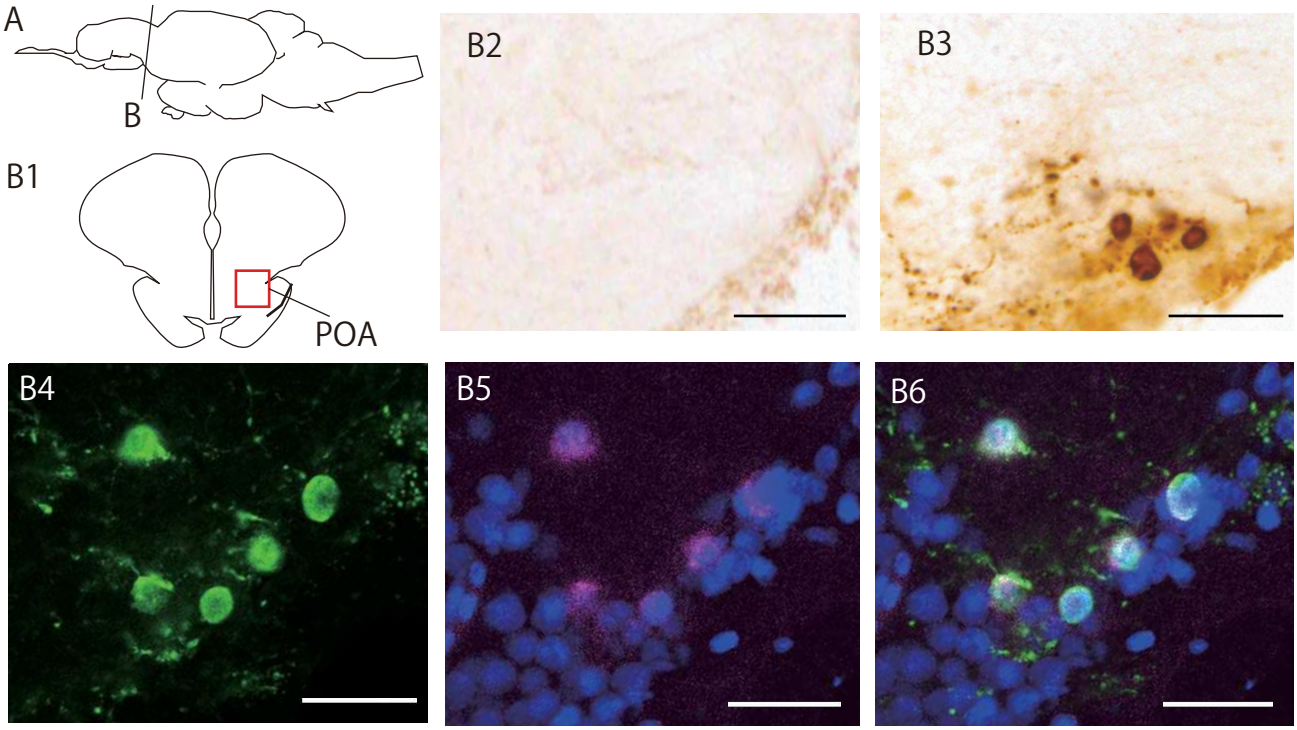

Figure 1-3

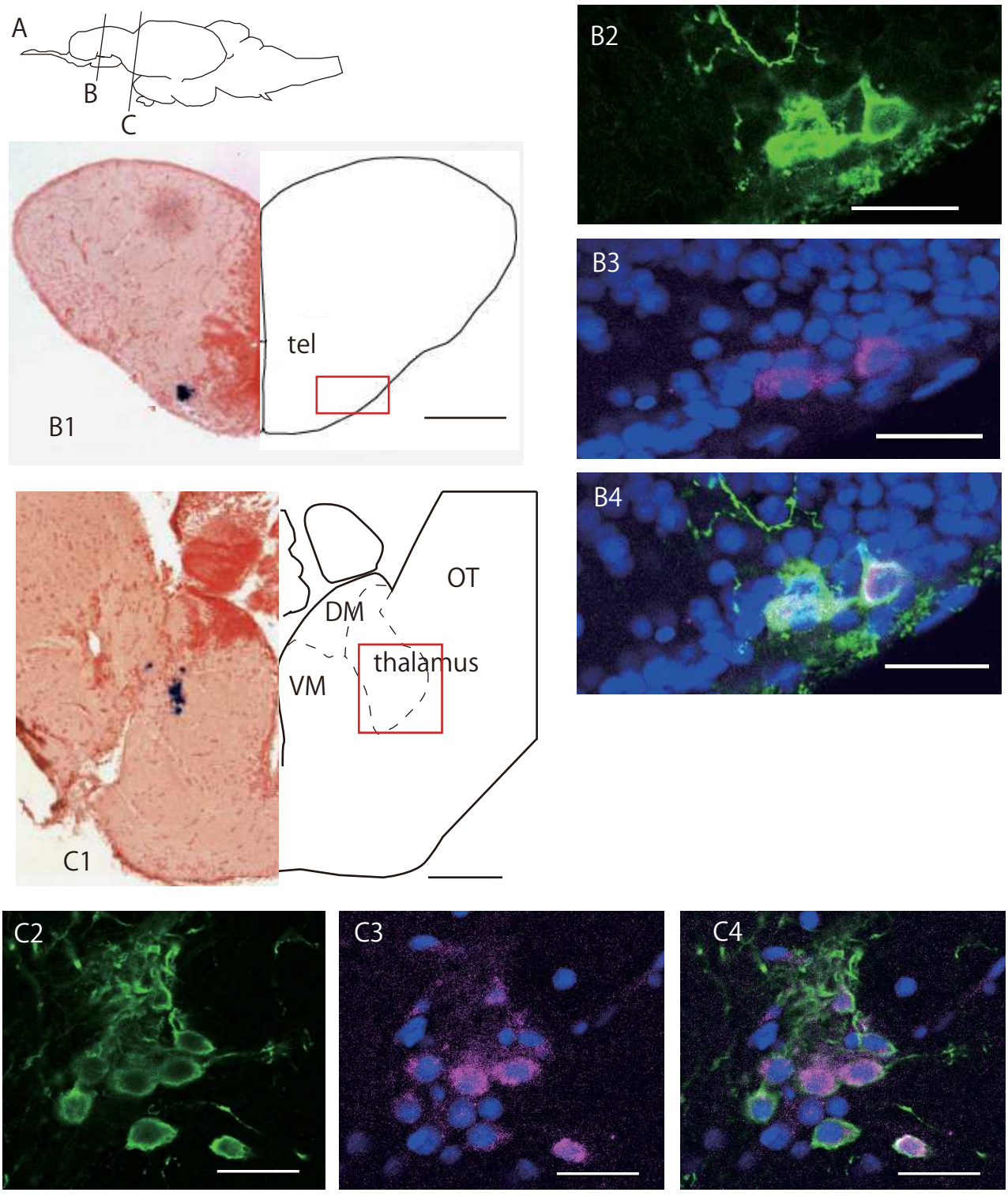

Figure 1-4

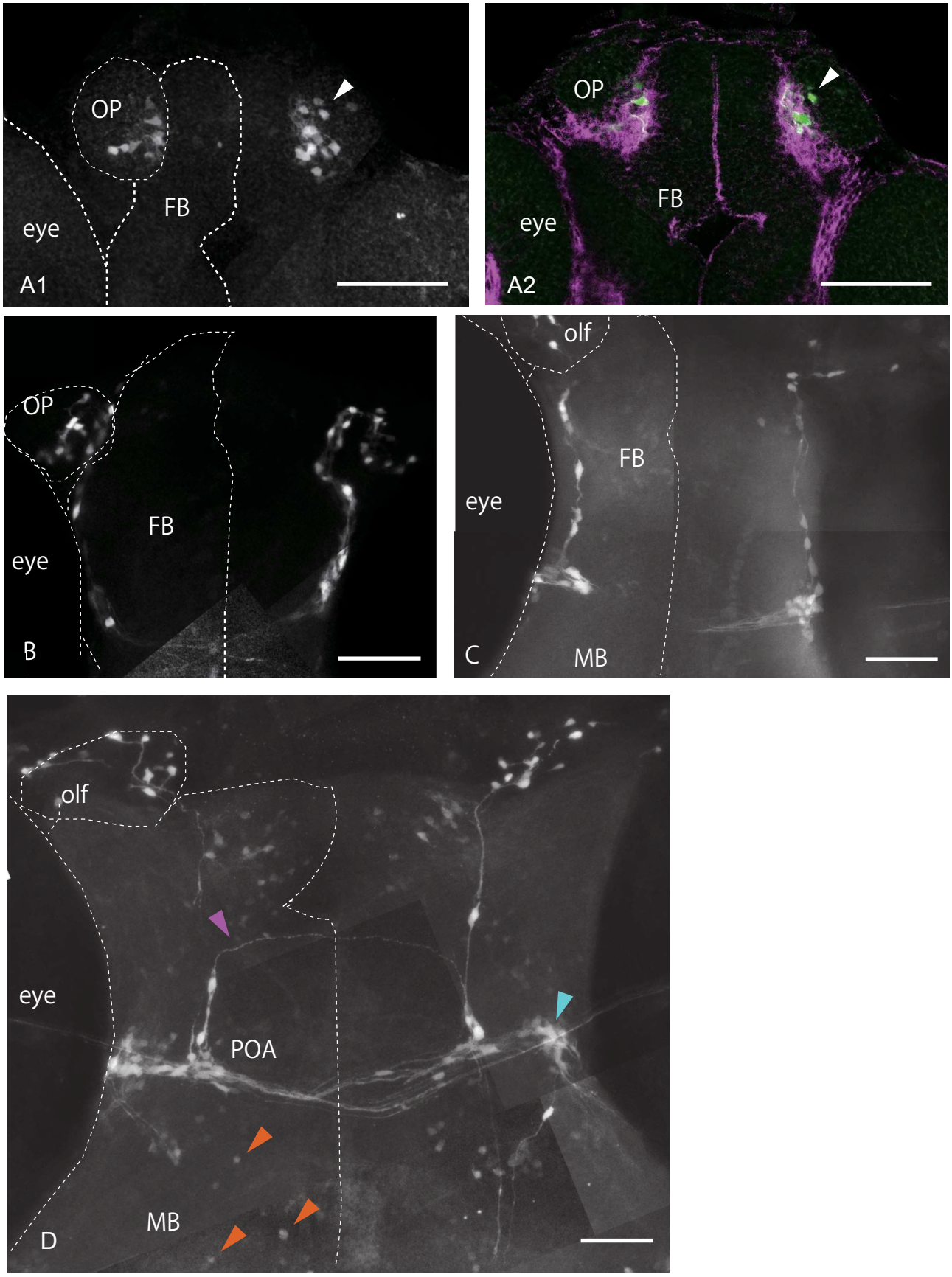

Figure 1-5

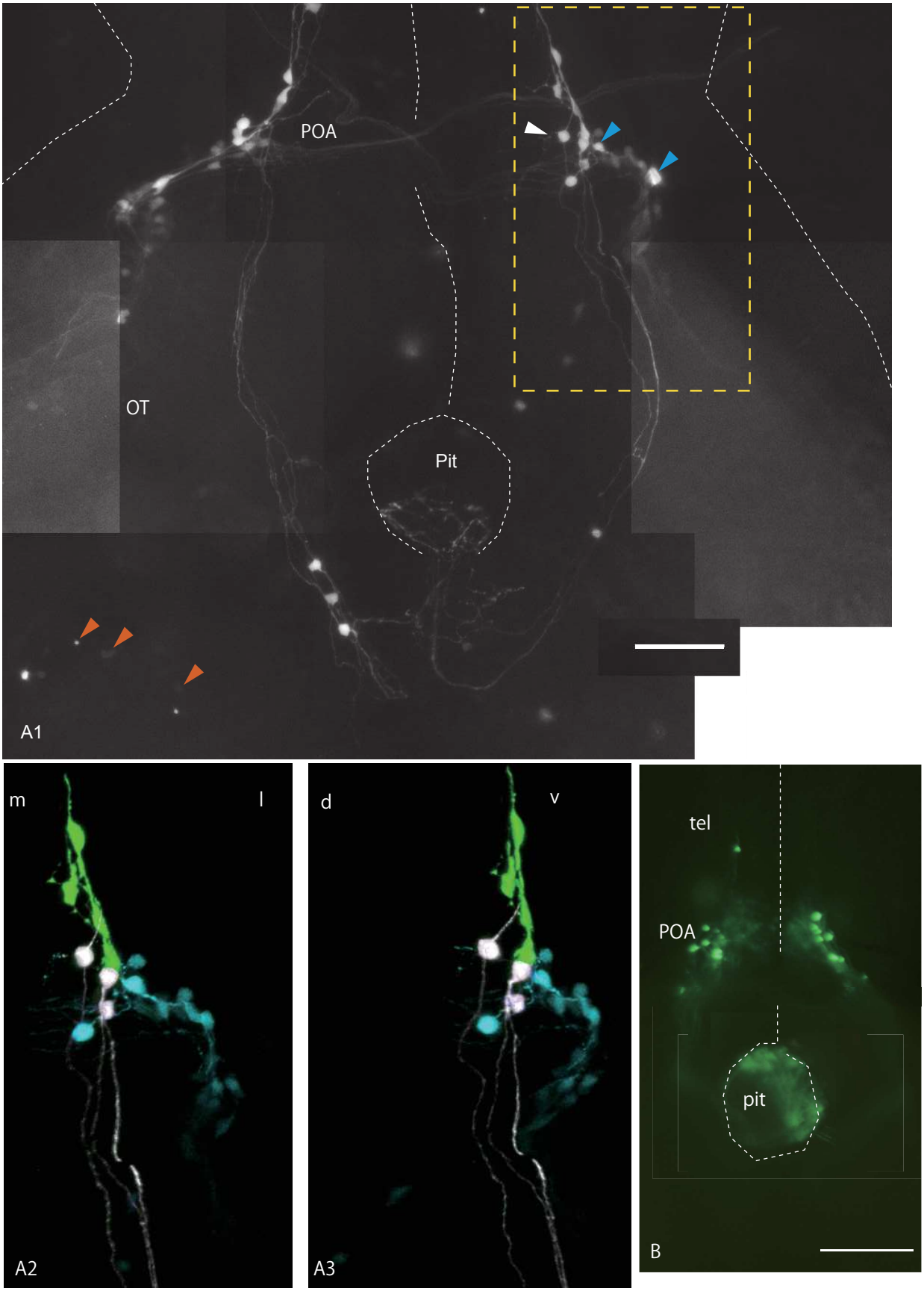

Figure 1-6

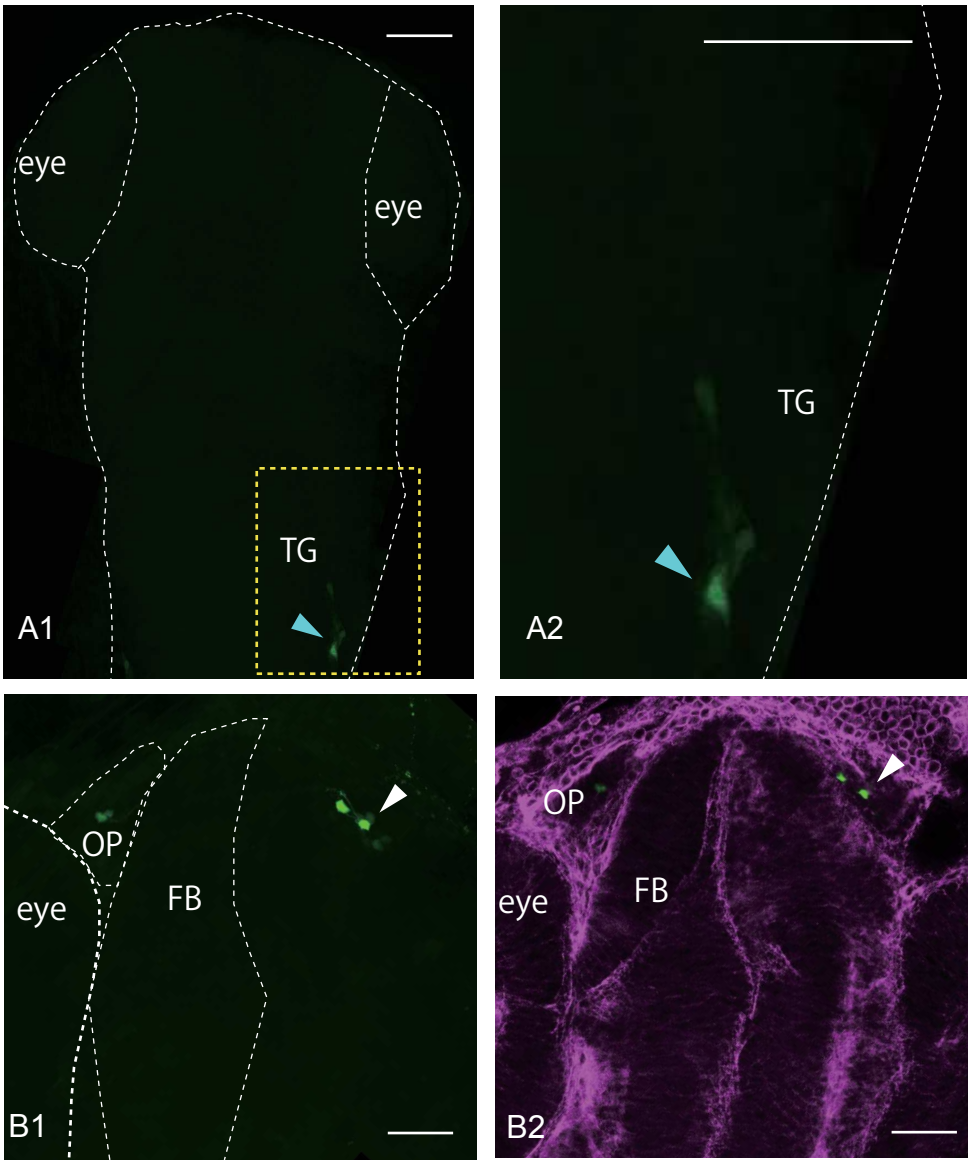

Figure 1-7

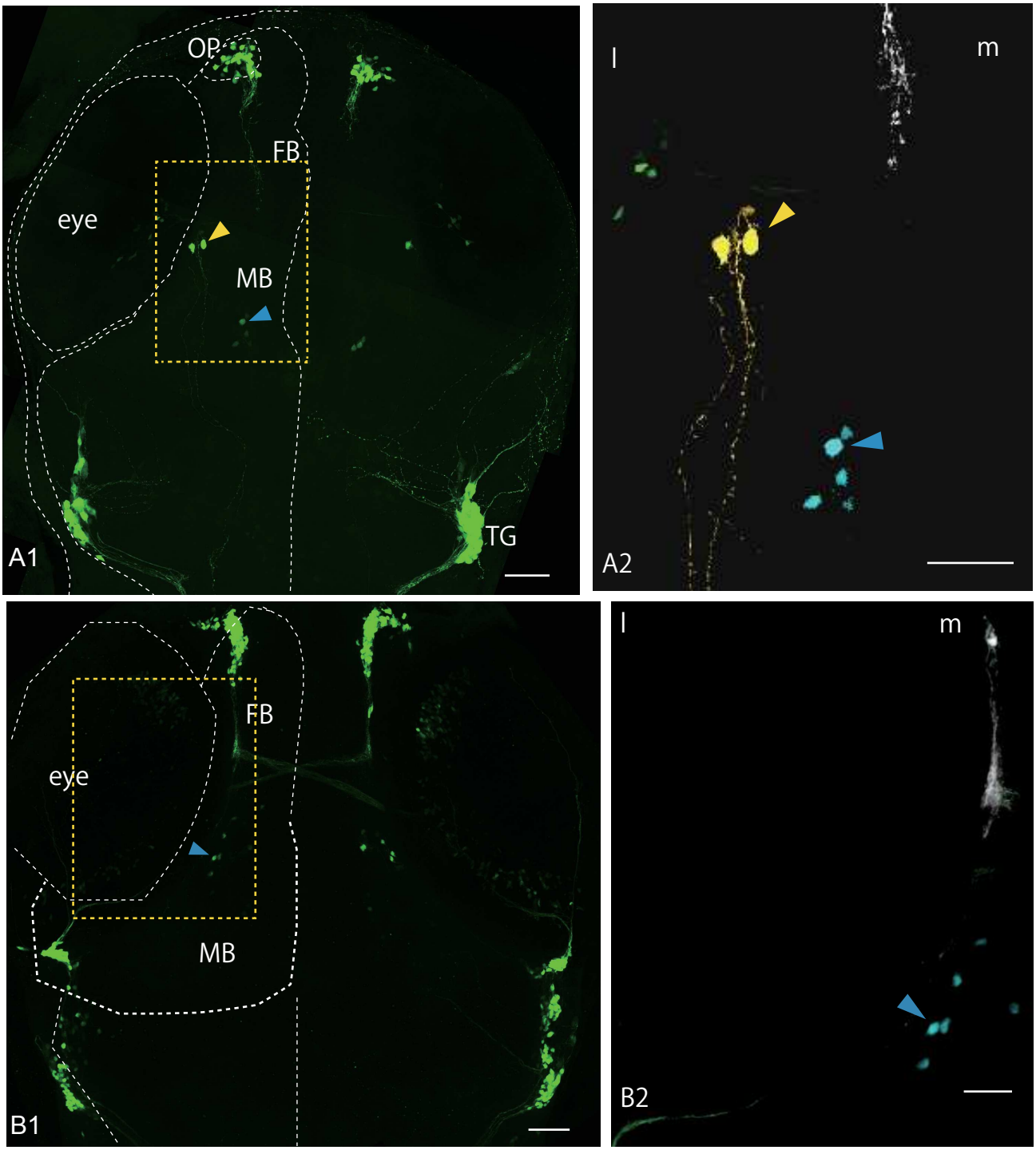

Figure 1-8

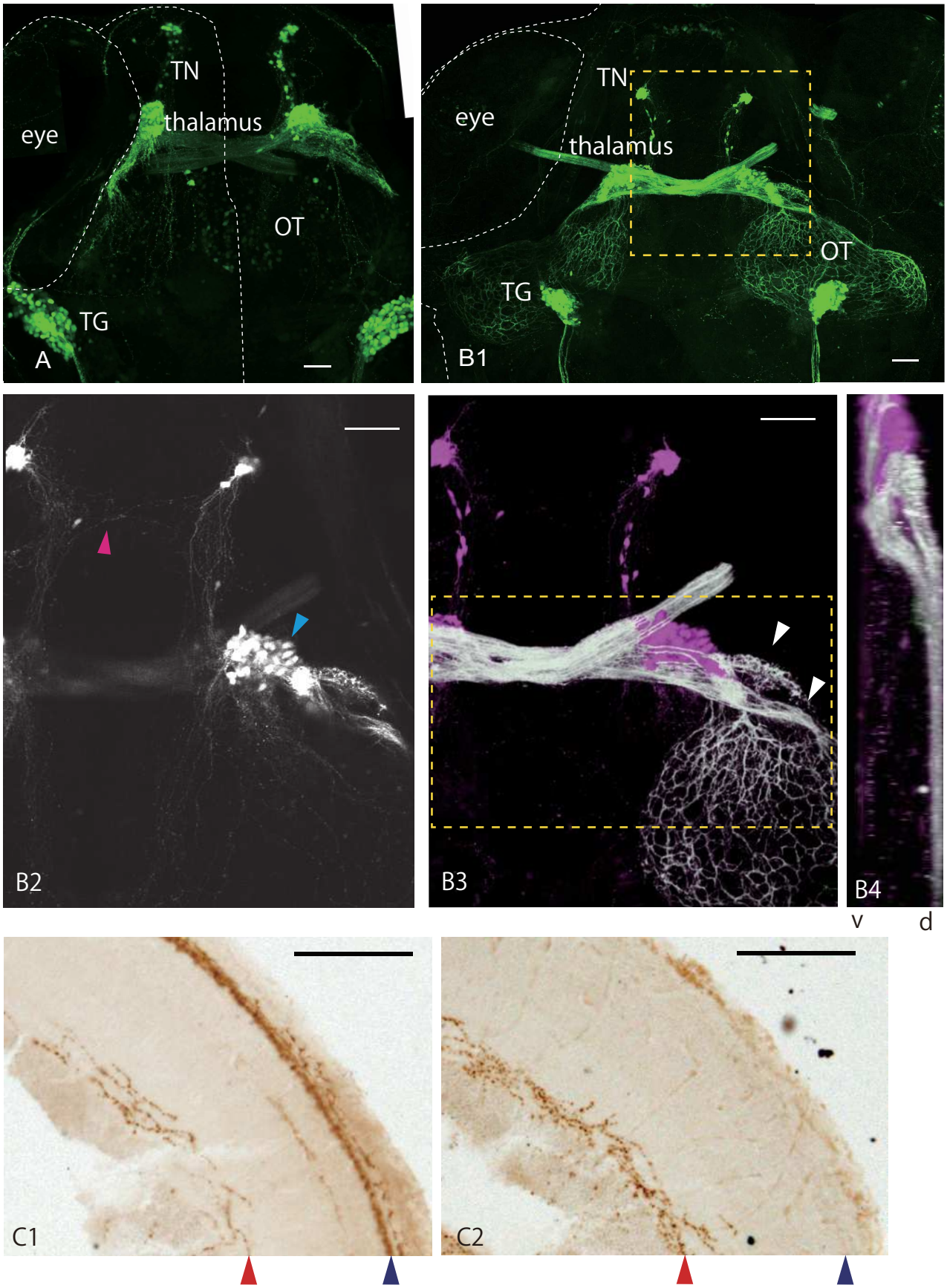

Figure 1-9

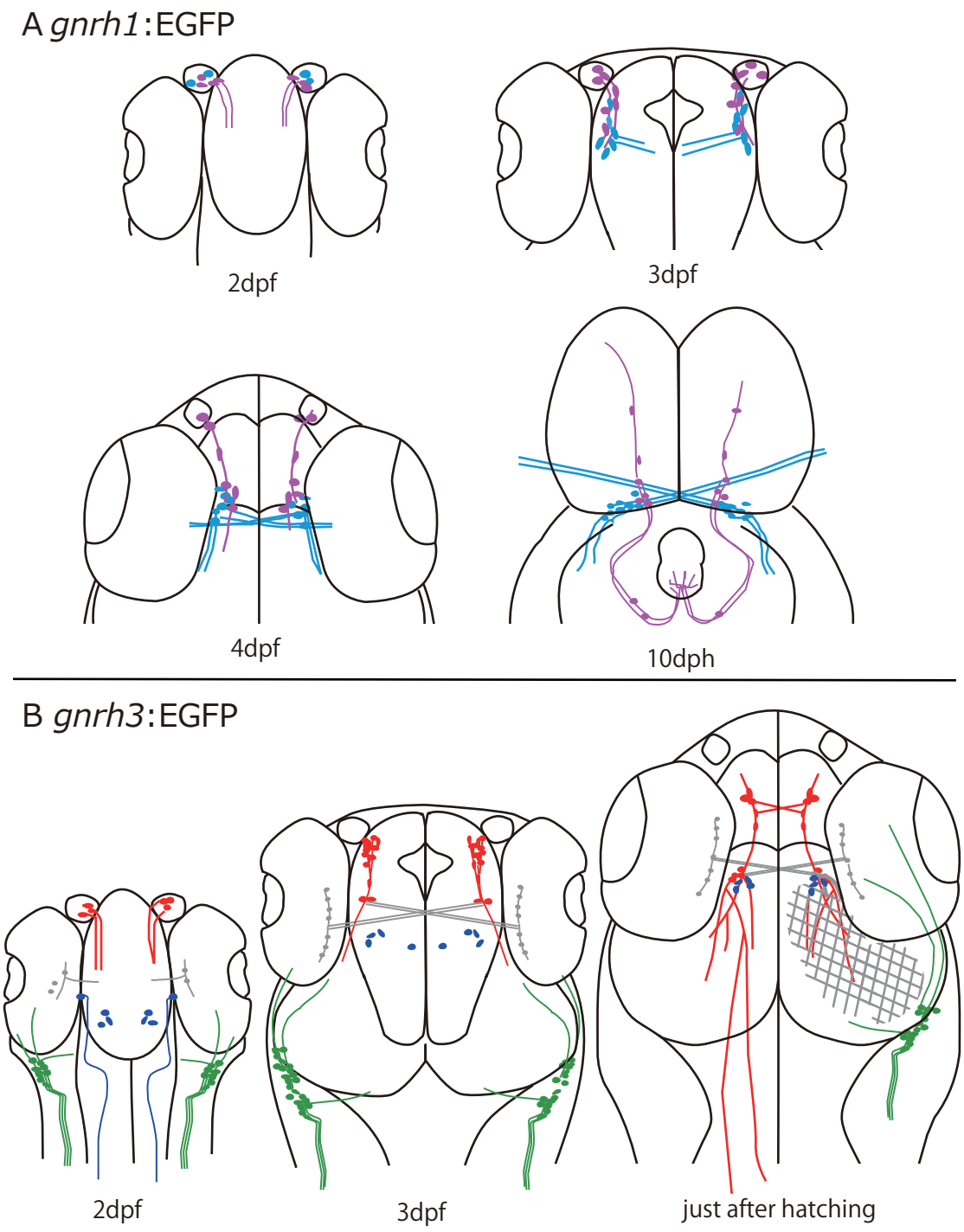
A *gnrh1*:EGFP
2dpf
3dpf
4dpf
10dph
B *gnrh3*:EGFP
2dpf
3dpf
just after hatching

Chapter 2

Functional analysis of GnRH, LH, and FSH in the HPG axis regulation by using knockout medaka

Introduction

Gonadotropin releasing hormone (GnRH) is widely accepted to be essential for regulation of reproduction by stimulating synthesis and release of luteinizing hormone (LH) and follicle stimulating hormone (FSH) in mammals. A natural mutation in *Gnrh* gene causes a decrease in serum LH and FSH concentrations, which leads to infertility in both male and female mice (Cattanach et al. 1977). Targeted gene knockout (KO) by using ES cell lines in mice revealed that LH/FSH null mice are sterile with immature gonads (Kumar et al. 1997, Abel et al. 2000, Ma et al. 2004).

However, such clear results seem to be limited to mice, and general functions of GnRH, LH, and FSH in vertebrates still remain unclear, although many studies have shown that GnRH peptides increase release and/or synthesis of LH and FSH in various species including amphibians and teleosts (Daniels and Licht 1980, Breton et al. 1998, Mananos et al. 1999, Weil et al. 1999, Dickey and Swanson 2000, Karigo et al. 2012a, Karigo et al. 2014). Unlike in mammals, many candidates for hypothalamic neurotransmitters that can be directly involved in the regulation of gonadotropin secretion have been reported in nonmammalian species, e.g. dopamine and gamma-aminobutyric acid (GABA) (Yaron et al. 2003). Thus, we even do not know for sure whether GnRH is essential and play a critical role in the regulation of reproduction or not in nonmammalian species.

LH and FSH are complex glycoproteins (Baenziger and Green 1988), and the functional analysis have lagged behind other simple peptide/protein hormones. In non-mammalian species, it has been reported that the expression level of *fshr* (FSH receptor gene) increase at mid-vitellogenic (MV) stage of ovarian development and that of LH

receptor gene increase at full-growth (FG) follicle stage in zebrafish (Kwok et al. 2005). Recently, some research groups have established a method for synthesizing recombinant glycoprotein hormones of teleosts, using Chinese hamster ovary cells (Ogiwara et al. 2013) or insect cells (Kamei et al. 2003, Aizen et al. 2007, Cui et al. 2007, Ko et al. 2007). By using such recombinant LH and FSH glycoproteins, in vivo and in vitro studies were performed (Kazeto et al. 2008, Hagiwara et al. 2014). It is suggested in non-mammalian species that FSH and LH play a role in the ovarian development and ovulation like in mammalian species. However, the function(s) of LH and FSH have not been clarified yet in detail.

Here, teleosts have some advantages for the elucidation of the essential components of reproduction in the hypothalamus and the pituitary from the following reasons. First, LH and FSH are secreted from distinct cell populations that express those hormones separately (Yaron et al. 2003, Kanda et al. 2011). By taking advantage of this, it has been demonstrated that LH and FSH cells show different $[Ca^{2+}]_i$ responses to GnRH (Karigo et al. 2014). Second, it is expected that features common to teleosts and mammals may be also common to the other vertebrates as well, because teleosts are evolutionarily distant from mammals. Among others, medaka is especially useful because of the ease of genetic manipulations and the wealth of knowledge on reproduction.

In Chapter 2, I analyzed the function(s) of GnRH, LH, and FSH and their interactions in medaka by using recently developed genome editing techniques; I generated and analyzed *gnrh1* KO medaka. As LH and FSH are heterodimeric glycoproteins, which consist of common α subunit and functionally unique β subunit, LHβ and FSHβ

(Baenziger and Green 1988), I generated and analyzed phenotypes of *lhb*/*fshb* KO medaka. Taken together with the previous literature, I proposed a dynamic interaction scheme among GnRH, LH, FSH, and gonads.

Materials and Methods

Animals

Male and female wild-type d-rR medaka (*Oryzias latipes*), *gnrh1* KO medaka, *lhb* KO medaka and *fshb* KO medaka (see below) were maintained under a 14-h light, 10-h dark photoperiod (lights-on at 08:00 h and lights-off at 22:00 h) at a water temperature of 27°C. Female subjects were sexually mature (older than 50 days post hatching (dph)). All experiments were conducted in accordance with the protocols approved by the Animal Care and Use Committee of the University of Tokyo (permission number: 15–3).

Generation of KO animals

gnrh1/*lhb*/*fshb* gene KO medaka were generated using TALEN. Specific TALEN target site were identified using an online tool (ZiFiT: supplied by ZINC FINGER CONSORTIUM; http://www.zincfingers.org/default2.htm). 5' region of exon2 of *gnrh1* (Fig. 1), 5' region of 1st exon of *lhb* (Fig. 2), and 5' region of 1st exon of *fshb* (Fig. 3) were selected for target regions of *gnrh1*, *lhb*, and *fshb* TALENs pairs, respectively. Gene-specific TALEN constructs were assembled using Joung Lab REAL Assembly TALEN kit (Addgene, Cambridge MA, USA) as described (Sander et al. 2011). Each left/right TALEN mRNA pairs were transcribed in vitro using mMessage mMachine T7 Transcription Kit (Life Technologies) in accordance with a manufacture

protocol. EGFP mRNA was transcribed using SP6 promoter in linearized pCS2+EGFP vector. TALEN solution containing left TALEN mRNA (20 ng/μL), right TALEN mRNA (20 ng/μL), EGFP mRNA (1-5ng/μL; for screening) and 0.02 % phenol red in 1 x PBS were injected into the cytoplasm of one- cell stage fertilized eggs with intact chorion. For screening, genomic DNA of candidate fish were extracted from their caudal fins using prepGem-tissue (ZyGEM, Hamilton, New Zealand) and were used as a template of real-time PCR for melting curve, or sequencing analyses using genome PCR primers described in the primer list (Table1).

Immunohistochemistry

Three-month-old wild type and KO medaka were deeply anesthetized with MS-222 (Sigma, St. Louis, MO). Brains with its pituitary were fixed in 4% paraformaldehyde (PFA) in 0.05 M phosphate-buffered saline (PBS) for overnight at 4 °C. Fixed specimens were immersed in PBS with 30 % sucrose for 3–6 hours, embedded in 5% agarose (type IX-A; Sigma) containing 20% sucrose in PBS, then frozen in *n*-hexane at −80 °C. Serial frontal sections were cut at 25 μm thickness using a cryostat (Leica CM3050S, Leica Microsystem Inc., IL). The cryosections were rinsed with 0.05 M PBS with 0.5 % Triton X-100 (PBST), and then incubated with rabbit anti-medaka GnRH antiserum (1:10,000, specific to medaka GnRH1 (Karigo et al. 2012a); generous gift from Dr. Okubo, The University of Tokyo, Tokyo, Japan), anti-medaka LH antiserum (1:10,000; (Ogiwara et al. 2013) ; generous gift from Drs. Ogiwara and Takahashi,), or anti-medaka FSH antiserum (1:10,000; (Ogiwara et al. 2013) ; generous gift from Drs. Ogiwara and Takahashi, Hokkaido University, Sapporo, Japan) diluted with PBST containing 10% normal goat serum for 8 hours at RT. After washout with

PBST, the sections were incubated with biotinylated goat anti-rabbit IgG antibody (1:200; Vector Laboratories, Burlingame, CA, USA) diluted in PBST for 2 hours at RT. They were then incubated with Vectastain Elite ABC (Vector Laboratories) for 1 hour at RT, washed in PBST, and then immunoreactivity was visualized with 3,3'-diaminobenzidine and 0.03 % H_2O_2.

Hematoxylin and eosin staining

The ovaries and testes were fixed with Bouin's fixative at 4 °C overnight. After fixation, each tissue sample was routinely processed and embedded in paraffin, and sections of 8 μm thickness were stained with hematoxylin and eosin (HE). Photographs were taken with a digital camera (DFC310FX; Leica Microsystems, Wetzlar, Germany) attached to an upright microscope (DM5000B; Leica Microsystems).

Ovariectomy and estrogen replacement

Ovariectomy and estrogen replacement were performed as previously described (Kanda et al. 2012). After the fish were anesthetized with 0.02% MS-222, the ovaries were totally removed with forceps (OVX). After the operation, the OVX fish were kept in 0.7% NaCl for one day without feeding, and then transferred to an aquarium, where they were kept under the breeding condition described above. They were fed with 17β-estradiol (E_2; Sigma, St Louis, MO, USA)-containing flake food for estrogen treatment (0.1 μg E/day) (Kanda et al. 2008) for three days. Their pituitaries were collected at 2hours after administration of E_2 by feeding at 5 days after OVX for real time PCR samples.

Quantitative realtime PCR

Three-month-old medaka were deeply anesthetized with 0.02% MS-222, and the pituitaries were collected for real-time PCR analysis at 10:00 h. For ovariectomy and estrogen treatment, three-month-old medaka were deeply anesthetized with 0.02% MS-222. Total RNA was extracted from the pituitaries using the NucleoSpin RNA XS (Takara, Shiga, Japan) according to the manufacture's protocol. Genomic DNA was removed by deoxyribonuclease I (Ambion, Applied Biosystems, Foster City, CA) treatment on a column membrane. Total RNA was reverse transcribed with a High Capacity PrimeScript Reverse Transcriptase (Takara) according to the manufacturer's instructions. For real-time PCR, the cDNA was amplified using a KAPA SYBR FAST qPCR Kit (Nippon Genetics Co, LTD, Tokyo, Japan) with the LightCycler 480 II system (Roche, Molecular Biochemicals GmbH, Mannheim, Germany). The temperature profile of the reaction was 95 °C for 5 min, 45 cycles of denaturation at 95 °C for 10 s, annealing at 60 °C for 10 s, and extension at 72 °C for 10 s. The PCR product was verified using melting curve analysis. The data was normalized to a housekeeping gene, ribosomal protein s13 (rps13). The primer pairs used in the real-time PCR are listed in Table1.

Recombinant medaka LH administration

Three month old *gnrh1*$^{-/-}$ or *lhb*$^{-/-}$ female medaka were anesthetized with 0.02 % MS-222 and were administrated with 10 μl recombinant medaka LH (rLH; 1:10 in PBS (Hagiwara et al. 2014)) or vehicle (PBS) by Intraperitoneal injection (IP) at 11:00-15:00, the predicted time of LH surge, which is 18-19 h before ovulation (Iwamatsu 1978b). Injected fish were pared with wild type adult male medaka overnight and ovaries of that were observed by HE staining at the next morning.

Data Analysis

All data were expressed as the mean ± SEM. The results of the experiments involving three groups in the wt, *gnrh1*$^{+/-}$, and *gnrh1*$^{-/-}$ were analyzed using steel test.

Results

Generation of KO medaka lines

After incross and/or outcross with wild type, sequence analyses of homozygous or heterozygous KO individuals were performed in the targeted genes of *gnrh1*$^{-/-}$, *lhb*$^{-/-}$, and *fshb*$^{-/-}$ medaka (Fig. 2-1A, 2A, 3A). Deduced amino acid sequences from these genomic sequence are shown in Fig. 2-1B, 2B, and 3B. The *gnrh1*$^{-/-}$ medaka completely lack GnRH peptide sequence. The *lhb*$^{-/-}$ and *fshb*$^{-/-}$ medaka produce peptides that is different from Lhb and Fshb, respectively. These peptides are considered to be nonfunctional, according to the previous reports (Baenziger and Green 1988). I have also shown by immunohistochemistry that each KO line lacks protein encoded by respective gene (Fig. 2-4). GnRH1 immunoreactive fibers could be detected in the pituitary of *gnrh1*$^{+/-}$, but not in that of *gnrh1*$^{-/-}$ (Fig. 2-4A, B). LH and FSH positive cells could be detected in the pituitary of *lhb*$^{+/-}$ (Fig. 2-4D) and *fshb*$^{+/-}$ (Fig. 2-4C), but not in that of *lhb*$^{-/-}$ (Fig. 2-4C) and *fshb*$^{-/-}$ (Fig. 2-4D), respectively. These results demonstrate that none of the KO line of medaka can produce functional protein encoded by the respective gene.

Fertility of *gnrh1*/*lhb*/*fshb* KO medaka lines

Although all male medaka of *gnrh1*$^{-/-}$, *lhb*$^{-/-}$, and *fshb*$^{-/-}$ were fertile, all female medaka of *gnrh1*$^{-/-}$, *lhb*$^{-/-}$, and *fshb*$^{-/-}$ were sterile. Meanwhile, all females of *gnrh1*$^{+/-}$, *lhb*$^{+/-}$, and *fshb*$^{+/-}$ were fertile. For further analysis, gonads of KO lines were sectioned and were histologically examined by HE staining (Fig. 2-5). As predicted by their fertility, the testis of each line normally grew up. On the other hand, although ovaries of *gnrh1*$^{-/-}$ and *lhb*$^{-/-}$ were fully developed to show full-growth (FG) or late vitellogenic (LV) follicle at

90 dph, ovulation was not detected in the ovaries of either line. The development of ovary of *fshb*$^{-/-}$ was insufficient and was halted at the yolk accumulation stage. No FG or LV ovum was observed in *fshb*$^{-/-}$ ovary even at 90 dph, when ovaries of other KO lines and wt showed FG or LV follicle (Fig. 2-5). These results demonstrate that FSH, but not LH, is necessary for follicular growth and the yolk accumulation of oocytes, whereas GnRH1 and LH are necessary for ovulation.

Expression level of gonadotropin genes in *gnrh1* KO medaka

The expression level of *lhb* and *fshb* mRNA in the pituitary of *gnrh1* KO line were measured by realtime PCR (Fig. 2-6). There was no significant difference in either the expression level of *lhb* or *fshb* of *gnrh1*$^{-/-}$ as well as *gnrh1*$^{+/-}$ male, compared with that of wt (Fig. 2-6A, C). Although there were no significant difference in the expression level of *fshb* of *gnrh1*$^{-/-}$or *gnrh1*$^{+/-}$ or wt female (Fig. 2-6D), the expression level of *lhb* in *gnrh1*$^{-/-}$ was significantly lower than that of *gnrh1*$^{+/-}$ or wt (Fig. 2-6B). To avoid the secondary effects of serum estrogen, the expression levels of *lhb* and *fshb* in *gnrh*$^{-/-}$ female were compared to those of wt/*gnrh*$^{+/-}$ under the condition of OVX+E (Fig. 2-6E, F). It was shown that there is no significant difference in the expression level of *fshb* among *gnrh1*$^{-/-}$, *gnrh1*$^{+/-}$, and wt females (Fig. 2-6F). Meanwhile, the expression level of *lhb* of *gnrh1*$^{-/-}$ was significantly lower than that of wt (Fig. 2-6E), although there is no significant difference between that of *gnrh1*$^{+/-}$and wt or *gnrh1*$^{-/-}$. These results indicate that GnRH1 plays an essential role in the stimulation of LH secretion, while it is dispensable for that of FSH secretion.

Sterility of *gnrh1*$^{-/-}$ and *lhb*$^{-/-}$ were rescued by intraperitoneal (IP) injection of medaka rLH or PMSG

As described above, both *gnrh1*$^{-/-}$ and *lhb*$^{-/-}$ female failed to ovulate, although their oocytes were full of accumulated yolk (Fig. 2-5A1, D1). On the other hand, the oocyte development of the ovary of *fshb*$^{-/-}$ was halted at the yolk accumulation stage (Fig. 5H1). These data suggest that FSH alone is sufficient for full accumulation of yolk, but insufficient release of LH in *gnrh1*$^{-/-}$ and *lhb*$^{-/-}$ medaka prevents ovulation. To verify this hypothesis, I tested whether IP injection of PMSG or rLH induces ovulation in *gnrh1*$^{-/-}$ and *lhb*$^{-/-}$ medaka. It has been reported that rLH activates both LH receptor and FSH receptor, whereas PMSG only activates LH receptor in medaka (Ogiwara et al., 2013). Although no ovulated ovum was detected in the ovary of *gnrh1*$^{-/-}$ and *lhb*$^{-/-}$ after IP injection of PBS as a control, ovulated ovum was detected in the ovary of *gnrh1*$^{-/-}$ and *lhb*$^{-/-}$ after IP injection of PMSG or rLH (Fig. 2-7). Thus, these results strongly support the above mentioned hypothesis.

Discussion

In Chapter 2, I used genome editing techniques to examine essentiality of the component of the hypothalamo-pituitary-gonadal (HPG) axis regulation, i.e., GnRH and two gonadotropins, LH, and FSH. Here, I generated KO medaka lines for each gene and scrutinized their phenotypes. I could clearly demonstrate that LH release, which is strongly suggested to be directly triggered by GnRH, is necessary for ovulation in female medaka. I demonstrated that FSH is necessary for the folliculogenesis, but that it does not require GnRH regulation. On the other hand, I unexpectedly found that males of all KO medaka were fertile, meaning that neither LH nor FSH release induced by GnRH is not essential in male medaka. Thus, the understanding of the hypothalamic

regulation of gonadotropins in medaka may open up a new window towards understanding the mechanisms of regulation of gonadotropin release, some of which are common to all vertebrates, and some of which are not.

The function of LH and FSH in teleosts

In the present Chapter, I have shown that FSH and LH have distinct roles in female gonadal maturation; FSH is necessary for the development of follicles, whereas LH is necessary for ovulation. In *fshb* KO female medaka, folliculogenesis is halted at pre-vitellogenic (PV) stage. On the other hand, in *lhb* KO females, ovulation did not occur, although the oocytes developed up to the FG-stage follicles. Moreover, I showed that a single injection of rLh or PMSG, which strongly activates medaka LH receptor (Ogiwara et al. 2013), induced ovulation. These lines of evidence indicate that FSH is required for oocyte development, whereas LH is essential for ovulation.

The phenotypes of *lhb*/*fshb* medaka provide evidence for LH and FSH functions

A previous report demonstrated that FSH receptor *(fshr)* gene KO female medaka is infertile from the failure of ovarian maturation, in which folliculogenesis was halted at the small-follicle stage (Murozumi et al. 2014). The authors also showed by *in situ* hybridization that the expression of *fshr* was detected in the layer of small and medium follicles but not the large follicles, whereas the expression of *lhr* was detected in all sizes of growing follicles (Ogiwara et al. 2013). Furthermore, rLH, PMSG or mammalian gonadotropins induced the ovulation in medaka in vitro (Iwamatsu 1978a, Ogiwara et al. 2013). The previous results and my present ones are spatiotemporally consistent; FSH is required for gonadal development, while LH is required for final maturation of the gonad.

The relationship between gonadotropin and gonadotropin receptors during ovarian development

It has been reported that female *lhb* KO zebrafish is infertile, even though the ovary develops normally. On the other hand, *fshb* KO zebrafish can eventually ovulate after delayed development of ovaries (Zhang et al. 2015b). It should be noted that the folliculogenesis is halted at pre-growth (PG) or PV stage in the *fshr* KO zebrafish ovary (Zhang et al. 2015a). Furthermore, Zhan and colleagues also report that *lhr* KO zebrafish is fertile. This apparent discrepancy may be explained by promiscuous relationship between ligands and receptors. In some teleosts, it has been reported that LH acts on FSH receptor promiscuously (Ge 2005, Kwok et al. 2005). Therefore, it is conceivable that LH acts through FSH receptor in the *lhr* KO zebrafish (Duan and Liu 2015). Meanwhile, there is a disagreement in the results in zebrafish and medaka; *fshb* KO female zebrafish was fertile (Zhang et al. 2015b), but *fshb* KO female medaka was infertile in present study. There is a report by *in situ* hybridization that the expression of both *lhr* and *fshr* was detected in both granulosa cells and theca cells in both early and late vitellogenic follicles in salmon (Andersson et al. 2009), unlike in medaka (Ogiwara et al. 2013). Although there is no such study in zebrafish, it is possible that such expressional deference in gonadotropin receptor genes or promiscuousness of them may lead to the species differences in the phenotypes of *gonadotropin* gene KO animals. It should be clarified by spatiotemporal analysis of *lhr* and *fshr* expression in the ovaries of zebrafish.

GnRH1 has an essential role in the regulation of reproduction via stimulation of LH secretion

The *gnrh1* KO female medaka showed infertility, which clearly demonstrates that GnRH1 has an essential role in the regulation of reproduction at least in female. The *gnrh1* KO female showed significantly low expression of *lhb*, which is considered to have caused disability of preovulatory LH surge and hence infertility. However, it should be noted that the expression level of *fshb* was normal. From the histological analysis, the late-vitellogenic (LV) and FG follicles were detected in the ovaries of both *gnrh1* and *lhb* KO female medaka. Furthermore, administration of rLh induced ovulation in the ovaries of both *gnrh1* and *lhb* KO female medaka. These results indicate that GnRH1 is essential for LH secretion, which causes ovulation, but not for FSH secretion in female medaka. Recent study in our laboratory demonstrated that the serum estrogen-dependent upregulation of *gnrhr* (GnRH receptor gene) expression in LH cells may be an important trigger for ovulation, which occurs when gonad is fully mature in medaka. (Arai et al., 2015). This is consistent with the previous report of our laboratory that the *lhb* expression is positively, while *fshb* expression is negatively, regulated by ovarian estrogen in medaka (Kanda et al. 2011). Taken together, my present results can be considered to suggest the following sequence of events occurring in the intact ovary; low serum concentration of estrogen upregulates FSH secretion via the negative feedback at early folliculogenesis stage, which induces gradual oocyte and follicle development, and then leads to the serum estrogen increase. The high serum estrogen may finally increase GnRH-mediated LH release via the positive feedback, and the ovulation occurs.

Regulation by GnRH is dispensable for FSH secretion

In teleosts, several reports have shown that administration of GnRH increase the serum concentration of both LH and FSH in the rainbow trout (Breton et al. 1998, Mananos et al. 1999, Weil et al. 1999) and the coho salmon (Dickey and Swanson 2000), and the expression level of both *lhb* and *fshb* in the male striped bass (Hassin et al. 1998) and the common carp (Kandel-Kfir et al. 2002). Furthermore, *in vitro* experiments have also shown that GnRH increase the release of LH and FSH in the goldfish (Khakoo et al. 1994), salmon (Ando et al. 2006), trout (Mananos et al. 1999), tilapia (Gur et al. 2002), and catfish (Bosma et al. 1997). On the other hand, it has been reported that administration of GnRH increase the expression level of *lhb* but not that of *fshb* in the European sea bass (Mateos et al. 2002). Given the different functions of LH and FSH as shown above, it seems probable that secretion of LH and FSH is regulated by different mechanisms. Furthermore, it has been reported that LH cells and FSH cells show different Ca^{2+} responses to GnRH peptide in medaka; LH cells show faster rise and fall of $[Ca^{2+}]_I$, compared to FSH cells (Karigo et al. 2014). Taken together with these previous reports, the results of Chapter 2 indicate that there is an essential and robust regulation of LH secretion by GnRH1 neurons, while regulation by GnRH is dispensable for FSH secretion. Yet, there may be other factors except GnRH that regulates FSH secretion in the hypothalamus (Yaron et al. 2003).

The role of gonadotropin in male teleosts

In medaka (present Chapter), it was shown that all KO male medaka (*fshb*$^{-/-}$, *lhb*$^{-/-}$, *gnrh1*$^{-/-}$) examined in the present study were fertile. In zebrafish, it has been reported that all the KO male fish examined, *fshb*$^{-/-}$, *lhb*$^{-/-}$, and double KO (*fshb*$^{-/-}$; *lhb*$^{-/-}$), were fertile, although spermatogenesis was delayed (Zhang et al. 2015b). My *gnrh1* KO

medaka is the first report in non-mammalian vertebrates, it is reasonable that male *gnrh1* KO medaka ashowed fertility, because GnRH is dispensable for FSH secretion in males.

Comparison of the functions of GnRH, LH, and FSH between mammals and teleosts

In mammals, both LH and FSH is required for normal development of the ovary and testis (Abel et al. 2000, Ma et al. 2004). Moreover, GnRH is required for the regulation of secretion of both LH and FSH (Cattanach et al. 1977). On the other hand, in teleosts, FSH but neither LH nor GnRH is required for the development of ovary unlike in mammals. Here, the tendency that FSH receptor is expressed in follicles during the early development of gonads, whereas LH receptor is mainly expressed during the later stages is widely observed in vertebrates including mammals and teleosts (Zhang et al. 1997, Donadeu and Ascoli 2005, Ogiwara et al. 2013). Thus, the function of FSH and LH receptors is considered to have been basically conserved, but the results of the present KO medaka suggested a strategic difference in the secretion of FSH and LH between mammals and teleosts. In mammals, it has been generally accepted that the pulsatile gonadotropin release caused by pulsatile GnRH release as the estrogen negative feedback regulation is necessary for gonadal development in both male and female (Knobil 1980). This pulsatile GnRH release is recently suggested to be regulated by kisspeptin neurons in mammals (Mayer et al. 2010, Wakabayashi et al. 2010). On the other hand, in teleosts, FSH is required for gonadal development, whereas LH or hypophysiotropic GnRH release is dispensable for ovarian development. These differences can be explained by the emergence of separate FSH and LH cells in the

teleost lineage, where FSH and LH release can be regulated completely independently of each other, because they are expressed in distinct cell types (Yaron et al. 2003, Kanda et al. 2011). It has been known that *lhb*, *fshb* and thyroid stimulating hormone β genes (*tshb*) branched from the common ancestral glycoprotein hormone β gene (Uchida et al. 2013). Presumably, the function of LH and FSH was differentiated during the evolutionary process, but the differential regulation of their release expressed in the same gonadotroph may have required more sophisticated mechanisms than the functional differentiation of LH and FSH. In conclusion, the differences in phenotypes of *gnrh1, fshb, and lhb* KO animals between teleosts and mammals may reflect the evolutionary different strategies; teleosts have distinct LH and FSH cells and their differential regulation mechanisms, while mammals have differential release modes of GnRH, pulsatile or surge, and their differential regulation mechanisms.

Figure legends

Figure 2-1

Genomic and deduced amino acid sequence of wild type (wt) and TALEN KO *gnrh1* gene. A, Alignment of genomic DNA sequence of *gnrh1* open reading frame (ORF) region of wt and a *gnrh1* KO line. Underlines indicate left and right TALEN targets. B, Alignment of deduced amino acid sequence of GnRH1 precursor taken from genomic data of wt and *gnrh1* KO line. Underline indicates a region in which amino acids were mutated. Shaded region indicates GnRH peptide sequence.

Figure 2-2

Genomic and deduced amino acid sequence of wt and TALEN KO *lhb* gene. A, Alignment of genomic DNA sequence of *lhb* ORF region of wt and a *lhb* KO line. Underlines indicate left and right TALEN targets. B, Alignment of deduced amino acid sequence of LHb from genomic data of wt and lhb KO line. Underline indicates a region in which amino acids were mutated.

Figure 2-3

Genomic and deduced amino acid sequence of wt and TALEN KO *fshb* gene. A, Alignment of genomic DNA sequence of *fshb* ORF region of wt and a *lhb* KO line. B, Alignment of deduced amino acid sequence of FSHb from genomic data of wt and *fshb* KO line. Underline indicates a region in which amino acids mutated.

Figure 2-4

Immunohistochemistry indicates that *gnrh1* KO, *lhb* KO, or *fshb* KO lines of medaka do not produce respective mature proteins. A, B. immunohistochemistry for GnRH1 in the pituitary of *gnrh1*$^{-/-}$ (A) and wt (B) medaka. Arrowheads indicate GnRH1 fibers labeled by rabbit anti-mdGnRH1 antibody. C,D. immunohistochemistry for LHb in the pituitary of *lhb*$^{-/-}$ (C) and wt (D) medaka. E,F. immunohistochemistry for FSH in the pituitary of *fshb*$^{-/-}$ (E) and wt (F) medaka. Scale bars, 50μm.

Figure 2-5

Hematoxylin and eosin-stained ovaries (90 dph) and testes (90 dph) of *gnrh1*, *lhb*, *or fshb* KO medaka. A-J, ovaries at 90 dph (1) and testes of 90 dph (2) of *gnrh1*$^{-/-}$ (A), *gnrh1*$^{+/-}$(B), *gnrh1*$^{+/+}$(C), *lhb*$^{-/-}$(D), *lhb*$^{+/-}$(E), *lhb*$^{+/+}$(F), *fshb*$^{-/-}$(G), *fshb*$^{+/-}$(H), and *fshb*$^{+/+}$(J). PG; primary growth stage, PV; previtellogenic stage, LV; late vitellogenic stage; FG; full-growth stage, sg; spermatogonia, sc; spermatocyte, and sz; spermatozoa. Scale bars of ovary images indicate 500 μm. Scale bars of testis images indicate 50 μm.

Figure 2-6

Expression level of gonadotropin genes in *gnrh1* KO medaka. A, B, expression level of *lhb* mRNA in the pituitary of *gnrh1*$^{+/+}$, *gnrh1*$^{+/-}$, and *gnrh1*$^{-/-}$ in male (A. and female (B). C, D, Expression level of *fshb* mRNA in the pituitary of *gnrh1*$^{+/+}$, *gnrh1*$^{+/-}$, and *gnrh1*$^{-/-}$ in male (C) and female (D). E, F, Effects of OVX and estrogen treatment on the expression of *lhb* (E) *fshb* (F) mRNA in the pituitary of *gnrh1*$^{+/+}$, *gnrh1*$^{+/-}$, and *gnrh1*$^{-/-}$. *$p<0.05$

Figure 2-7

Recombinant LH protein (rLH) induces ovulation in *gnrh1*$^{-/-}$ *and lhb*$^{-/-}$ medaka. A,B. Histological section of *gnrh1*$^{-/-}$ ovaries IP injected rLH (A), or saline (B). C. Number of ovulated eggs in gnrh1-/- medaka with or without PMSG injection. D,E. Histological section of *lhb*$^{-/-}$ ovaries IP injected rLH (D), or saline (E). F. Number of ovulated eggs in *lhb*$^{-/-}$ medaka with or without PMSG injection. Arrowheads indicate ovulated egg. Scale bars, 500 μm.

Primer name	purpose	sequence
gnrh1TALcheckSE	gnrh1 genome PCR, sequence primer	5’-TGTGTTCTGCAGGAATGGTGGTA-3’
gnrh1TALcheckAS	gnrh1 genome PCR	5’- GATGCTTACATTTTCCAGTGTGTTTGG -3’
gnrh1TAL17WTSE	gnrh1 genome PCR check	5’- GGGCTGCTGCCAGCACT -3’
rps13 SE	ribosomal protein subunit 13 (rps13) qRT PCR	5’-GTGTTCCCACTTGGCTCAAGC-3’
rps13 AS	rps13 qRT PCR	5’-CACCAATTTGAGAGGGAGTGAGAC-3’
qPCR LHb Fw new	lhb qRT PCR	5’-AGGGTATGTGACTGACGGATCCAC-3’
qPCR LHb Rv new	lhb qRT PCR	5’-TGCCTTACCAAGGACCCCTTGATG-3’
qPCR FSHb Fw new	fshb qRT PCR	5’-TGGAGATCTACAGGCGTCGGTAC-3’
qPCR FSHb Fw new	fshb qRT PCR	5’-AGCTCTCCACAGGGATGCTG-3’

Table 2-1

The list of primers.

Figure 2-1

A. ORF sequence of *gnrh1*

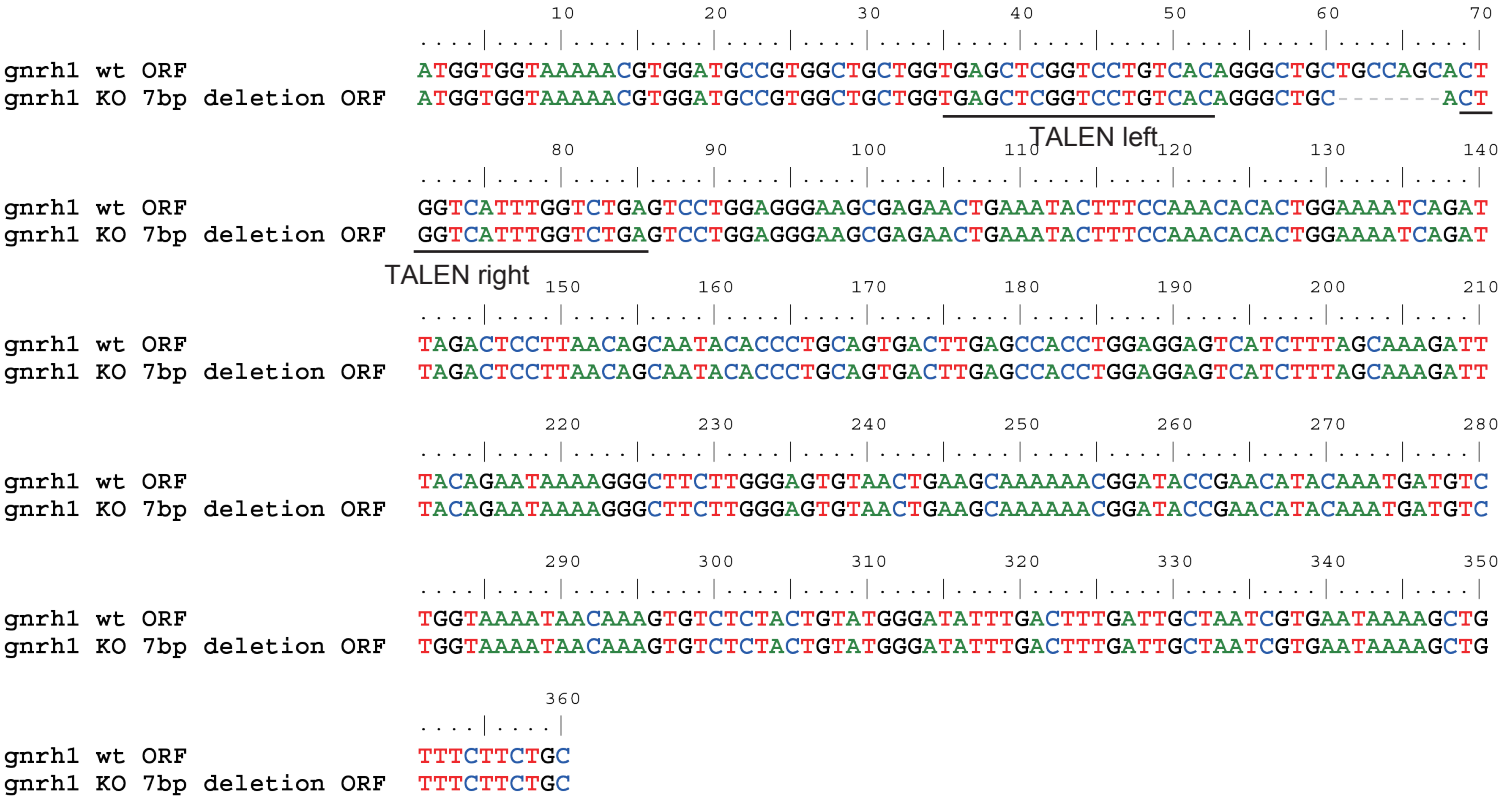

B. deduced peptide sequence of GnRH1

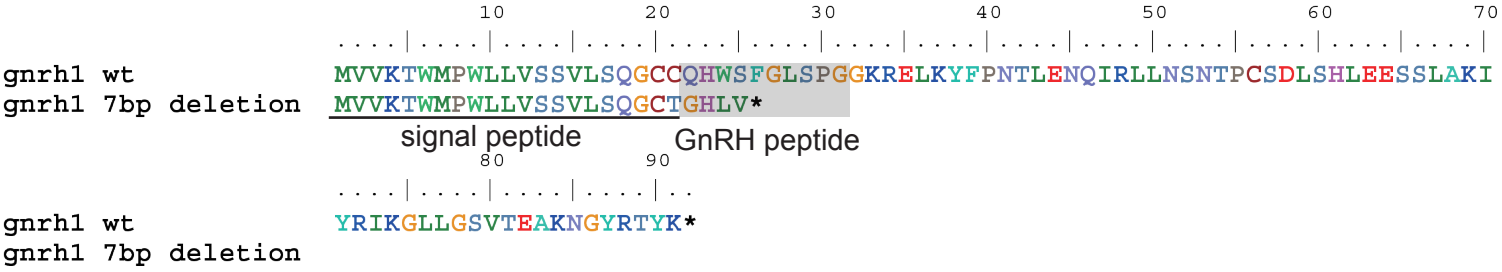

Figure 2-2

A. ORF sequence of *lhb*

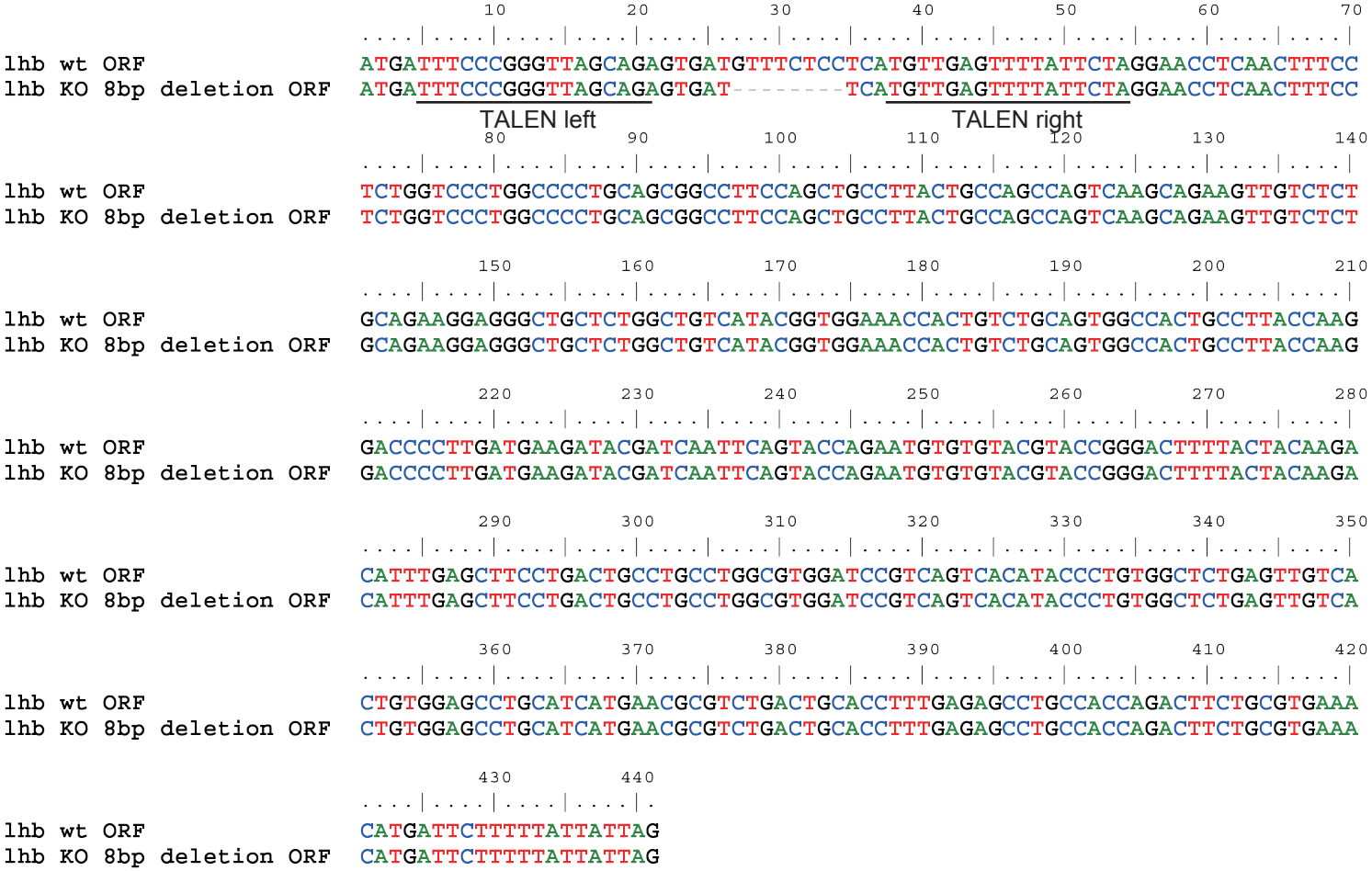

B. deduced peptide sequence of LHb

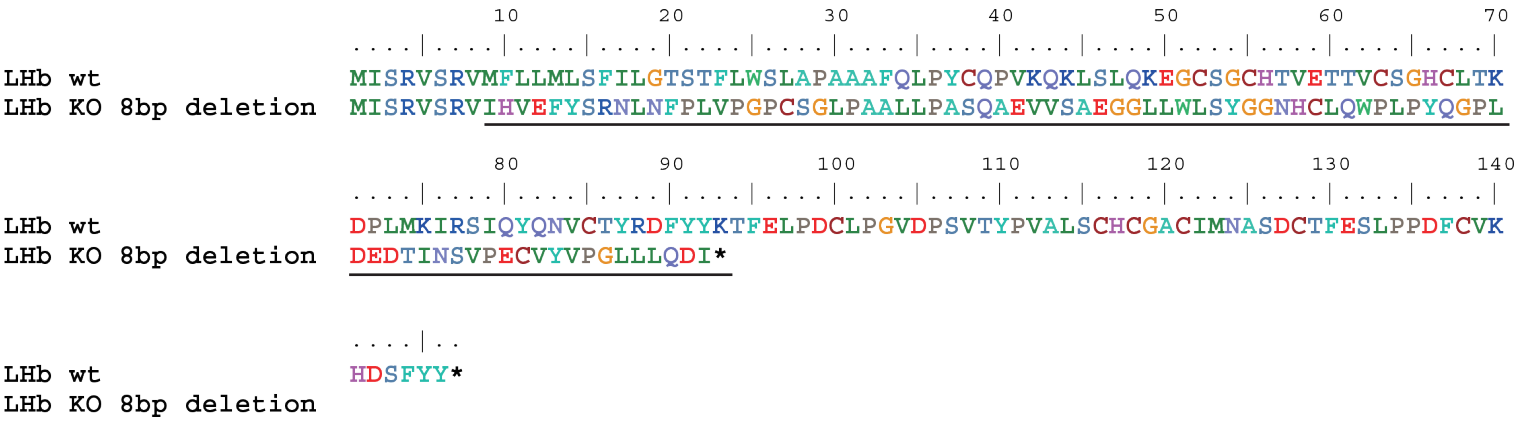

Figure 2-3

A. ORF sequence of *fshb*

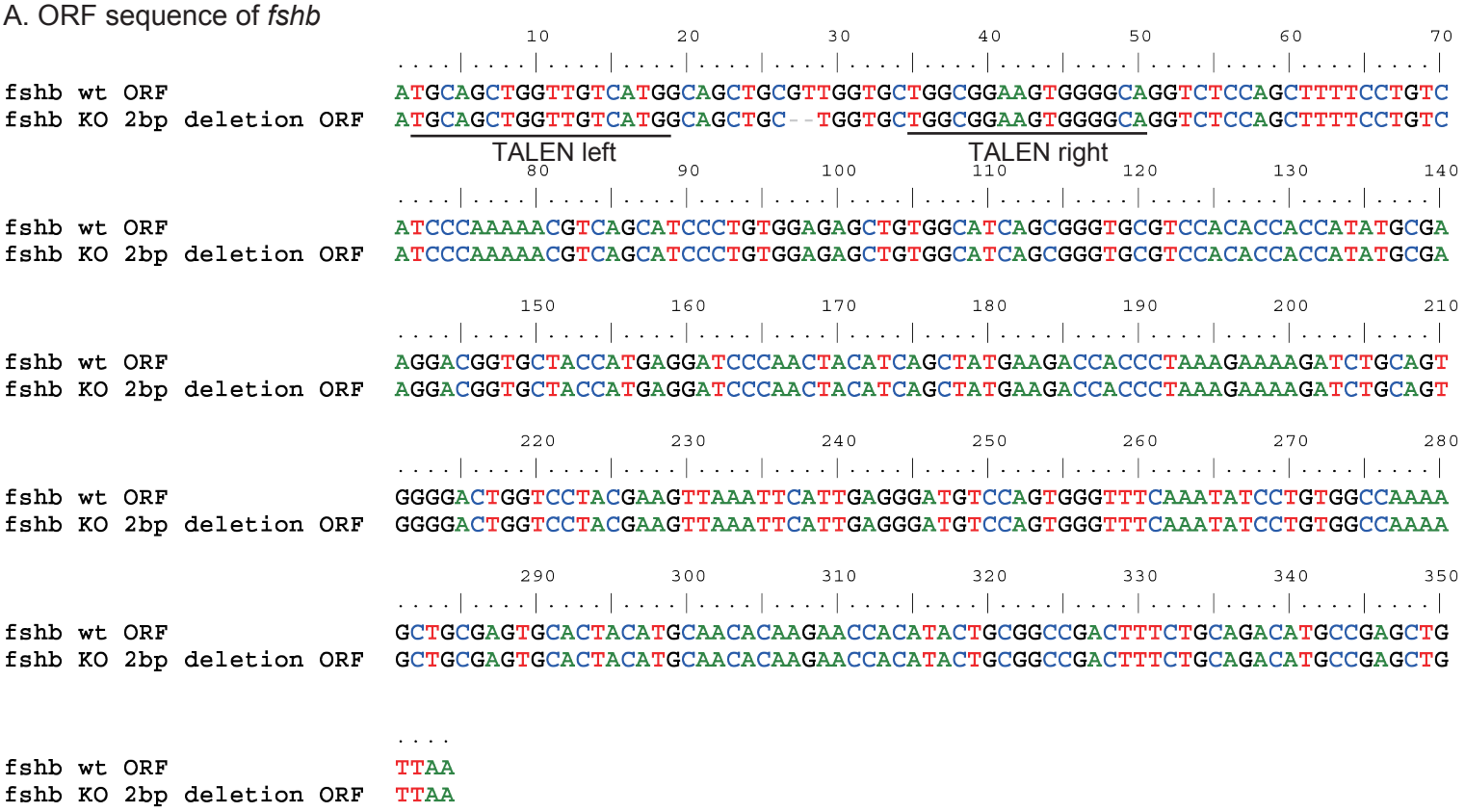

B. deduced peptide sequence of FSHb

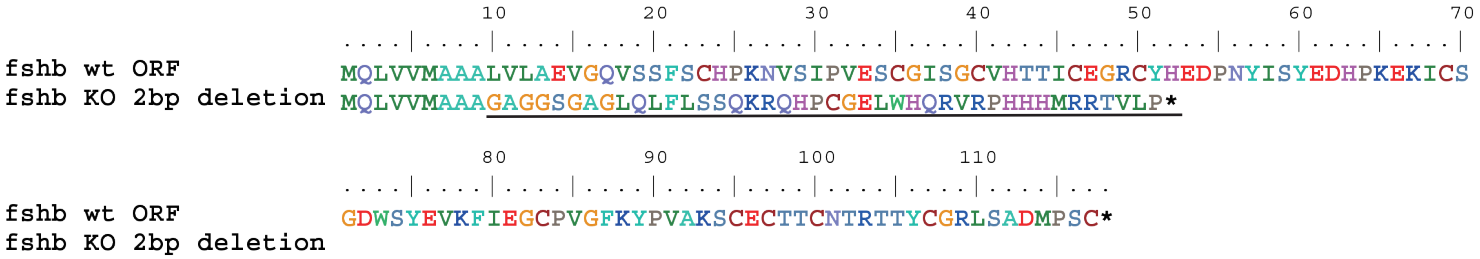

Figure 2-4

Immunohistochemistry for GnRH1

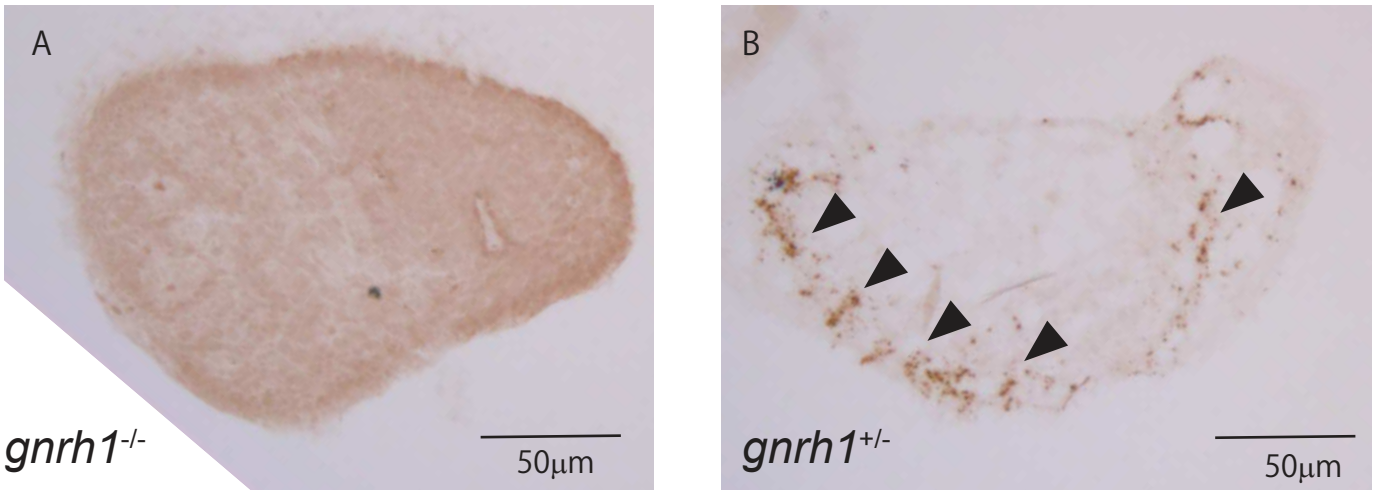

Immunohistochemistry for LH

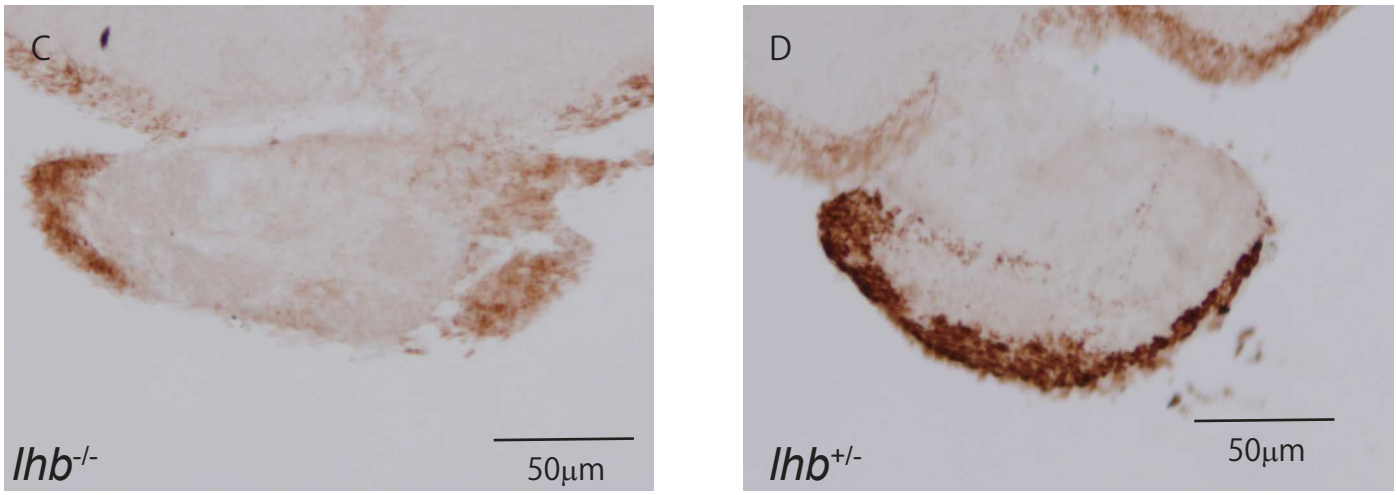

Immunohistochemistry for FSH

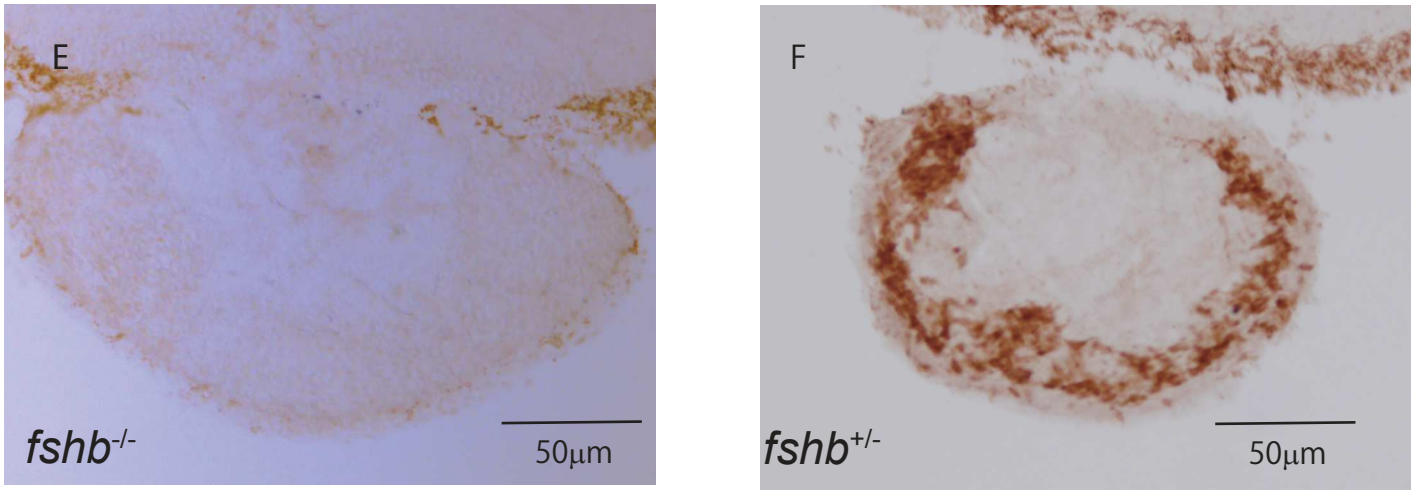

Figure 2-5

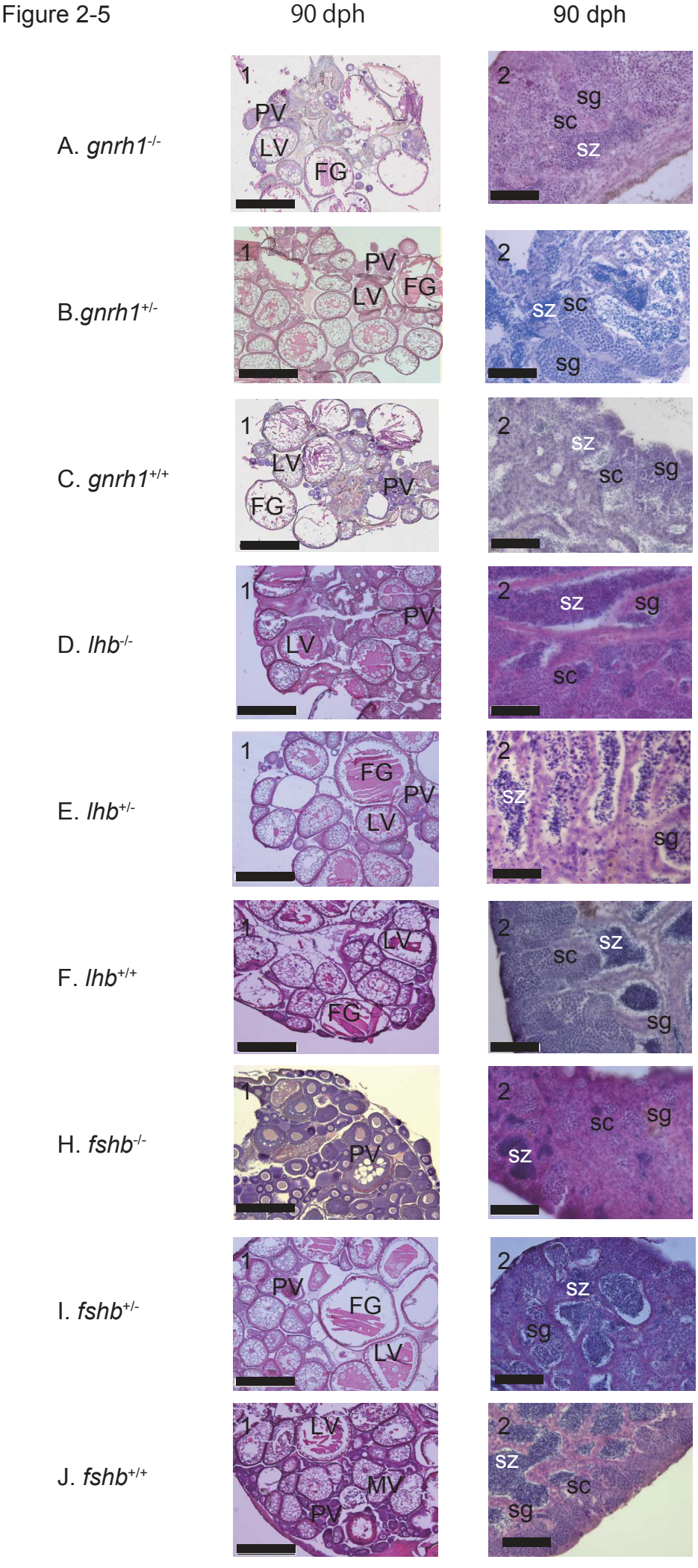
90 dph
90 dph
A. gnrh1-/-
1
PV
LV
FG
2
sg
sc
sz
B.gnrh1+/-
1
PV
LV
FG
2
sz
sc
sg
C. gnrh1+/+
1
LV
PV
FG
2
sz
sc
sg
D. lhb-/-
1
PV
LV
2
sz
sg
sc
E. lhb+/-
1
FG
PV
LV
2
sz
sg
F. lhb+/+
1
LV
FG
2
sc
sz
sg
H. fshb-/-
1
PV
2
sc
sg
sz
I. fshb+/-
1
PV
FG
LV
2
sz
sg
J. fshb+/+
1
LV
MV
PV
2
sz
sc
sg

Figure 2-6

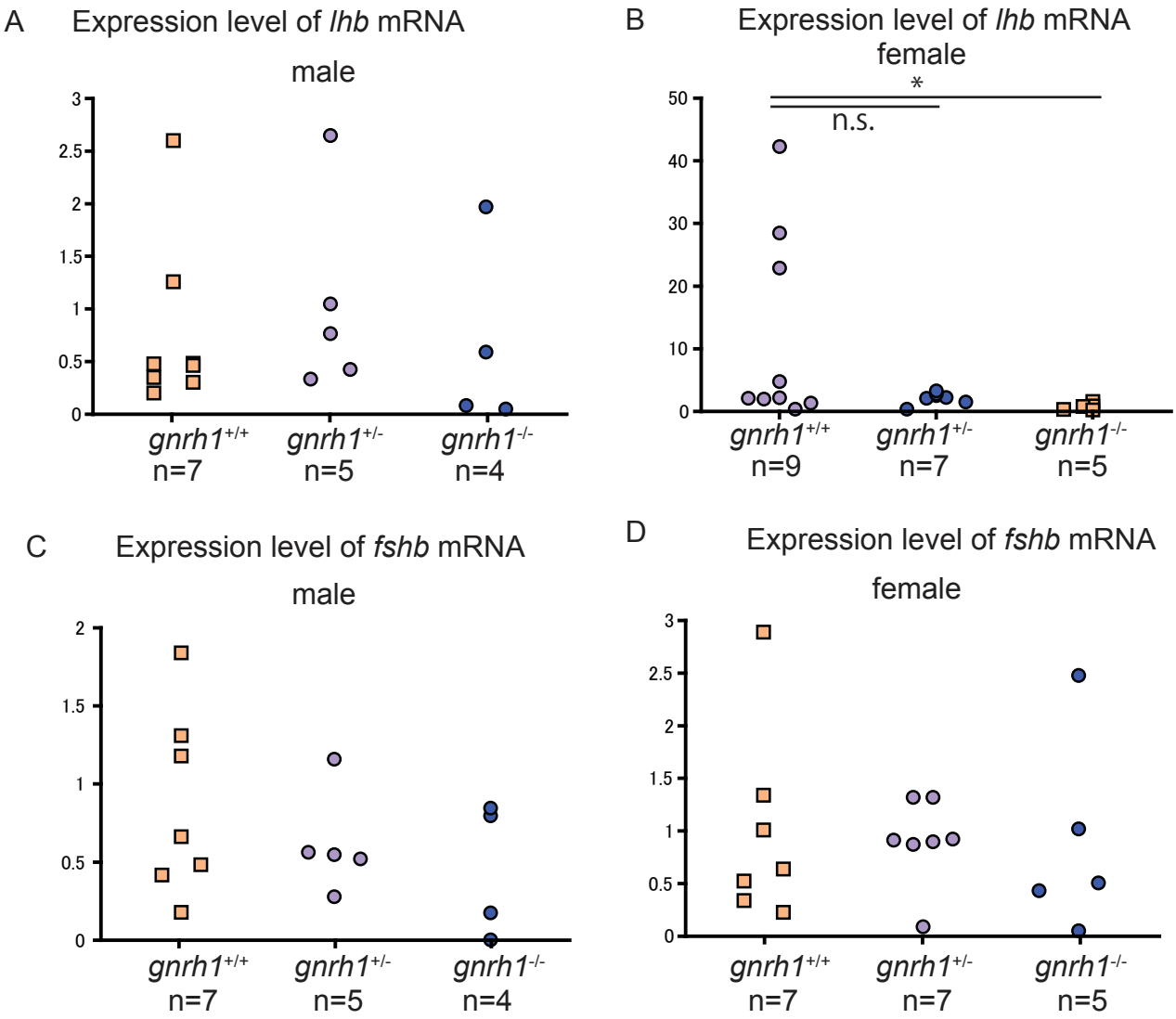
A
Expression level of lhb mRNA
male
3
2.5
2
1.5
1
0.5
0
gnrh1+/+ n=7
gnrh1+/- n=5
gnrh1-/- n=4
B
Expression level of lhb mRNA
female
*
n.s.
50
40
30
20
10
0
gnrh1+/+ n=9
gnrh1+/- n=7
gnrh1-/- n=5
C
Expression level of fshb mRNA
male
2
1.5
1
0.5
0
gnrh1+/+ n=7
gnrh1+/- n=5
gnrh1-/- n=4
D
Expression level of fshb mRNA
female
3
2.5
2
1.5
1
0.5
0
gnrh1+/+ n=7
gnrh1+/- n=7
gnrh1-/- n=5

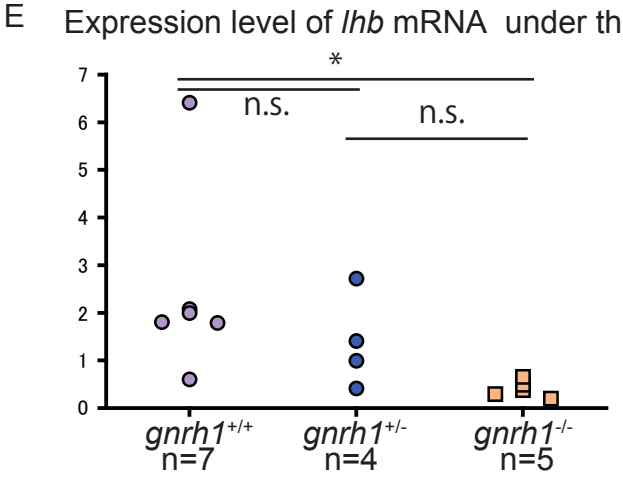
E
Expression level of lhb mRNA under the OVX and E2 administration
*
n.s.
n.s.
7
6
5
4
3
2
1
0
gnrh1+/+ n=7
gnrh1+/- n=4
gnrh1-/- n=5

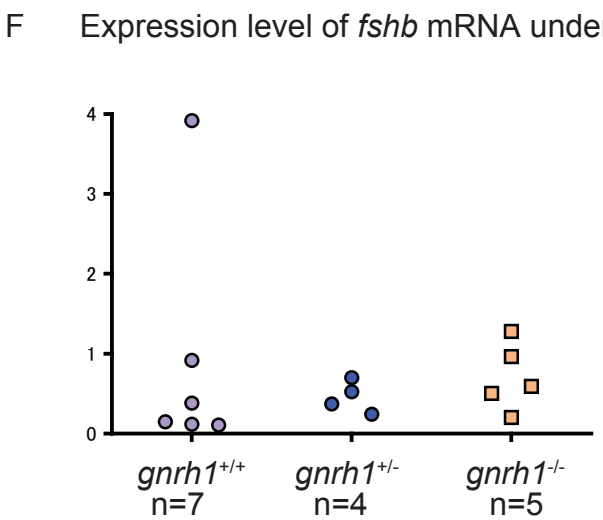
F
Expression level of fshb mRNA under the OVX and E2 administration
4
3
2
1
0
gnrh1+/+ n=7
gnrh1+/- n=4
gnrh1-/- n=5

Figure 2-7

A

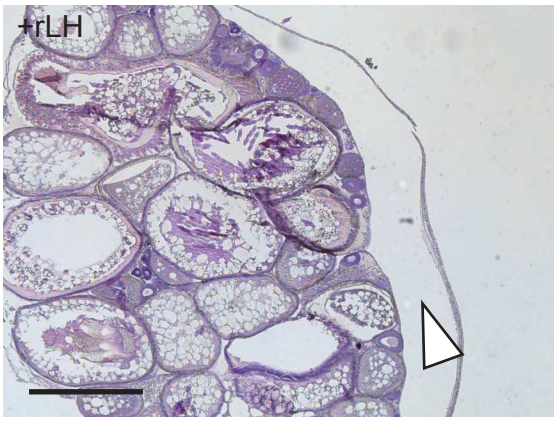

B

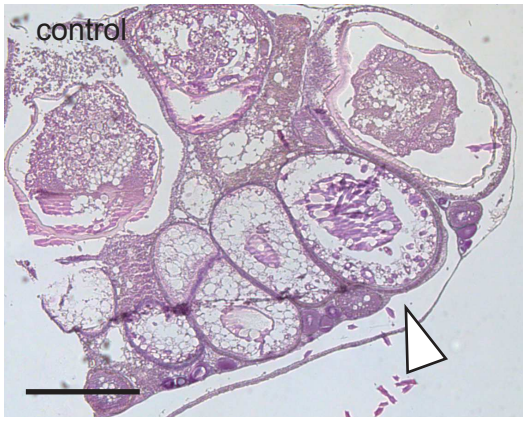

gnrh1$^{-/-}$

C The number of spawned eggs

After injection	day1	day2	day3
20 IU PMSG	0	9	6
PBS	0	0	0

D

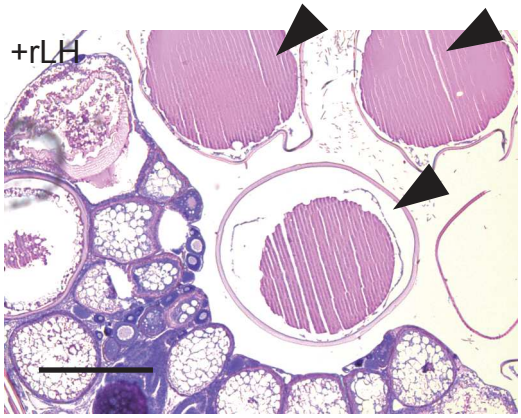

E

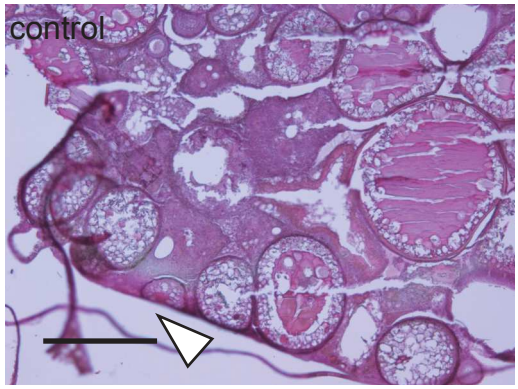

Ihb$^{-/-}$

F The number of spawned eggs

After injection	day1	day2	day3
20 IU PMSG	0	21	2
20 IU PMSG	0	15	12
20 IU PMSG	0	9	4
20 IU PMSG	0	11	6
PBS	0	0	0

Chapter 3

Functional analysis of kisspeptin signaling by using knockout medaka of kisspeptin and kisspeptin receptor genes

Introduction

In Chapter 2, I demonstrated that folliculogenesis and ovulation is elaborately regulated by the essential players that are common to vertebrates in general: hypothalamic gonadotropin-releasing hormone (GnRH) neurons, pituitary luteinizing hormone (LH), and follicle stimulating hormone (FSH), with some difference in the regulation mechanisms between mammals and teleosts. However, it remains unclear how the GnRH1 neurons, which is generally considered to be the final common pathway in the HPG axis regulation of vertebrates including teleosts, receives inputs from gonadal steroids and alters its regulation on gonadotrophs (feedback regulation by estrogen). It has been suggested that estrogen receptor α (*erα*), which is essential for the estrogen feedback (Couse et al. 2003, Glidewell-Kenney et al. 2007), is not expressed in GnRH neurons (Herbison and Pape 2001), and the neurons expressing *erα* and directly regulates the GnRH1 neurons have been called the "missing link" for the estrogen feedback. Meanwhile, a neuropeptide kisspeptin has been found to fulfill the criteria for the missing link, based on the following body of evidence. Kisspeptin, coded by *Kiss1* gene, is a ligand for a G-protein coupled receptor (GPR54) that is coded by a causative gene for hypogonadism in mammals (Kauffman et al. 2007). It has been shown that synthetic kisspeptin peptide increases the serum concentration of luteinizing hormone (LH) *in vivo* in several mammals (Smith 2013) and directly depolarizes GnRH neurons *in vitro* (Han et al. 2005, Zhang et al. 2008) by activating *Gpr54* expressed by them (Irwig et al. 2004). Furthermore, the expression of *Kiss1* mRNA in KISS1 neurons changes according to the serum estrogen level (Smith et al. 2005). In fact, it has been demonstrated that knockout (KO) of ERα gene specifically in KISS1 neurons suppress

the increase in LH after ovariectomy (OVX), which normally occurs in wild type mice (Mayer et al. 2010). Furthermore, estrous cyclicity was disturbed by acute ablation of *Kiss1*-expressing cells (Mayer and Boehm 2011). Thus, it has been widely accepted that kisspeptin neurons play a key role in the hypothalamic-pituitary-gonadal (HPG) axis by receiving estrogen feedback signal and modulating GnRH neuron firing in mammals (Ohkura et al. 2009, Smith 2013).

There are two homologous genes coding kisspeptin, *kiss1* and *kiss2*, one or both of which is conserved in vertebrates except the avian species (Lee et al. 2009b, Akazome et al. 2010). It is unclear whether the kisspeptin signaling that is dependent on the HPG axis regulation has been lost specifically in avian species or has appeared in mammals. This is a critical question for the elucidation of regulatory mechanisms of reproduction that may be common to various vertebrate species.

In teleosts, it has been reported that the expression of *kiss1* or *kiss2* in specific neuronal population is changed by the serum estrogen (Kanda et al. 2008, Servili et al. 2011, Kanda et al. 2012). Moreover, Kiss1 or Kiss2 neurons in the hypothalamus project to the preoptic area (POA), where hypophysiotropic GnRH neurons are localized in medaka and zebrafish brain (Servili et al. 2011, Hasebe et al. 2014). However, accumulating evidence suggests that kisspeptin does not regulate GnRH neurons in teleosts. First, intraperitoneal (i.p.) injection of kisspeptin did not induce serum LH increase in goldfish (Karigo et al., 2012b), although there are some reports in other teleosts that serum LH or *lhb* mRNA increased after kisspeptin i.p. injection (Felip et al. 2009, Chang et al. 2012, Ohga et al. 2014). Second, double *in situ* hybridization studies failed to show co-localization of *gnrh1* and *gpr54* mRNA in a wide variety of teleosts,

e.g. medaka, cichlid, and seabass (Grone et al. 2010, Escobar et al. 2013, Kanda et al. 2013). Thus, it is still controversial whether kisspeptin is involved in the reproductive regulation in vertebrates other than mammals.

In Chapter 3, I generated and analyzed KO medaka for kisspeptin genes, *kiss1* and *kiss2*, and kisspeptin receptor genes, *gpr54-1* and *gpr54-2*[1], to examine functional significance of kisspeptin signaling in the regulation of reproduction.

Materials and Methods

Animals

Male and female wild-type (wt) d-rR medaka (*Oryzias latipes*) and knockout medaka lines, established as described below, were maintained under a 14-h light and 10-h dark photoperiod (lights-on at 08:00 h and lights-off at 22:00 h) at a water temperature of 27°C. Female subjects were sexually mature (older than 50 days post hatching (dph). All experiments were conducted in accordance with the protocols approved by the Animal Care and Use Committee of the University of Tokyo (permission number: 15–3)

Establishment of medaka knockout lines

I generated *kiss1* gene KO medaka using TALEN (Sander et al. 2011), while I generated *kiss2*, *gpr54-1*, *gpr54-2* KO medaka using CRISPR/Cas9 (Hwang et al. 2013), because some of the TALEN pairs did not work for these genes. The specific

[1] It has been reported in various vertebrate species that there are two paralogous genes for kisspeptin (*kiss1* and *kiss2*) and its receptor (*gpr54-1* and *gpr54-2*). Medaka is known to have all of these paralogous genes ((Akazome et al. 2010)

TALEN and CRISPR/Cas9 target sites were identified using an online tool (ZiFiT: supplied by ZINC FINGER CONSORTIUM; http://www.zincfingers.org/default2.htm). Exon 3 of *kiss1* gene and exon 2 of *kiss2* gene, which codes the core sequence of kisspeptin, were selected for target sites (Fig. 3-1A, 2A). Exon 4 of *gpr54-1* gene, which codes the transmembrane region, was selected for the CRISPR target site (Fig. 3-3A). Approximately 50bp downstream of the first methionine of *gpr54-2* was selected for the CRISPR target site (Fig. 3-4A). Gene-specific TALEN constructs were assembled using Joung Lab REAL Assembly TALEN kit (Addgene, Cambridge MA, USA) as described (Sander et al. 2011). TALEN coding region was transferred to pCold II (Takara), which contains the cold shock promoter, His- tag, and polyadenylation signal. NiCo21 (DE3) E. coli cells (NEB, Ipswich, MA, USA) were transfected by TALEN expression plasmid. TALEN proteins were purified by His-bind column (BIO-RAD, CA, USA) and by Heparin chromatography (QIAGEN, Hilden, Germany). For generation of gRNA, Oligo DNA (2μM) for gRNA listed in Table 3-1 were annealed and ligated with gRNA expression vector (DR274; Addgene) digested by BsaI (NEB) according to Hwang et al., 2013. After cloning and digestion by DraI (NEB), gRNA was transcribed by T7 polymerase (Roche). The Cas9 mRNA was transcribed using PmeI-digested Cas9 expression vector (MLM 3613; Addgene) by mMessage mMachine T7 ULTRA kit (Life technologies). EGFP mRNA was transcribed using SP6 promoter in linearized pCS2+EGFP vector. TALEN solution containing left and right TALEN protein, or CRISPR/Cas9 solution containing gRNA (12.5 ng/μL) and Cas9 mRNA (300 ng/μL), with EGFP mRNA (1-5ng/μL; for validation of successful microinjection) and 0.02 % phenol red in 1 x PBS were injected into the cytoplasm of fertilized one-cell

stage medaka eggs with intact chorion. Genomic DNA of F1 fish was extracted from the caudal fin using Mag Extractor -Genome- (TOYOBO CO, Tokyo, Japan) or prepGem-tissue (ZyGEM, Hamilton, New Zealand) according to the respective manufacturer's instructions. Amplicon that include the target region of each gene was generated by PCR using LightCycler 480 SYBER Green I Master (Roche), Thunderbird SYBR qPCR Mix (TOYOBO CO) and corresponding primers (Table 3-3). Candidate fish were chosen by comparing the peaks of the melting curves between wild type and F1 fish. After PCR reaction, primers were digested by Exonuclease I (Takara, Shiga, Japan), and dNTPs were dephosphorylated by Shrimp Alkaline Phosphatase (Takara). Amplicons of the candidate fish were sequenced. F1 fish that had mutation were intercrossed. Homozygous KO F2 fish were selected by genome sequence as described above.

Quantitative real-time PCR

Three-month-old medaka were deeply anesthetized with 0.02% MS-222, and the pituitaries were collected for real-time PCR analysis at 10:00 h. Total RNA was extracted from the pituitaries using the NucleoSpin RNA XS (Takara, Shiga, Japan) or the brain using the NucleoSpin II (Takara) according to the manufacture's protocol. Genomic DNA was removed by deoxyribonuclease I (Ambion, Applied Biosystems, Foster City, CA) treatment on a column membrane. Total RNA was reverse transcribed with High Capacity PrimeScript Reverse Transcriptase (Takara) according to the manufacturer's instructions. For real-time PCR, the cDNA was amplified using Thunderbird SYBR qPCR Mix (TOYOBO CO) or KAPA SYBR FAST qPCR Kit (Nippon Genetics Co, LTD, Tokyo, Japan) with the LightCycler 480 II system (Roche, Molecular Biochemicals GmbH, Mannheim, Germany). The temperature profile of the

reaction was 95 °C for 5 min, 45 cycles of denaturation at 95 °C for 10 s, annealing at 60 °C for 10 s, and extension at 72 °C for 10 s. The PCR product was verified using the melting curve analysis. The data was normalized to a housekeeping gene, ribosomal protein s13 (rps13). The primer pairs used in the real-time PCR are listed in Table 3-3.

Hematoxylin and eosin (HE) staining

The ovaries and testes were fixed with Bouin's fixative at 4 °C overnight. After fixation, each tissue sample was routinely processed and embedded in paraffin, and sections of 8 μm thickness were stained with hematoxylin and eosin (HE). Photographs were taken with a digital camera (DFC310FX; Leica Microsystems, Wetzlar, Germany) attached to an upright microscope (DM5000B; Leica Microsystems).

Observation of courtship behavior

Circle dance, which is a specific and remarkable courtship behavior of medaka (Ono and Uematsu 1957), of each pair was observed for 10 min after start of mating, which was initiated by removing a transparent separator between male and female that had been set from the previous night. Behavioral observation was done between 10:00 to 11:00 AM. The fertilization rate was calculated from the total number of fertilized eggs divided by that of spawned eggs.

Open field test and diving test

Two types of white acrylic resin tanks were used as test tanks in open-field and diving test experiments: open field test tank (size of the inner side, 15 cm square, water depth, 3cm, center region was defined as 7.5 cm square), and diving test tank (size of the inner side, 15 cm x 3 cm rectangle, water depth 15 cm, surface region was defined as 6 cm top of the tank). The temperature of the tank water was at 23-25 ◦C. Medaka was softly

put into the tank by using net. Animal behavior was recorded from above (open field test) or from the side (diving test) using web camera and analyzed using software for analysis of locus of movement (QtFish6; provided by Dr. Hosokawa (Kyoto University)).

Statistical analysis

All values are shown as mean ± SEM. Expression levels measured by real-time PCR were analyzed using Mann–Whitney U test.

Results

Generation of KO medaka lines

After incross and/or outcross with wild type, sequence analyses of homozygous or heterozygous KO individuals were performed in the targeted genes of *kiss1*$^{-/-}$, *kiss2*$^{-/-}$, *gpr54-1*$^{-/-}$, and *gpr54-2*$^{-/-}$ medaka (Fig. 3-1A, 2A, 3A, 4A). The sequence of each mRNA transcribed from respective gene was estimated by reading PCR product of cDNA reverse-transcribed from mRNA extracted from fish brain of each KO line. These changes in mRNA sequence coincided with the corresponding genomic data (data not shown). Deduced amino acid sequences from these genomic sequences are shown in Fig. 3-1B, 2B, 3B and 4B. The *kiss1*$^{-/-}$ and *kiss2*$^{-/-}$ medaka lacked kisspeptin core-peptide sequence. The *gpr54-1*$^{-/-}$ and *gpr54-2*$^{-/-}$ medaka produced peptides that are different from Gpr54-1 or Gpr54-2 and lacked typical 7-transmembrain structure, respectively. These peptides are considered to be nonfunctional, according to the previous reports (Lee et al. 2009a). I used the fish that showed 11 base pair (bp) deletion/2 bp deletion/10 bp deletion and 2 bp replacement/1 bp insertion in

kiss1/kiss2/*gpr54-1/gpr54-2* genes as representative knockout lines for *kiss1*/*kiss2/gpr54-1*/*gpr54-2*, respectively.

Kisspeptin signaling is not necessary for the HPG axis regulation

To reveal the role of kisspeptin in the HPG axis regulation of teleosts, I analyzed the expression levels of gonadotropin genes, histology of gonad, courtship behavior, and fertility of each KO line medaka.

The expression level of gonadotropin genes

There was no significant difference in the expression level of *lhb* nor *fshb* among all generated KO lines of medaka (Fig. 3-5A-F).

Morphological analysis of gonads

The histology of HE-stained gonad of each KO line of fish and of wt fish is shown in Fig. 3-6. The ovary of each KO fish normally developed, with no difference from that of wt (Fig. 3-6A1-F1). Full-growth follicle (FG) and late-vitellogenic follicle (LV) were observed in the ovary of each KO fish. Also, the testis of each KO line of fish normally developed, compared with that of wt (Fig. 3-6A2-F2). Spermatozoa (SZ) were observed in the testis of each KO fish.

Fertility

To examine the fertility of each KO line of fish, I observed the courtship behavior, spawning, and the ratio of fertilized eggs (Table 3-2). Each KO male medaka showed circle dance, a characteristic courtship behavior of medaka, toward its partner female (Table 3-2). Moreover, spawning was observed in each KO medaka pair.

All of these results indicate that Kisspeptin signaling is not necessary for the HPG axis regulation at least in medaka.

Exploration of functions of kisspeptin neuronal system

In teleosts, the kiss1 neurons are roughly divided two anatomically distinct populations, the one in habenula and the other in hypothalamus/POA. kiss1 is reported to be expressed in the habenular neurons that project to the interpeduncular nucleus (IPN) (Ogawa et al., 2012, Hasebe et al., 2014), which is suggested to be involved in the emotional behavior (Matsumoto and Hikosaka, 2007). The axon projections of Kiss1 neurons could be detected in the hypothalamus, which is known to be involved in homeostatic regulations and the pituitary functions (Ogawa et al. 2012, Hasebe et al. 2014).

Observation of behavior

To explore functions of kisspeptin neuronal system in emotional behavior, I observed behavior of KO medaka by open field test and diving test, and examined the change of serotonin-related genes, *pet1* and solute carrier family 6, member 4 (*slc6a4*), which are reported to be changed by administration of Kiss1 (Ogawa et al. 2014). However there is no significant difference in behavior (Figure 3-7,8) and expression level of serotonin-related genes (Figure 3-9).

Exploration of changes in gene expression in KO medaka

I examined changes in gene expressions in the brain of KO medaka of genes for kisspeptin and their receptors by using real-time PCR. Among the genes in the pituitary and the brain related to homeostasis, I found that the expression level of thyroid stimulating hormone b2 (*tshb2*; Kitano et al. 2010) was increased in male *kiss2*/*gpr54-2* KO medaka, compared with the wild type medaka (Figure 3-10).

Discussion

In Chapter 3, I used genome editing techniques, TALEN and CRISPR, and generated KO medaka lines for kisspeptin-related genes. I demonstrated that *kiss1*/*kiss2*/*gpr54-1*/*gpr54-2* KO medaka show normal expression level of *lhb*/*fshb*, gonadal development, and fertility. These results clearly show that the HPG axis regulation in teleost is not dependent on kisspeptin signaling, unlike that in mammals.

The HPG axis regulation in teleosts is not dependent on kisspeptin signaling

Compared to the conventional knockdown methods, the two genome editing techniques mentioned above are reported to be drastically improved in specificity and reproducibility (Kok et al. 2015). Especially for the analysis of adult phenotypes, such as reproduction, it is virtually impossible to apply morpholino oligo, because it is reported to be digested within ~10 days after injection. Thus, at present, TALEN/CRISPR should be the best method of choice for the loss-of-function analysis of kisspeptin signaling. There is only one knockdown study of medaka *kiss1* and *kiss2* during the developmental stages (Hodne et al. 2013). The present knockout medaka study did not replicate the lethal phenotype observed in the knockdown study. Although we cannot rule out a possibility that functional compensation occurred in TALEN/CRISPR during development, it is more likely, according to the previous comparison of these methods (Kanda et al. 2008, Mitani et al. 2010, Kok et al. 2015), that small fragment(s) of artificial nucleotides produced off-target effects. The possibility of compensation in *kiss1* or *kiss2* KO medaka by their respective paralogue is excluded by the results that *kiss1* and *kiss2* double KO medaka also showed normal

fertility. The expression level of *lhb* in each KO medaka showed no significant difference from that in wt, unlike in mammals.

My present conclusion that the HPG axis regulation in teleost is not dependent on the kisspeptin signaling is also supported by results of the morphological studies that the expression of *gpr54-1* and *gpr54-2* are not detected in hypophysiotropic GnRH neurons in teleosts (Grone et al. 2010, Escobar et al. 2013, Kanda et al. 2013), and those of i.p. Kisspeptin administration studies that it did not increase the serum concentration of LH in goldfish (Karigo et al., 2012b). Furthermore, in zebrafish, which is phylogenetically distinct from medaka (diverged ~245 million years ago, (Broughton et al. 2013)), knockout animals for *kiss1*/*kiss2*/*gpr54-1*/*gpr54-2* also showed normal reproduction (Tang et al. 2015). Given these lines of evidence, it may be further suggested that kisspeptin have minimum influence, if any, on teleost reproduction in general.

The HPG axis regulation by kisspeptin signaling may be specific to mammals

In mammals, kisspeptin neurons play an essential role in the HPG axis regulation by receiving estrogen feedback signal and modulating GnRH release (Ohkura et al. 2009, Smith 2013). On the other hand, my present results and previous ones in teleosts, together with the fact that avian species completely lack kisspeptin-related genes, strongly suggest that the HPG axis regulation by kisspeptin signaling may not be common to vertebrates in general, but may have emerged rather specifically in mammalian lineage. Interestingly, in teleosts, which can reproduce normally without kisspeptin, kisspeptin expression of the kisspeptin neuron drastically changes in accordance with serum estrogen (Kanda et al. 2008, Servili et al. 2011), and their axons project to the brain region near the GnRH neurons (Servili et al. 2011, Hasebe et al.

2014). Thus, the only large difference in the kisspeptin systems in teleosts and mammals is gpr54 expression in GnRH neurons. In other words, the kisspeptin neurons in non-mammalian species could contribute to reproduction only if gpr54 were somehow expressed in GnRH neurons. As mammals gained kisspeptin regulation of GnRH neurons, they may have lost other important regulatory mechanism of reproduction, which is important for the non-mammalian vertebrates, and this may have led to the essentiality of kisspeptin genes for mammalian reproduction. Several regulator of GnRH and gonadotropins have been found in various teleosts, such as dopamine (Chang et al. 1984a, Chang et al. 1984b, Sokolowska et al. 1985) and gamma-aminobutyric acid (GABA) (Trudeau et al. 1993a, Trudeau et al. 1993b). In addition, inhibitory regulation of the secretion of GnRH and gonadotropins by gonadotropin-inhibitory hormone (GnIH; GnIH coding gene is the orthologous gene of RF amide-related peptide 3 of mammals) is considered to be important for the HPG axis regulation in the avian species (Tsutsui et al. 2010), which have completely lost kisspeptin genes. Because *rfrp* gene was shown to be dispensable for medaka reproduction (Kaise et al., unpublished), another important regulatory system may exist in medaka. Thus, the gene knockout technique of neuropeptides is a very clear method to find the essential regulatory component(s) of reproduction, which was actually used to demonstrate the essentiality of GnRH1 in Chapter 2. In summary, I propose that the HPG axis regulation through kisspeptin signaling is specific to mammals, and that there may be more ancestral and more conservative mechanism(s) in the HPG axis regulation that are common to various vertebrates.

Exploration of the unknown function(s) of kisspeptin

Because the kisspeptin neurons were suggested not to be involved in the HPG axis regulation in non-mammalian species, the question then arises: what are the unknown functions of kisspeptin that are common to a wide variety of vertebrates?

In teleosts, the *kiss1* neurons are roughly divided two anatomically distinct populations, the one in habenula and the other in hypothalamus/POA. *kiss1* is reported to be expressed in the habenular neurons that project to the IPN (Ogawa et al. 2012, Hasebe et al. 2014), which is suggested to be involved in the emotional behavior (Matsumoto and Hikosaka 2007). However my *kiss1* KO medaka showed no significant difference from the wild type in two typical "habituation tests" to examine the emotional change (Karl et al. 2003, Matsunaga and Watanabe 2010), in the open field test and the diving test (Fig. 3-7, 8). It should be noted that loss of *kiss1* expression in the habenula was not compensated by *kiss2*, because *kiss2* mRNA was not detected by *in situ* hybridization in the habenula in *kiss1* KO medaka (data not shown).In *kiss1* KO medaka, there was no significant difference in serotonin-related genes, *pet1* or *slc6a4* (Fig. 3-9). My present result thus apparently disagrees with a previous report in zebrafish that *kiss1* is important for the emotional changes and the increase in serotonin-related gene expression (Ogawa et al. 2014). However, this discrepancy may be explained by the difference in the method; they ablated Kiss1 neurons in the habenula by using saporin, whereas I eliminated Kiss1 expression in habenula by *kiss1* knockout. In their behavioral test, they used Kiss1 peptide injection at extremely low dose (10^{-15} mol in ~350 mg body weight) to cause suppression of alert substance-induced fear response. Unfortunately, the alert substance-induced fear response could not be observed in medaka, and I could not perform similar behavioral experiment in medaka. Behavioral

experiments using *kiss1* and *gpr54-1* KO zebrafish may elucidate reasons for the puzzling discrepancy mentioned above. Anyway, my present results indicate that Kiss1 is not a major regulator of fear behavior at least in medaka.

The axon projections of Kiss1 neurons could be detected in the hypothalamus, which is known to be involved in homeostatic regulations and the pituitary functions (Ogawa et al. 2012, Hasebe et al. 2014). By real-time PCR analysis, among the genes in the pituitary and the brain, I found that the expression level of *tshb2* (Kitano et al. 2010) was increased in male *kiss2*/*gpr54-2* KO medaka, compared with the wild type medaka (Figure 3-10). It has been reported that the expression of *tshb2* in the pituitary is changed by day length, and *tshb2* has been suggested to be involved in seasonal breeding of the stickleback (Kitano et al. 2010). Because this increase was detected even in the heterogenic KO medaka of these genes, further analysis is necessary. It has also been reported that kisspeptin increase the release, but not transcription, of somatolactin in the pituitary of the goldfish (Jiang et al. 2014). Further analysis of the present KO medaka should be the key to reveal the unknown functions of the kisspeptin neurons that may be common to a wide variety of vertebrates.

Figure legends

Table 3-1

The list of oligo DNA for gRNA.

Table 3-2

Properties of reproductive functions of KO medaka lines.

Table 3-3

List of primers for quantitative reverse transcription realtime PCR (qRT PCR).

Figure 3-1

Genomic and deduced amino acids sequence of wild type (wt) and TALEN knockout *kiss1* gene. A, Alignment of genomic DNA sequence of kiss1 open reading frame (ORF) region of wt and a *kiss1* KO line. Underlines indicate left and right TALEN targets. B, Alignment of deduced amino acids sequence of precursor of Kiss1 from genomic data of wt and *kiss1* KO line. Shaded region indicates kisspeptin core-peptide sequence. D; deletion, I; insertion, R; replacement.

Figure 3-2

Genomic and deduced amino acids sequence of wild type (wt) and CRISPR/Cas9 knockout *kiss2* gene. A, Alignment of genomic DNA sequence of *kiss2* open reading frame (ORF) region of wt and a *kiss2* KO line. Underline indicates gRNA target. B, Alignment of deduced amino acids sequence of precursor of Kiss2 from genomic data of wt and *kiss2* KO medaka. Shaded region indicates kisspeptin peptide sequence. D; deletion.

Figure 3-3

Genomic and deduced amino acids sequence of wild type (wt) and CRISPR/Cas9 KO *gpr54-1* gene. A, Alignment of genomic DNA sequence of *gpr54-1* open reading frame (ORF) region of wt and a *gpr54-1* KO line. Underline indicates gRNA target. B, Alignment of deduced amino acids sequence of precursor of Gpr54-1 from genomic data of wt and *gpr54-1* KO line. Shaded region indicates transmembrane domain (TM). D; deletion.

Figure 3-4

Genomic and deduced amino acids sequence of wild type (wt) and CRISPR/Cas9 KO *gpr54-2* gene. A, Alignment of genomic DNA sequence of *gpr54-2* open reading frame (ORF) region of wt and a *gpr54-2* KO line. Underline indicates gRNA target. B, Alignment of deduced amino acids sequence of precursor of Gpr54-2 from genomic data of wt and *gpr54-2* KO line. Shaded region indicates transmembrane domain (TM). D; deletion, R; replacement.

Figure 3-5

Expression level of gonadotropin genes in KO medaka. Expression level of *lhb* (A) and *fshb* (B) mRNA in the pituitary of wt male, *kiss1*$^{-/-}$ male, wt female, and *kiss1*$^{-/-}$ female. Expression level of *lhb* mRNA in the pituitary of *kiss1*$^{+/-}$*kiss2*$^{-/-}$, *kiss1*$^{+/-}$*kiss2*$^{+/-}$, *kiss1*$^{-/-}$*kiss2*$^{-/-}$, *gpr54-1*$^{-/-}$, *gpr54-1*$^{+/-}$, *gpr54-2*$^{-/-}$, and *gpr54-2*$^{+/-}$ male (C) and female (D). Expression level of *fshb* mRNA in the pituitary of *kiss1*$^{+/-}$*kiss2*$^{-/-}$, *kiss1*$^{+/-}$*kiss2*$^{+/-}$, *kiss1*$^{-/-}$ *kiss2*$^{-/-}$, *gpr54-1*$^{-/-}$, *gpr54-1*$^{+/-}$, *gpr54-2*$^{-/-}$, and *gpr54-2*$^{+/-}$ male (E) and female (F).

Figure 3-6

Hematoxylin and eoxin stained sections of ovaries (90 dph) or testes (90 dph) of *kiss1*, *kiss2*, *gpr54-1*, or *gpr54-2* knockout medaka. A-F, Ovaries at 90 dph (1) and testes of 90

dph (2) of wt (A), *kiss1*$^{-/-}$(B), *kiss2*$^{-/-}$(C), *kiss1*$^{-/-}$ *kiss2*$^{-/-}$ (D), *gpr54-1*$^{-/-}$(E), and *gpr54-2*$^{-/-}$ (F). PG; primary growth, PV; previtellogenic, LV; late vitellogenic; FG; full-growth, sg; spermatogonia, sc; spermatocyte, and sz; spermatozoa. Scale bars of ovary images indicate 500 μm. Scale bars of testis images indicate 50 μm.

Figure 3-7

Open field test. A, Moving distance of lateral motion in one minute (min) for 10 min of wt and *kiss1*$^{-/-}$ medaka. B, Center stay time (seconds, s) for 10 min of wt and *kiss1*$^{-/-}$ medaka.

Figure 3-8

Diving test. A, Moving distance of vertical motion in one minute (min) for 10 min of wt and *kiss1*$^{-/-}$ medaka. B, Surface stay time (s) for 10 min of wt and *kiss1*$^{-/-}$ medaka.

Figure 3-9

Expression level of serotonin-related genes, *pet1* and *slc6a4*, in *kiss1*$^{-/-}$ medaka. Expression level of *pet1* (A) and *slc6a4* (B) mRNA in the brain of wt male, *kiss1*$^{-/-}$ male, wt female, and *kiss1*$^{-/-}$ female.

Figure 3-10

Expression level of *tshb2* genes in KO medaka. Expression level of *tshb2* mRNA in the pituitary of male (A) and female (B). A. *kiss1*$^{-/-}$, *kiss1*$^{+/-}$*kiss2*$^{-/-}$, *kiss1*$^{+/-}$*kiss2*$^{+/-}$, *kiss1*$^{-/-}$ *kiss2*$^{-/-}$, *gpr54-2*$^{-/-}$, *gpr54-2*$^{+/-}$, *gpr54-1*$^{-/-}$, *gpr54-1*$^{+/-}$, and wt male. B. *kiss1*$^{-/-}$, *kiss1*$^{+/-}$ *kiss2*$^{-/-}$, *kiss1*$^{+/-}$*kiss2*$^{+/-}$, *kiss1*$^{-/-}$*kiss2*$^{-/-}$, *gpr54-2*$^{-/-}$, *gpr54-2*$^{+/-}$, *gpr54-1*$^{-/-}$, and wt female.

name	purpose	sequence
kiss2casoligo_2_1	kiss2 gRNA template	5’-TAGGACGACTCTGCGGCAGGGG-3’
kiss2casoligo_2_2	kiss2 gRNA template	5’-AAACCCCCTGCCGCAGAGTCGT-3’
gpr54-1ex3-R-1	gpr54-1 gRNA template	5’-TAGGTCCACGCTCATGGCAGAC-3’
gpr54-1ex3-R-2	gpr54-1 gRNA template	5’-AAACGTCTGCCATGAGCGTGGA-3’
gpr54-2ex1_1F	gpr54-2 gRNA template	5’-TAGGTGGGGGTCAACAGATCCG-3’
gpr54-2ex1_1R	gpr54-2 gRNA template	5’-AAACCGGATCTGTTGACCCCCA-3’

Table 3-1. Oligo DNA list for gRNA.

genotype				
male	**female**	**male courtship behavior (number of circle dance) in 10 min**	**number of pairs that laid eggs**	**fertilization rate**
kiss1$^{-/-}$	*kiss1*$^{-/-}$	3.5±1.6 (n=7)	4/7	97 % (n=4)
kiss2$^{-/-}$	*kiss2*$^{-/-}$	3.2±1.2 (n=5)	3/5	100 % (n=3)
kiss1$^{-/-}$ *kiss2*$^{-/-}$	*kiss1*$^{-/-}$ *kiss2*$^{-/-}$	2.2±0.90 (n=6)	3/9	100 % (n=3)
gpr54-1$^{-/-}$	*gpr54-1*$^{-/-}$	8.1±2.5 (n=7)	3/7	78 % (n=3)
gpr54-2$^{-/-}$	*gpr54-2*$^{-/-}$	4.0±2.0 (n=6)	4/6	93 % (n=4)
wt	wt	5.5±1.6 (n=4)	3/4	96 % (n=3)

Table 3-2

Properties of reproductive functions of KO medaka.

Primer name		sequence
mdkiss1 check F1	kiss1 genome PCR, sequence primer	5'-CATGTGTTTCTCCTGCAGATAATGC-3'
mdkiss1 check R1	kiss1 genome PCR	5'-CGTTTCTTTATAGCCACAGGGTG-3'
kiss1hcheck11bpf2	kiss1 genome PCR check	5'-GAAGGAGTGGCCAAAGAGTG-3'
kiss2seq-3f	kiss2 genome PCR	5'-GGTAAAGTCTCCGCCTCCTC-3'
kiss2_check_r3	kiss2 genome PCR, sequence primer	5'-AACGGGTTGTAGTTAAACTTGCTG-3'
gpr54-1_check_f3	gpr54-1 genome PCR	5'- CAAAGACAAGAATTCTGTGTAAACTG-3'
gpr54-1_check_r1	gpr54-1 genome PCR, sequence primer	5'- ATGGACACAGAGACGGCCAGAG -3'
gpr54-2-f2	gpr54-2 genome PCR	5'- CCTGACACCATGCACTCCTC-3'
gpr54-2_check_r1	gpr54-2 genome PCR, sequence primer	5'- CTCCTTCCTCCTCATCCTCGT-3'
rps13 SE	ribosomal protein subunit 13 (rps13) qRT PCR	5'-GTGTTCCCACTTGGCTCAAGC-3'
rps13 AS	rps13 qRT PC	5'-CACCAATTTGAGAGGGAGTGAGAC-3'
qPCR LHb Fw new	lhb qRT PCR	5'-AGGGTATGTGACTGACGGATCCAC-3'
qPCR LHb Rv new	lhb qRT PCR	5'-TGCCTTACCAAGGACCCCTTGATG-3'
qPCR FSHb Fw new	fshb qRT PCR	5'-TGGAGATCTACAGGCGTCGGTAC-3'
qPCR FSHb Fw new	fshb qRT PCR	5'-AGCTCTCCACAGGGATGCTG-3'
TSHb2-rt-SE	tshb qRT PCR	5'-ACTGCTACTCAAGGGATACC-3'
TSHb2-rt-AS	tshb qRT PCR	5'-GAGGGCAGCCAGGAATATGAG-3'
pet1 se	qRT PCR	5'- GCGGAGGAAAGCTCATGTTC-3'
pet1 as	qRT PCR	5'-AGGAACTGCCACAGCTGGAT-3'
slc6a4 se	qRT PCR	5'-CGTGACTTGGTCCAACTTATCC-3'
slc6a4 as	qRT PCR	5'-AGCTGGTGCAGACCTGATGA-3'

Table 3-3

The list of primers.

Figure 3-1

A. ORF sequence of *kiss1*

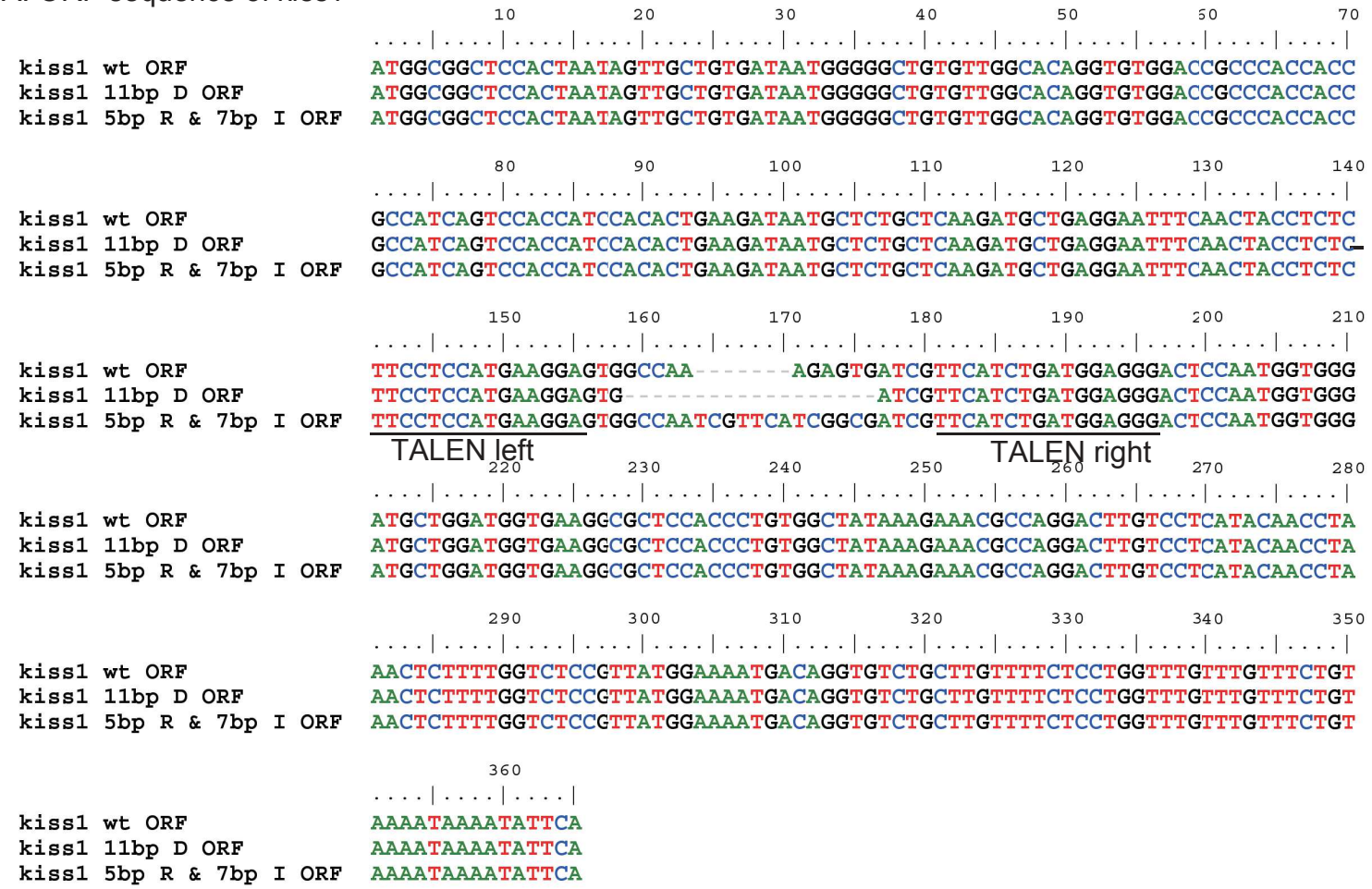

B. deduced amino acid sequence of Kiss1

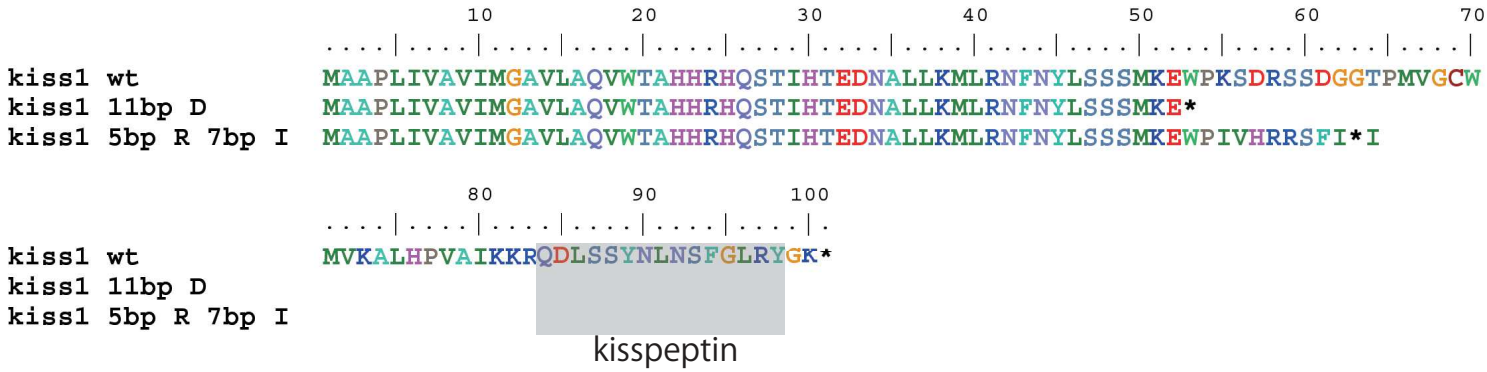

Figure 3-2

A. ORF sequence of *kiss2*

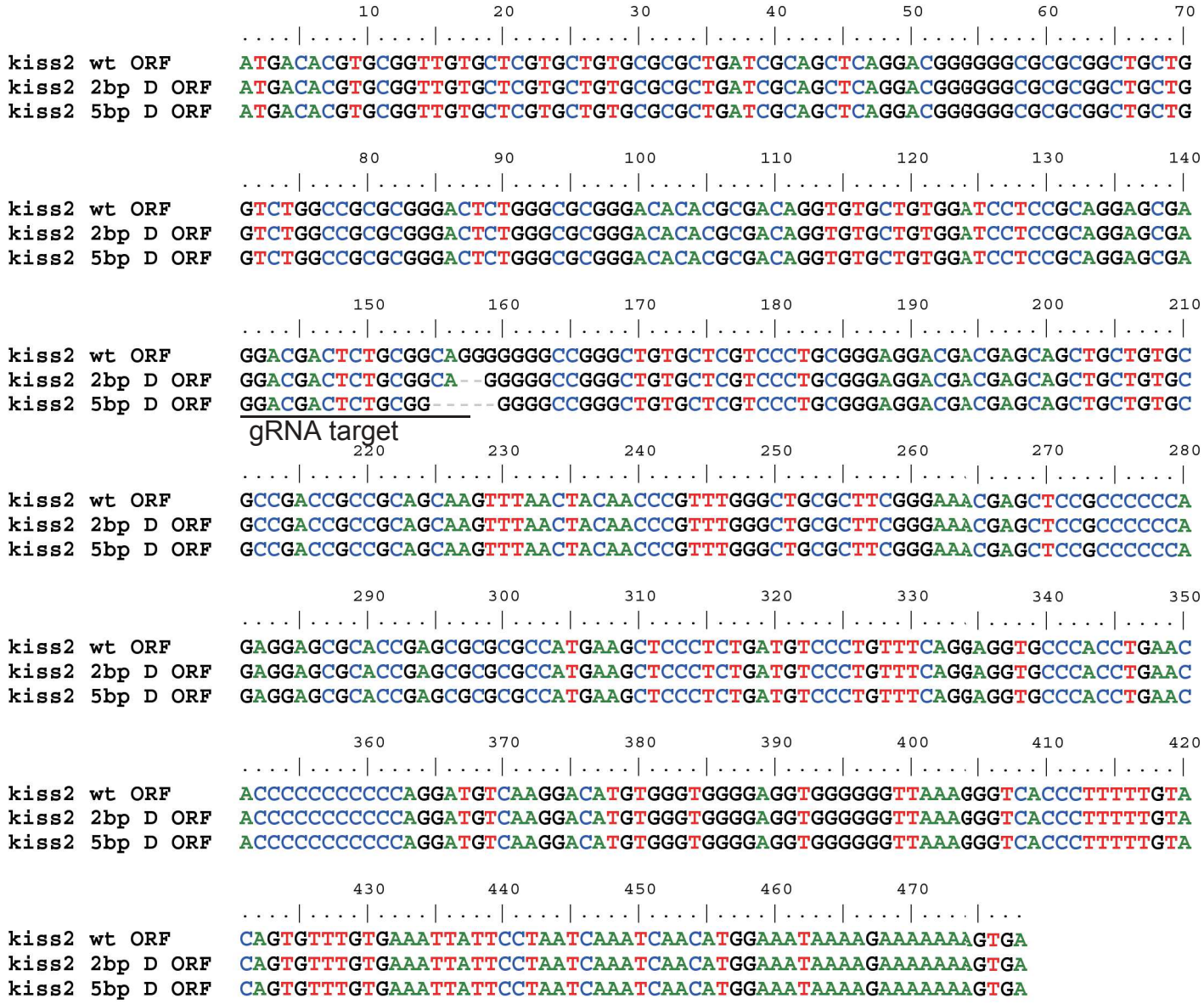

B. deduced amino acid sequence of Kiss2

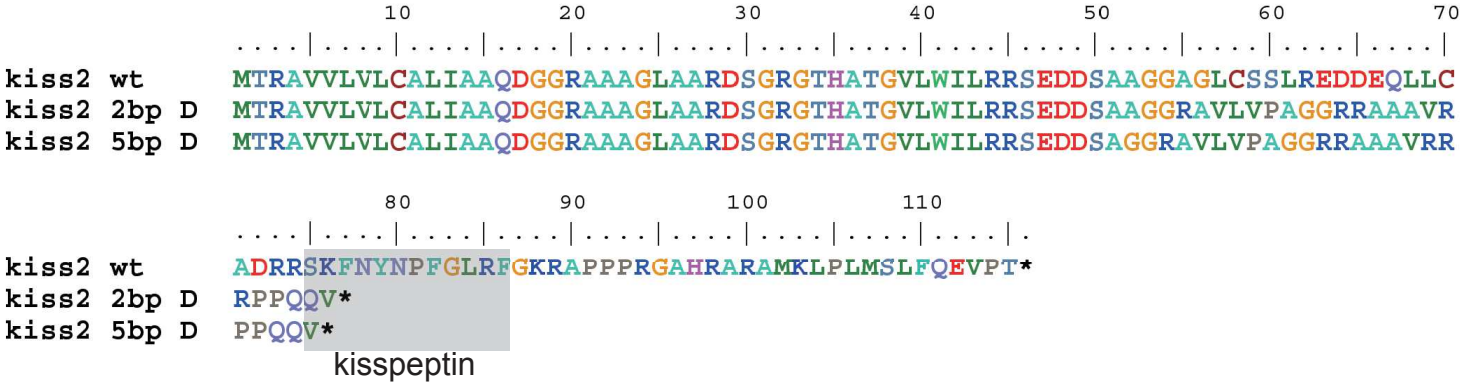

Figure 3-3

A. ORF sequence of *gpr54-1*

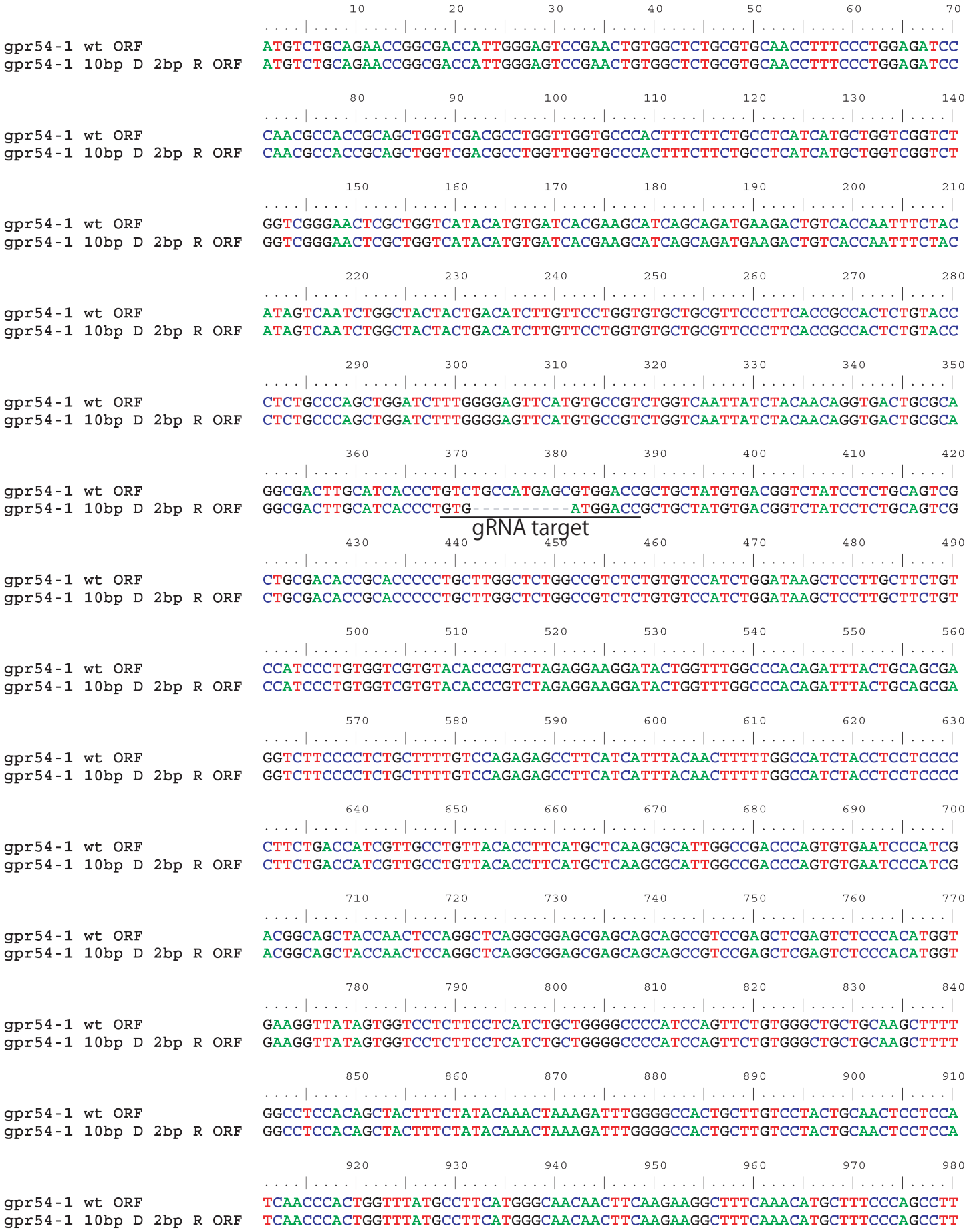

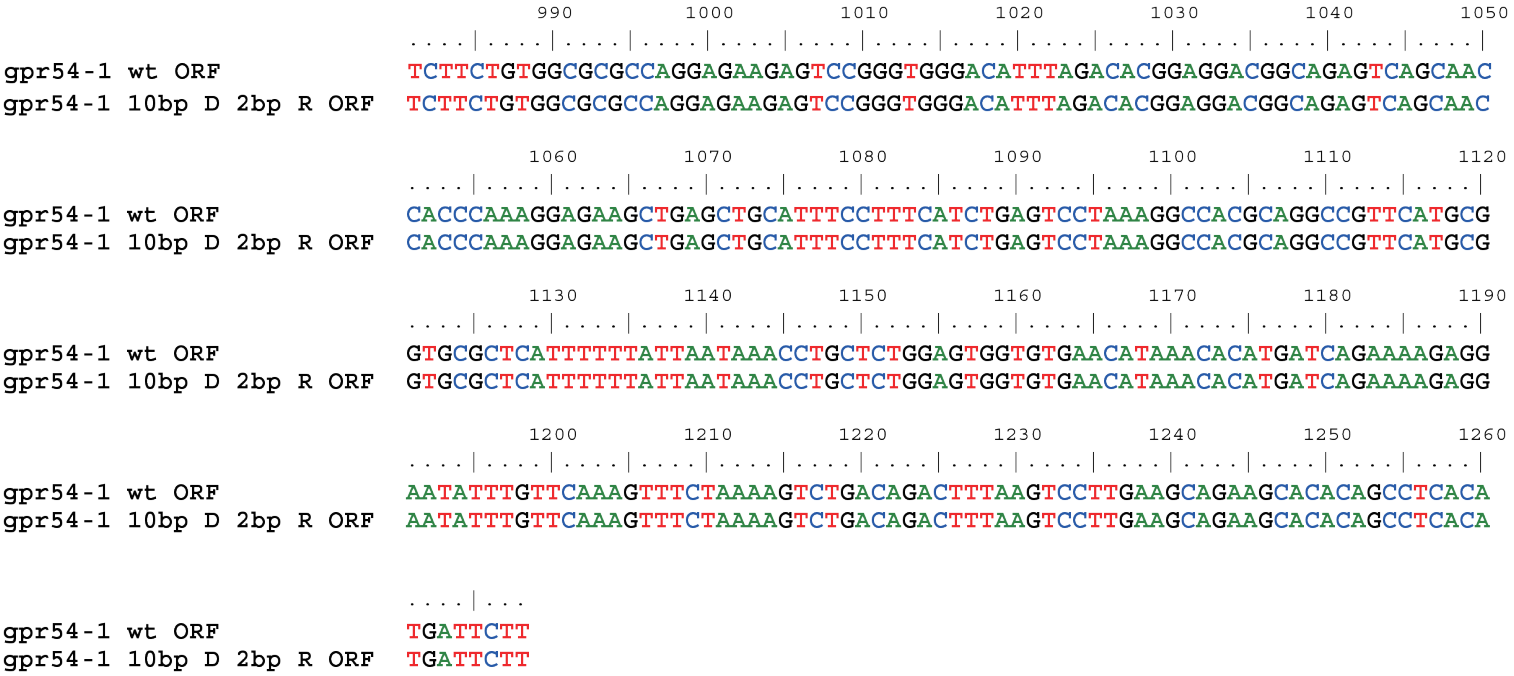

B. deduced amino acid sequence of Gpr54-1

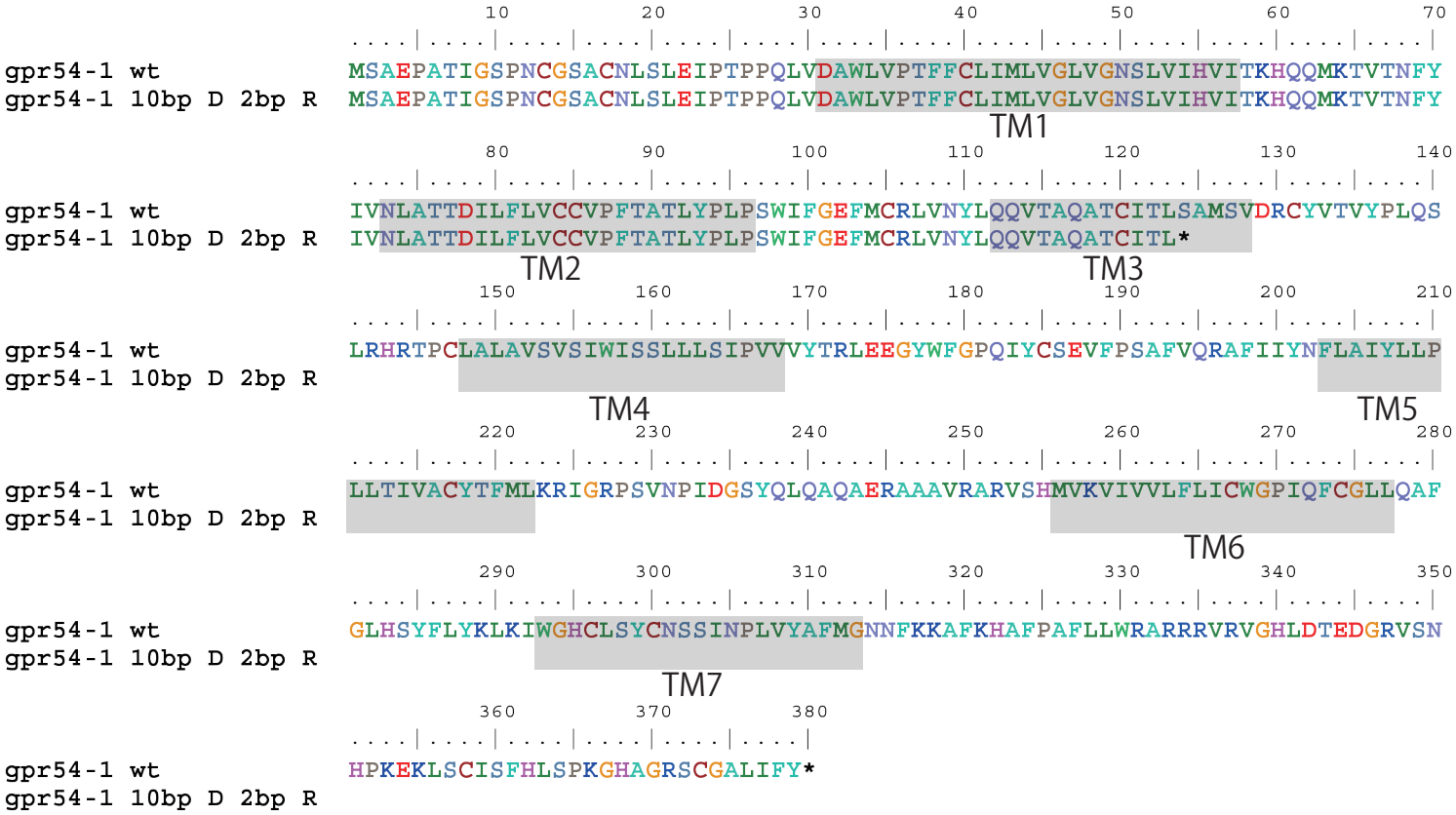

Figure 3-4

ORF sequence of *gpr54-2*

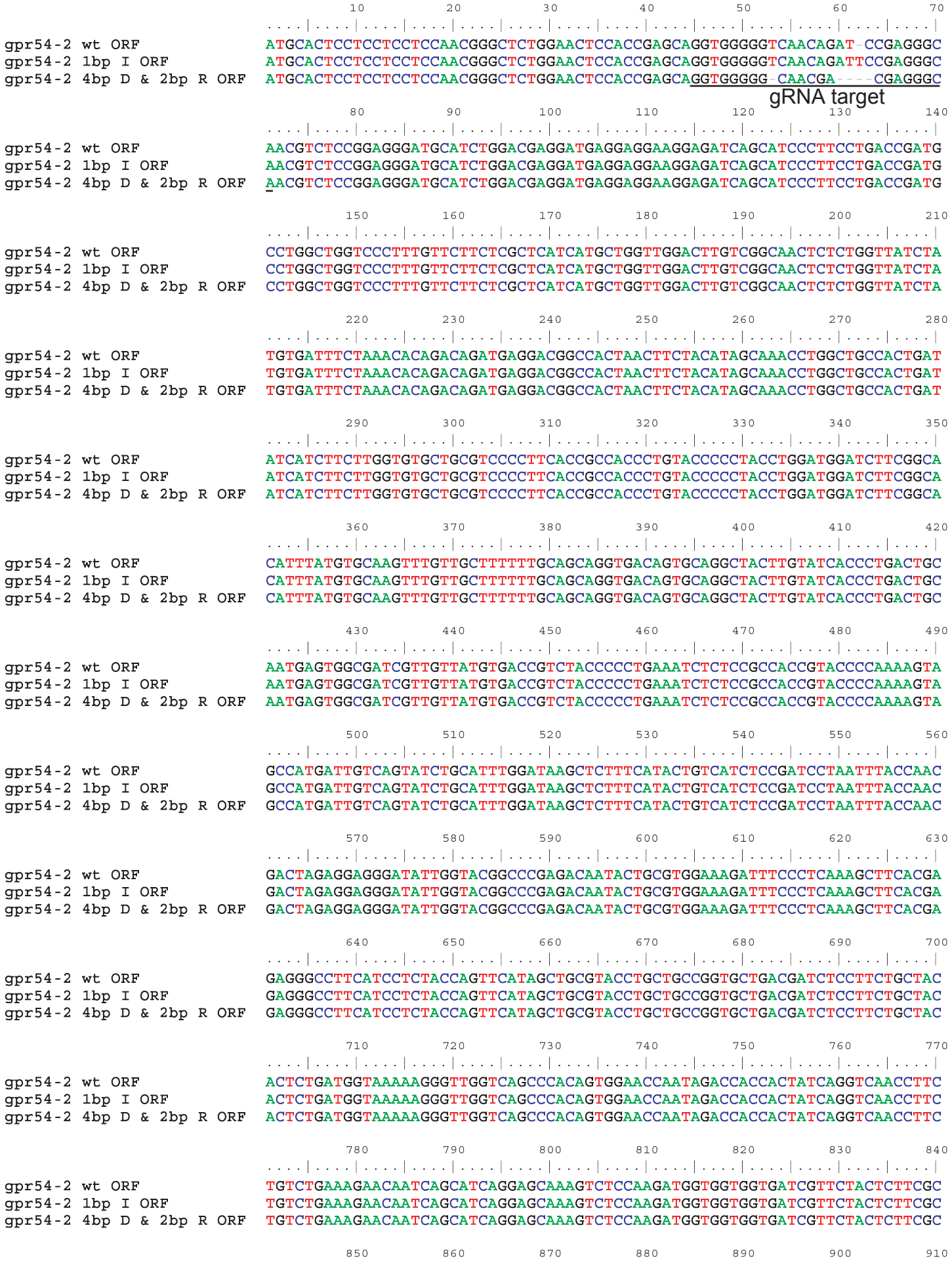

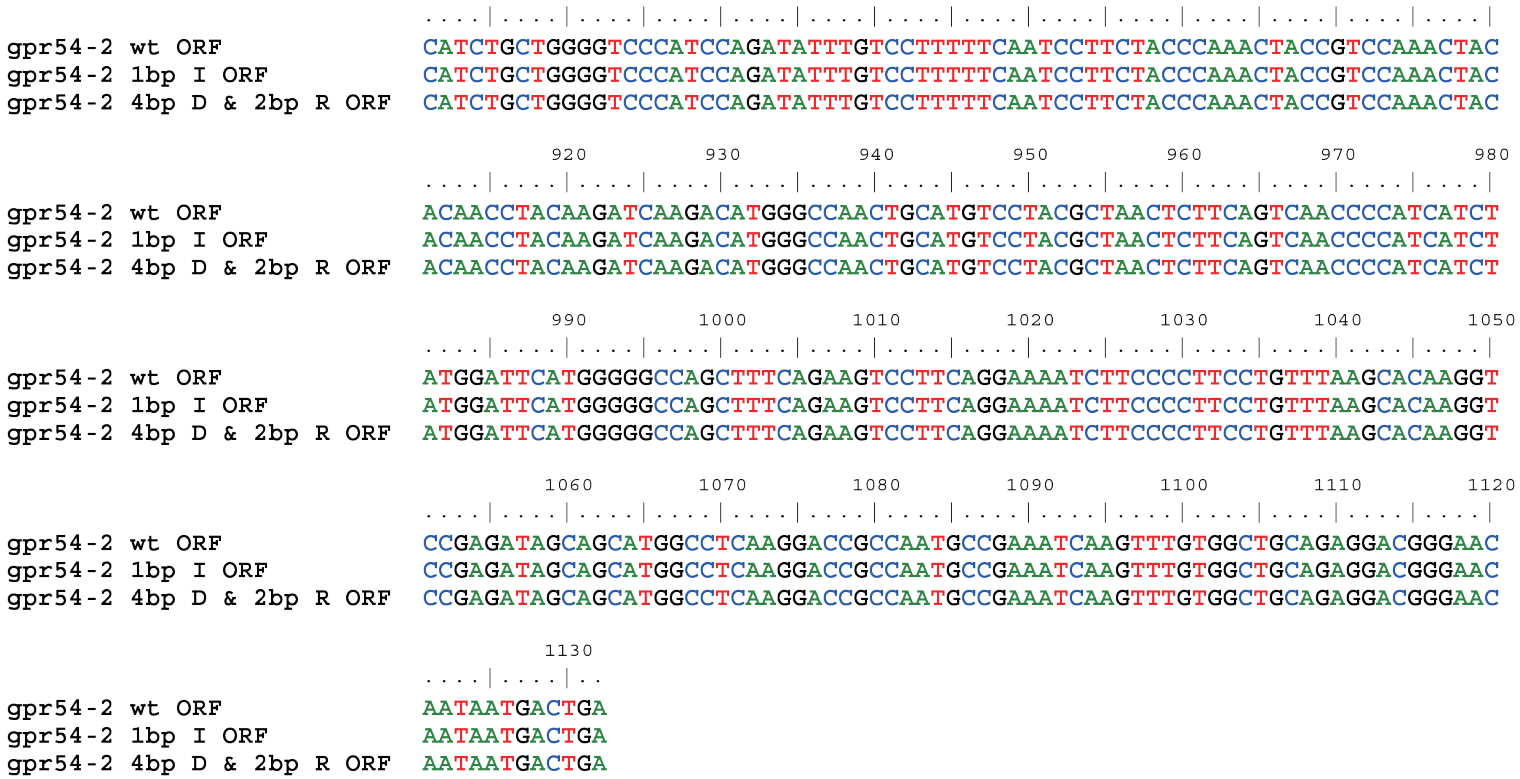

B. deduced amino acid sequence of Gpr54-2

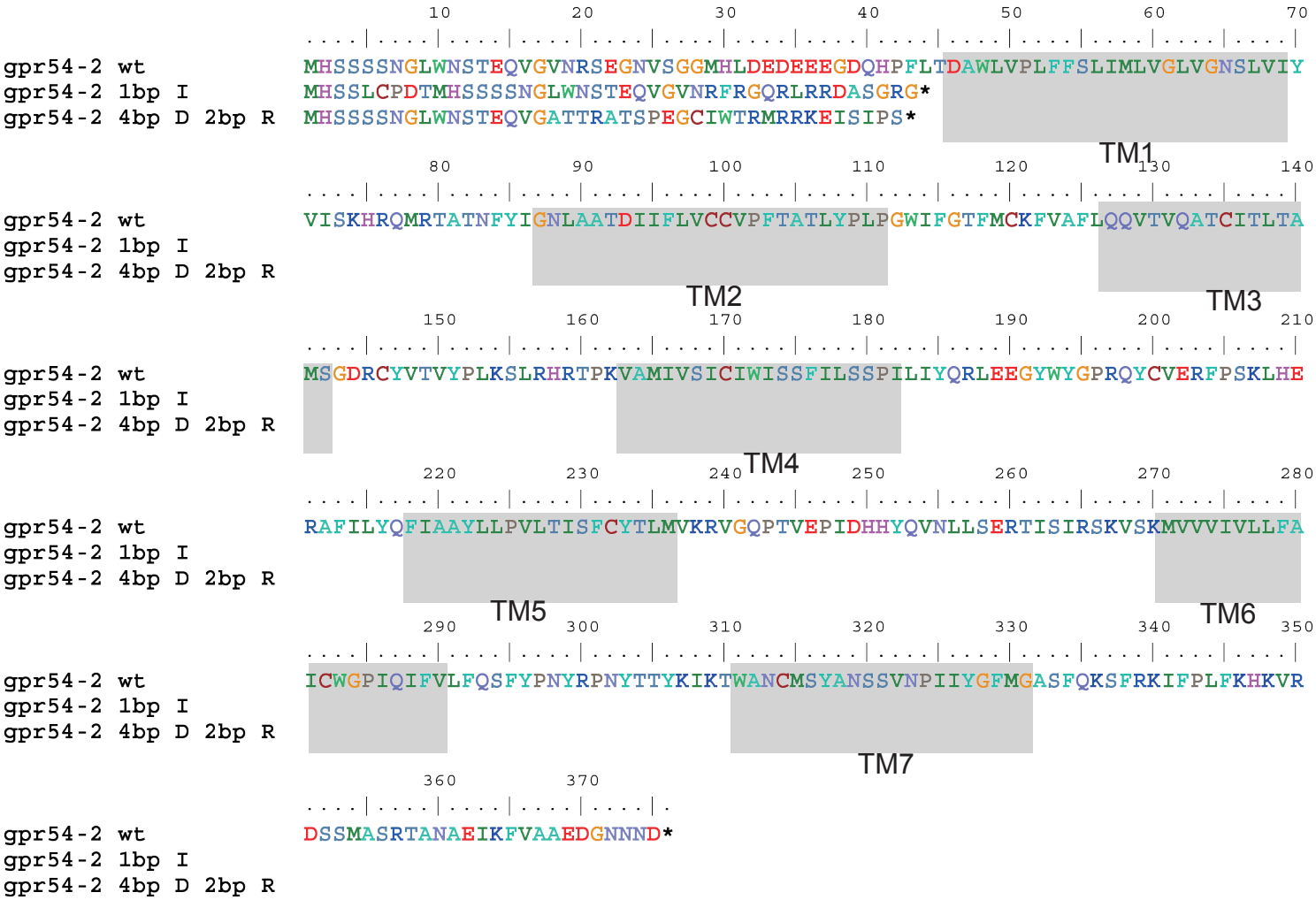

Figure 3-5

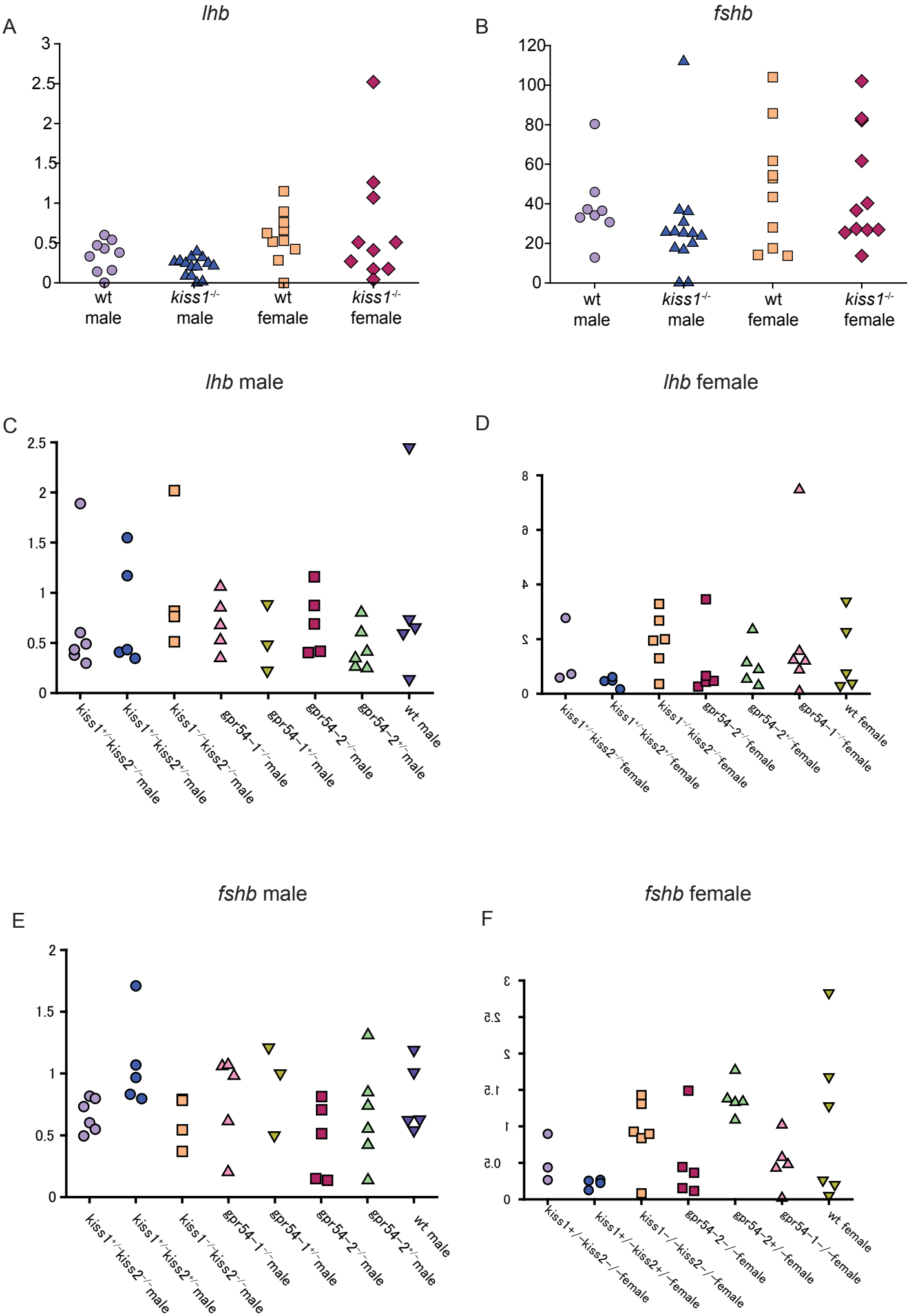
A
lhb
3
2.5
2
1.5
1
0.5
0
wt male
kiss1-/- male
wt female
kiss1-/- female
B
fshb
120
100
80
60
40
20
0
wt male
kiss1-/- male
wt female
kiss1-/- female
lhb male
C
2.5
2
1.5
1
0.5
0
kiss1+/-kiss2-/- male
kiss1+/-kiss2+/- male
kiss1-/-kiss2-/- male
gpr54-1-/- male
gpr54-1+/- male
gpr54-2-/- male
gpr54-2+/- male
wt male
lhb female
D
8
6
4
2
0
kiss1+/-kiss2-/- female
kiss1+/-kiss2+/- female
kiss1-/-kiss2-/- female
gpr54-2-/- female
gpr54-2+/- female
gpr54-1-/- female
wt female
fshb male
E
2
1.5
1
0.5
0
kiss1+/-kiss2-/- male
kiss1+/-kiss2+/- male
kiss1-/-kiss2-/- male
gpr54-1-/- male
gpr54-1+/- male
gpr54-2-/- male
gpr54-2+/- male
wt male
fshb female
F
3
2.5
2
1.5
1
0.5
0
kiss1+/-kiss2-/- female
kiss1+/-kiss2+/- female
kiss1-/-kiss2-/- female
gpr54-2-/- female
gpr54-2+/- female
gpr54-1-/- female
wt female

Figure 3-6

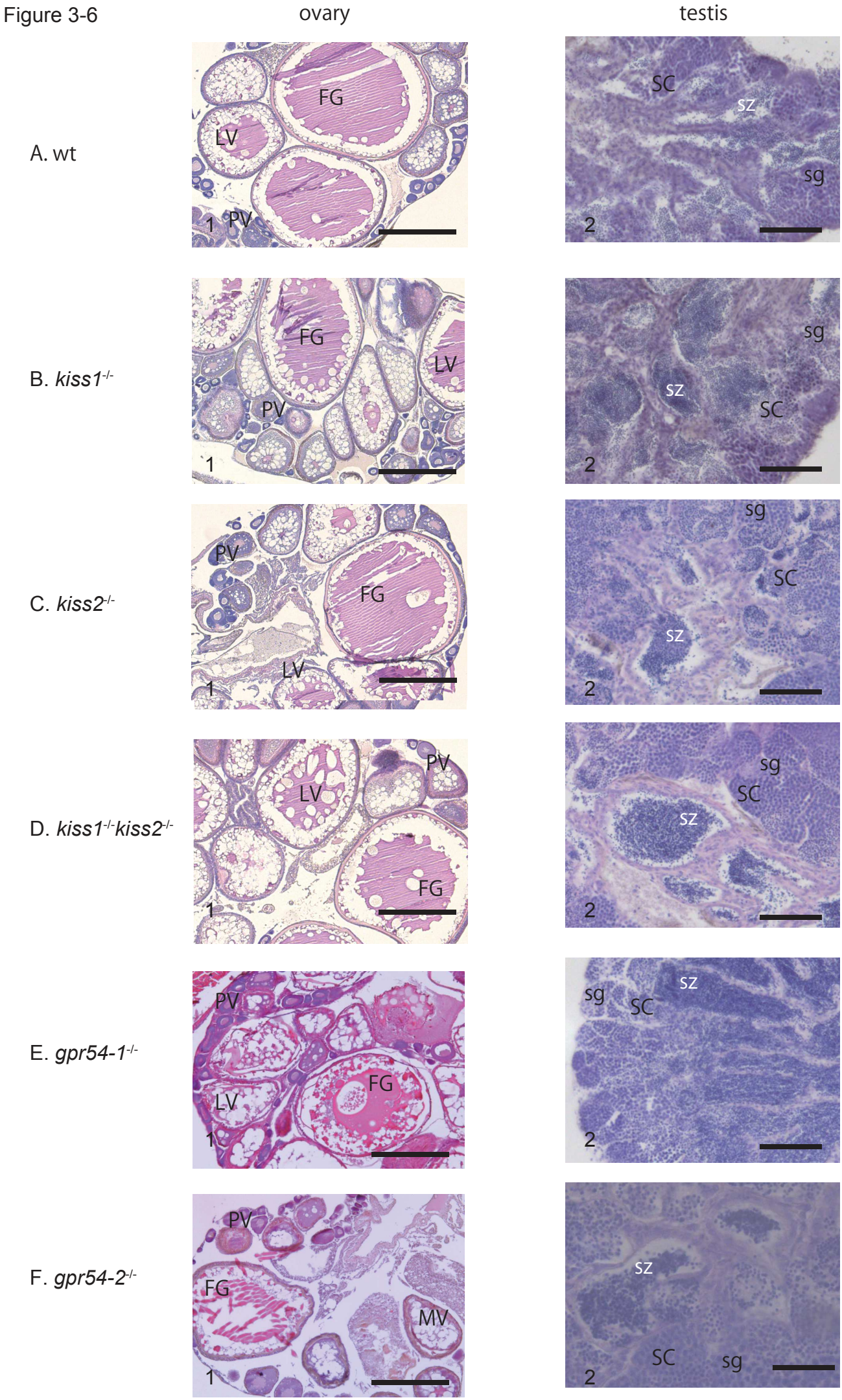
ovary
testis
A. wt
FG
LV
PV
1
SC
SZ
sg
2
B. kiss1-/-
FG
LV
PV
1
sg
SZ
SC
2
C. kiss2-/-
PV
FG
LV
1
sg
SC
SZ
2
D. kiss1-/-kiss2-/-
PV
LV
FG
1
sg
SC
SZ
2
E. gpr54-1-/-
PV
FG
LV
1
SZ
sg
SC
2
F. gpr54-2-/-
PV
FG
MV
1
SZ
SC
sg
2

Figure 3-7

Open field test

A

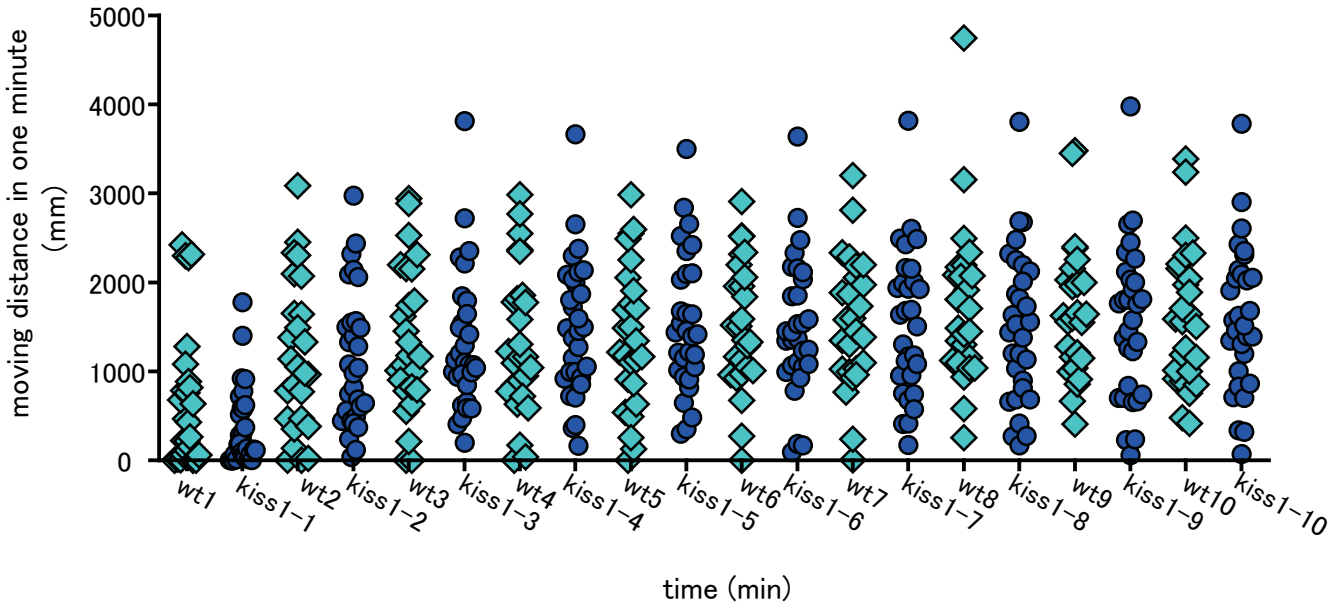

B

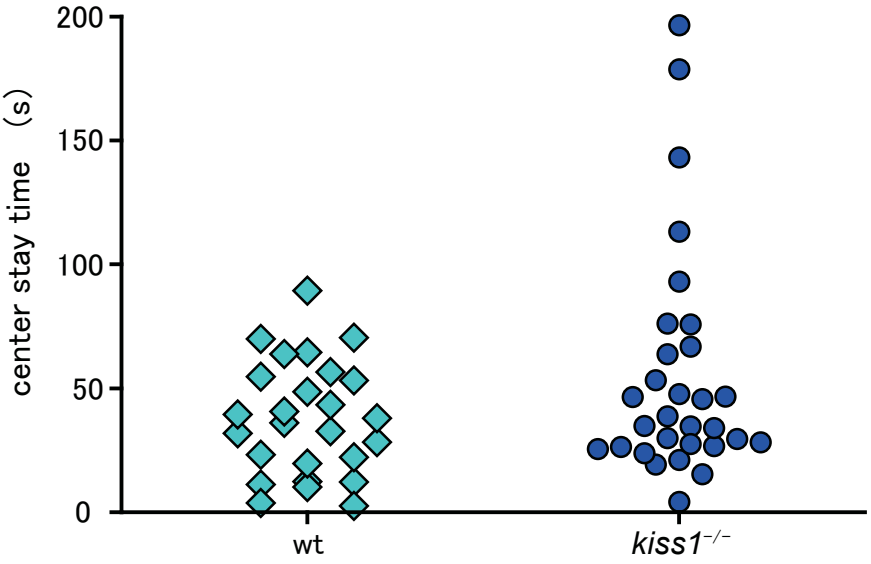

Figure 3-8

Diving test

A

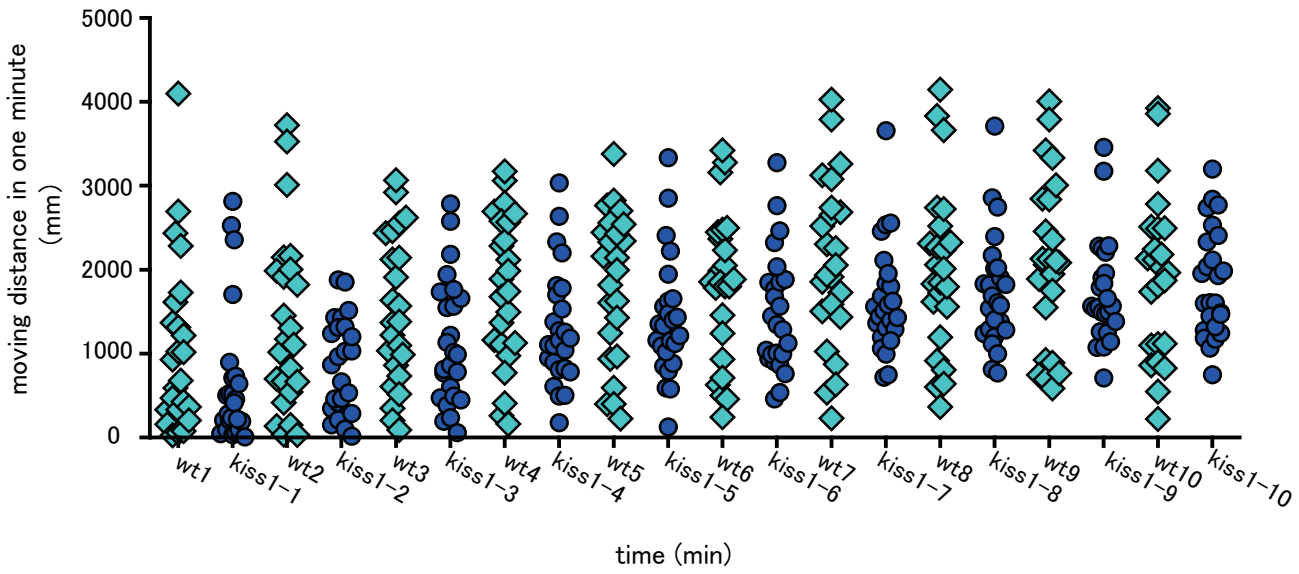

B

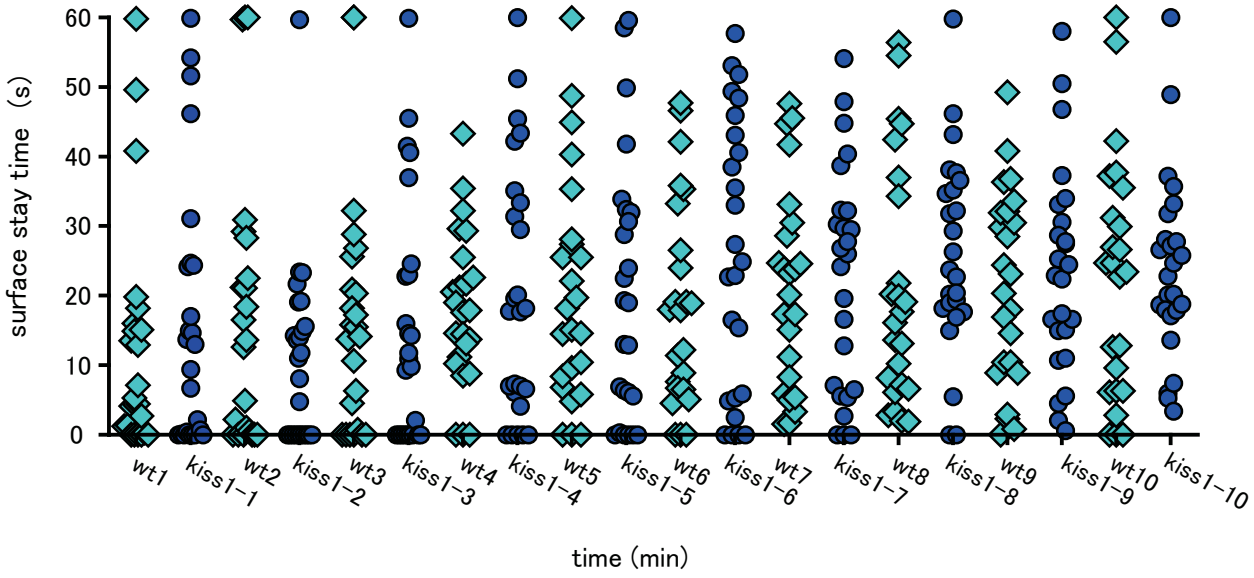

Figure 3-9

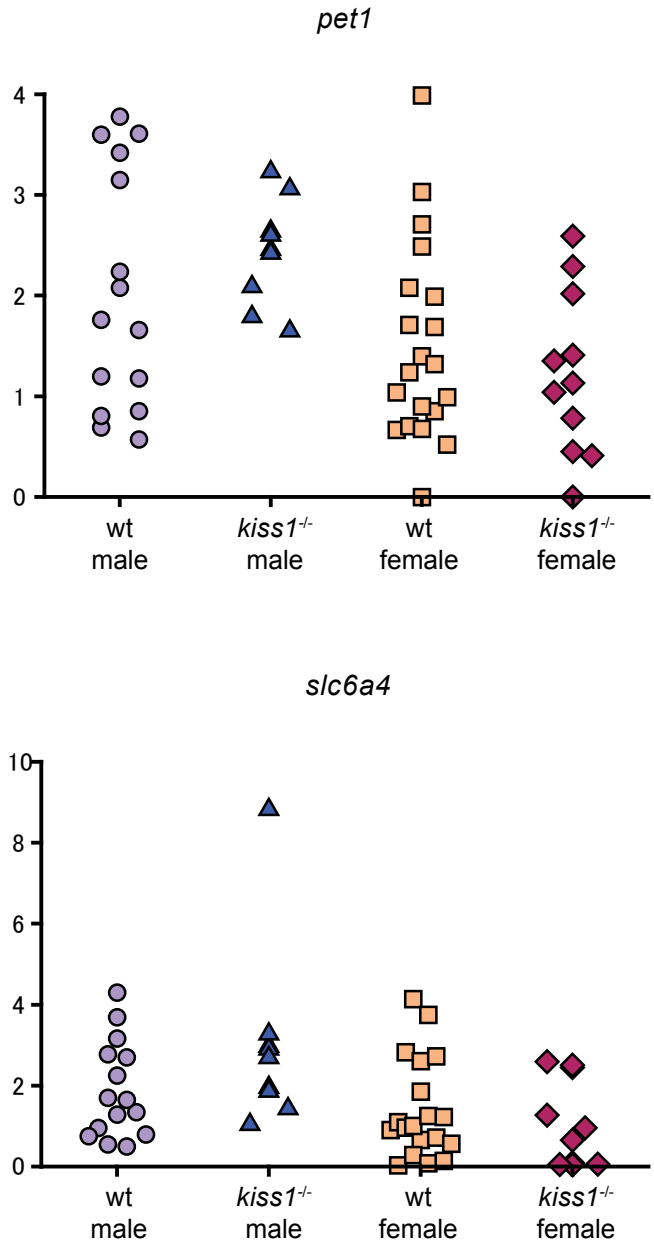
pet1
4
3
2
1
0
wt male
kiss1-/- male
wt female
kiss1-/- female
slc6a4
10
8
6
4
2
0
wt male
kiss1-/- male
wt female
kiss1-/- female

Figure 3-10

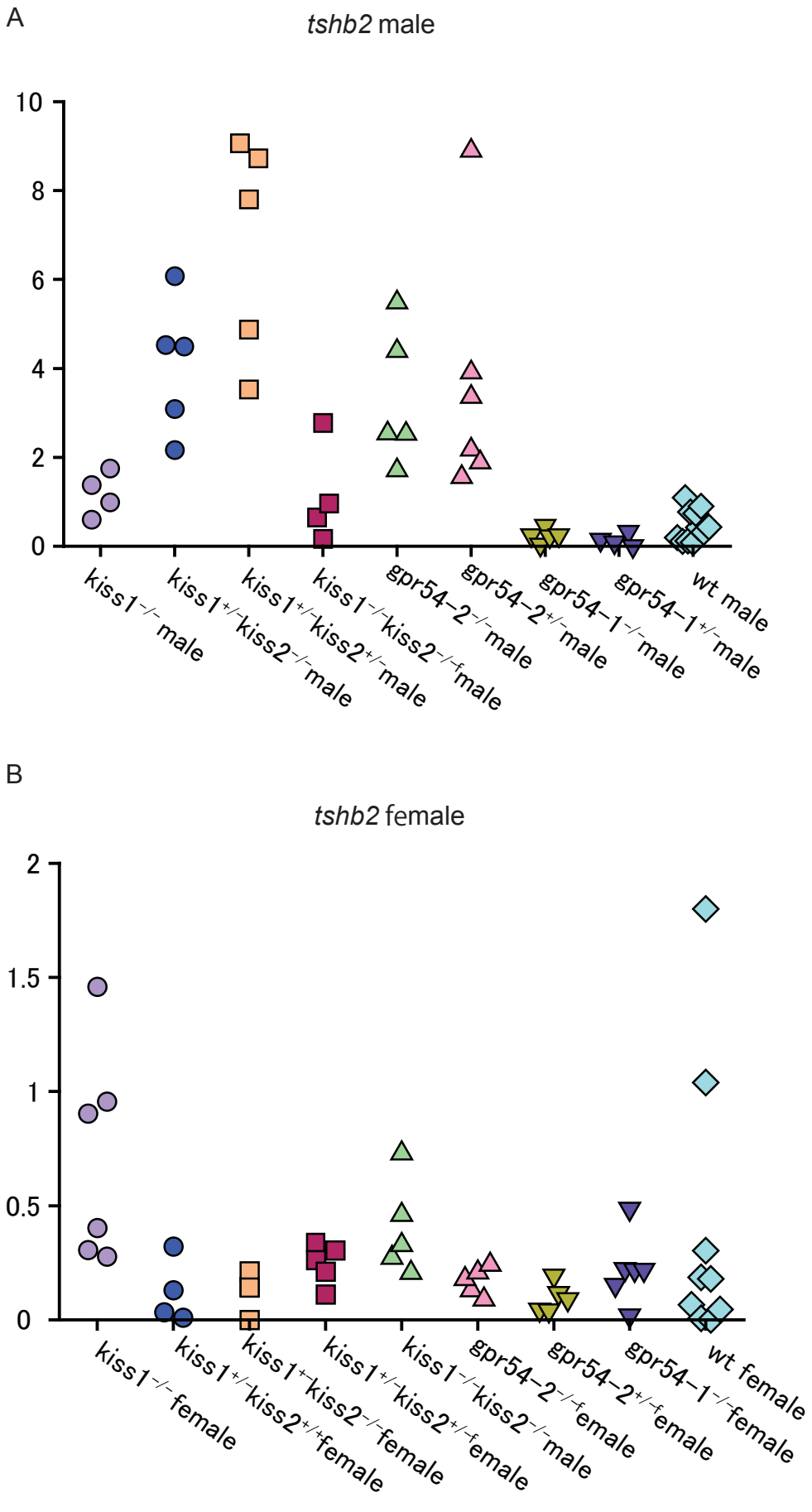
A
tshb2 male
10
8
6
4
2
0
kiss1−/− male
kiss1+/−kiss2−/− male
kiss1+/−kiss2+/− male
kiss1−/−kiss2−/−male
gpr54−2−/− male
gpr54−2+/− male
gpr54−1−/− male
gpr54−1+/− male
wt male
B
tshb2 female
2
1.5
1
0.5
0
kiss1−/−female
kiss1+/−kiss2+/+female
kiss1+/−kiss2−/−female
kiss1+/−kiss2+/−female
kiss1−/−kiss2−/− male
gpr54−2−/−female
gpr54−2+/−female
gpr54−1−/−female
wt female

General Discussion

In the present thesis, I aimed to clarify what is important for the HPG axis regulation in vertebrates, by focusing on the key components of the HPG axis regulation known in mammals, i.e. GnRH, LH, FSH, and kisspeptin, with special reference to the functional conservation of its mechanisms. I demonstrated that FSH, LH, and GnRH functions are roughly similar between mammals and teleosts, with newly found significant differences. I here emphasize the commonalities and specificities of the HPG axis regulation I have shown in this study. In addition, I propose from the kisspeptin knockout (KO) study that non-mammalian species like medaka may have an estrogen feedback loop not dependent on kisspeptin neurons. These points will be discussed here in General Discussion.

The commonality and specificity of the HPG axis regulation in vertebrates

I demonstrated that LH release triggered by GnRH is necessary for ovulation, and that FSH is necessary for folliculogenesis in medaka. These observations were basically consistent with their function, as suggested by their names. Given that the expression level of *lhb* and *fshb* is changed by serum estrogen level in fish (Yaron et al. 2003) as in mammals, it is suggested that the basic HPG axis regulation mechanism may be highly conserved in vertebrates especially in female. However, there are also several differences in their functions. (1) GnRH effect on gonadotropin release is mediated by hypophyseal portal vessel in mammals, whereas GnRH neurons directly innervate gonadotrophs in medaka. (2) GnRH and LH are also essential for folliculogenesis in mammals, whereas they are not essential in medaka. (3) Kisspeptin neurons are the essential mediator of estrogen signal to GnRH neurons in mammals, whereas they are not essential in medaka.

While mammalian GnRH neurons project to the median eminence and release GnRH peptide, which reach the gonadotrophs through the hypophyseal portal vessel (Charlton 2008), medaka GnRH1 neurons directly project to the pituitary, as in other teleosts (Dubois et al. 2000, Ishizaki and Oka 2001). However, my analyses in both morphology and knockout phenotypes indicated that this difference does not change the function of hypophysiotropic GnRH neurons in stimulating LH secretion. I demonstrated that the regulation of LH cells by GnRH neuron is essential regardless of their drastic morphological changes.

In mammals, mutant of GnRH genes showed a striking decrease in expression level and release of not only LH but also FSH (Cattanach et al. 1977) and insufficient folliculogenesis. In contrast, my *gnrh1* KO medaka showed a decrease in *lhb* expression level, but no change in *fshb* expression level and showed apparently intact preovulatory follicles. It indicates that the GnRH regulation is not required for physiological level of secretion of FSH in teleosts, unlike in mammals. Moreover, it should be noted that *lhb* KO medaka as shown in the present study showed well developed gonad with preovulatory follicles, while LH null mice showed insufficient gonadal development (Ma et al. 2004). Thus, I suggest that the function of FSH and LH is differentiated more clearly in teleosts, compared to that in mammals.

Furthermore, I demonstrated that, unlike in mammals, kisspeptin signaling is not necessary for normal HPG axis functions in medaka. However, it is presumable that estrogen feedback regulation is conserved also in teleosts including medaka, because there are several literature reporting that the expression level of gonadotropin genes are changed by serum estrogen level in several teleost species (Yaron et al. 2003, Kanda et

al. 2011). Recent study in our laboratory also demonstrated that the serum estrogen-dependent upregulation of *gnrhr* (GnRH receptor gene) expression in LH cells may be an important trigger for ovulation, which occurs when gonad is fully mature in medaka (Arai et al., 2015). This regulation can be one of the candidates for estrogen feedback regulation in teleosts. They reported that GnRH neuron firing and probably GnRH release do not change between breeding and non-breeding conditions, while GnRH sensitivity of LH cells are the important switch for LH release. Thus, current results indicate that in spite of high level of conservation of the mechanism of HPG axis regulation as a regulatory system of reproduction in vertebrates, especially in females, there is also a diversity between mammals and teleosts in the role of each component of the HPG axis in gonadal regulation (Figure 4-1).

Estrogen negative feedback signaling for gonadal development and positive feedback signaling for ovulation

In mammals, kisspeptin neurons in the arcuate nucleus, which is also known as KNDy neurons because they co-express neurokinin B and dynorphin in addition to kisspeptin, are involved in the negative estrogen feedback and regulate pulsatile GnRH release, which is suggested to be important for folliculogenesis in mammals (Wakabayashi et al. 2010). On the other hand, in contrast to many reports for the occurrence of LH surge in mammals, (Ching 1982, Hatanaka and Wada 1988, Canosa et al. 2008), there has been no clear evidence for pulsatile LH secretion in non-mammalian species. This difference between mammalian and non-mammalian species may be related to the reason why pulsatile LH release is essential for follicular growth in mammalian species but not in non-mammalian species (chapter 2) as follows. From the results of my thesis, I assume

that the HPG axis through kisspeptin signaling is required for the pulsatile LH release during gonadal development only in tetrapod, because *Lhb* and *Fshb* are expressed in the same cell in mammals. During immature stage of ovaries in mammalian species, FSH regulation and pulsatile LH release simultaneously occur by the action of negative estrogen feedback through kisspeptin-GnRH signaling, both of which promotes the ovarian development (Mayer and Boehm 2011). After the development of the ovary, surge release of GnRH and subsequent LH induces ovulation, by the action of positive estrogen feedback (Smith 2013). By taking advantage of these differential modes of GnRH release, pulse and surge, mammalian species successfully separate the regulation of ovarian development and ovulation. On the other hand, in non-mammalian species including teleosts (Yaron et al. 2003) , FSH and LH are distinctly expressed in separate cells in the pituitary, so that they can take advantage of it to use different regulatory pathways. I propose that this may be the reason why teleosts do not need kisspeptin for reproduction. It is strongly suggested that *lhb* and *fshb* may have been expressed in the same cell in the common ancestor of teleosts and mammals, because *lhb* and *fshb* were originally duplicated from the ancestral glycoprotein hormone b gene (Uchida et al. 2013), and they should be expressed in a single cell at the time of duplication. In fact, LH and FSH are detected in the same cell in frogs (Pinelli et al. 1996) and some tetrapods, leaving an exception, birds (Proudman et al. 1999). Given that kisspeptin neurons express *er*α and project to the POA in medaka (Hasebe et al. 2014), where GnRH neurons are localized (Chapter 1, (Abraham et al. 2010)) but not the kisspeptin receptors in medaka (Kanda et al. 2013), it is presumable that the mammalian type of kisspeptin neuron-GnRH neuron circuitry should be complete only if kisspeptin

receptor genes are expressed in GnRH neurons. Further studies of kisspeptin neurons in non-mammalian tetrapods should reveal the ancestral regulatory mechanisms and the timing when kisspeptin became essential for reproductive regulation during the tetrapod lineage.

Exploration of functions of kisspeptin neurons

Because I demonstrated that kisspeptin neurons are not involved in the HPG axis regulation in non-mammalian vertebrates, the question then arises; what are the unknown functions of kisspeptin that are common to a wide variety of vertebrates?
I also demonstrated by real-time PCR analysis of multiple genes in pituitary and brain that the pituitary expression of thyroid stimulating hormone b2 (*tshb2*) was increased in *kiss1*/*kiss2*/*gpr54-2* KO medaka compared to the wild type medaka. *tshb2* in the pituitary changes with day length and suggested to be involved in seasonal breeding in stickleback (Kitano et al. 2010). Because this increase was detected even in heterogenic KO of these genes, further analysis is necessary. Further analysis of these KO medaka will be the key to finding the unknown functions of kisspeptin that are widely common to a wide variety of vertebrates.

In summary, by making the most of genetically modified animals, I elucidated the essential components of the HPG axis. By comparing my results with those of the previous reports, I proposed a hypothetical prototype of the HPG axis regulation of common ancestors of teleosts and mammals. The commonalities and specificities in the HPG axis regulation of reproduction I found in the present thesis will give insights into the understanding of the evolutionary process of one of the most essential regulatory mechanisms of life, reproduction.

Figure legend

Figure 4-1

Schematic illustration of the HPG axis regulatory pathway of female reproduction in mammals and medaka (teleosts). The circled numbers in the figure correspond to the Chapters in this thesis. In mammals, GnRH increases secretion of FSH, which promotes the early folliculogenesis and generation of LH pulse, which promotes the late folliculogenesis (Kumar 2005). This GnRH release is negatively regulated by kisspeptin neurons (negative feedback), in accordance with the increase of serum estrogen (Mayer and Boehm 2011). On the other hand, in teleosts, FSH, instead of LH pulse, promotes folliculogenesis up to the preovulatory follicle stage, which is not dependent on GnRH (Chapter 2). After the increase of serum estrogen, LH surge, which is triggered by the ventrolateral POA GnRH neurons (Chapter 1), induces ovulation. Kisspeptin was demonstrated to be dispensable for folliculogenesis as well as for ovulation in medaka (Chapter 3). Kisspeptin signaling may have other functions, e.g. expressional change of *tshb2* (Chapter 3).

Figure 4-1

mammals

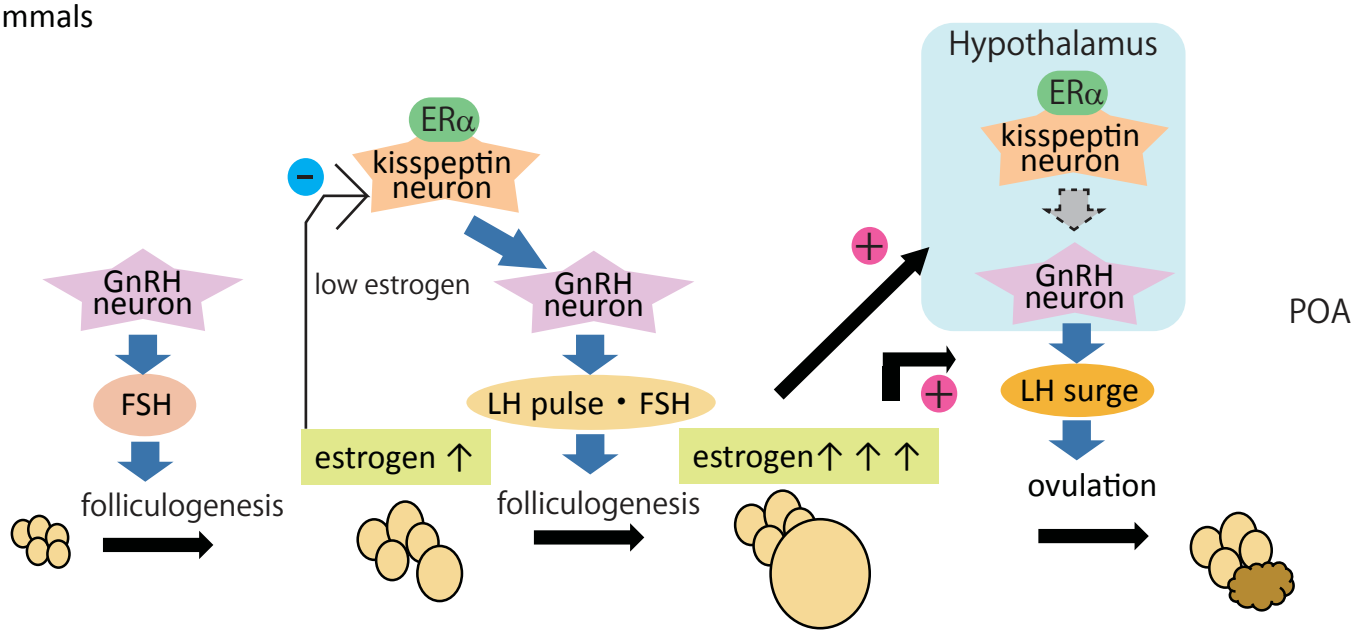

medaka (teleosts)

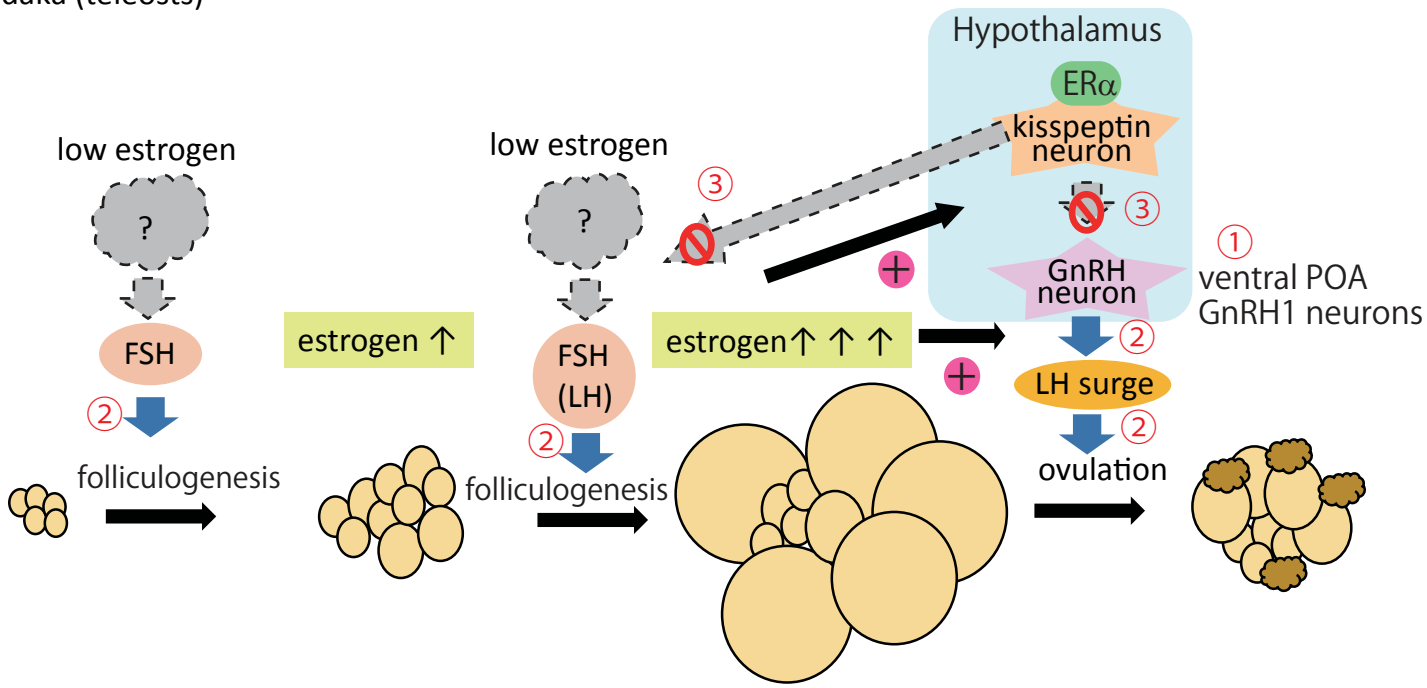

Acknowledgments

I heartily express my great gratitude to Professor Yoshitaka Oka, laboratory of Biological Signaling, Department of Biological Science, Graduate School of Science, The University of Tokyo, for his constant guidance, encouragement, and valuable discussion during the course of my study. I am also indebted to Drs. Min Kyun Park, Shinji Kanda (Graduate school of Science, The University of Tokyo), Yasuhisa Akazome (St. Marianna University School of Medicine), and Hideki Abe (Nagoya University) for insightful instruction, discussion, and encouragement. I am grateful to Drs. Naoyuki Yamamoto (Nagoya University) and Kataaki Okubo (Graduate School of Agriculture and Life Science, The University of Tokyo) for helpful advice and discussion. I appreciate Dr. Okuzawa (National Fisheries Research Agency) for the gift of anti-sGnRH antibody. I appreciate Dr. Hiroyuki Takeda (The University of Tokyo) for the gift of Rhodamine-Phalloidin and Dr. Sachiko Tsuda (Saitama University) for helpful advice. I appreciate Dr. Hiroshi Hosokawa (Kyoto University) for providing QtFish6, software for behavior analysis. I appreciate Drs. Takayuki Takahashi and Kastueki Ogiwara (Hokkaido University) for the gift of rLH and anti-mdLH, mdFSH antibody. I greatly thank Mr. Tomohiro Abe for his technical support and helpful advice and discussion. I appreciate Mr. Yuta Mitani (University of Tshkuba) for generating constructions of TALENs for *gnrh1*, *lhb* and *fshb*. I also thank Ms. Miho Kyokuwa and Ms. Hisako Kohno (the University of Tokyo) for their excellent care of the fish used in this study.

I am sincerely grateful to Prof. Hiroyuki Takeda, Yoshio Takei (Ocean Research Institute, The University of Tokyo), Associate Prof. Kataaki Okubo, Min Kyun Park for critical reading of the present thesis and valuable discussion.

Finally I would like to extend my deep gratitude to my parents, Haruki and Masako Takahashi for their constant understanding, support, and encouragement throughout my study.

References

Abel, M. H., A. N. Wootton, V. Wilkins, I. Huhtaniemi, P. G. Knight, and H. M. Charlton. 2000. The effect of a null mutation in the follicle-stimulating hormone receptor gene on mouse reproduction. Endocrinology **141**:1795-1803.

Abraham, E., O. Palevitch, Y. Gothilf, and Y. Zohar. 2010. Targeted gonadotropin-releasing hormone-3 neuron ablation in zebrafish: effects on neurogenesis, neuronal migration, and reproduction. Endocrinology **151**:332-340.

Abraham, E., O. Palevitch, S. Ijiri, S. J. Du, Y. Gothilf, and Y. Zohar. 2008. Early development of forebrain gonadotrophin-releasing hormone (GnRH) neurones and the role of GnRH as an autocrine migration factor. J Neuroendocrinol **20**:394-405.

Aizen, J., H. Kasuto, M. Golan, H. Zakay, and B. Levavi-Sivan. 2007. Tilapia follicle-stimulating hormone (FSH): immunochemistry, stimulation by gonadotropin-releasing hormone, and effect of biologically active recombinant FSH on steroid secretion. Biol Reprod **76**:692-700.

Akazome, Y., S. Kanda, K. Okubo, and Y. Oka. 2010. Functional and evolutionary insights into vertebrate kisspeptin systems from studies of fish brain. J Fish Biol **76**:161-182.

Andersson, E., W. Nijenhuis, R. Male, P. Swanson, J. Bogerd, G. L. Taranger, and R. W. Schulz. 2009. Pharmacological characterization, localization and quantification of expression of gonadotropin receptors in Atlantic salmon (*Salmo salar L.*) ovaries. Gen Comp Endocrinol **163**:329-339.

Ando, H., Q. Luo, N. Koide, H. Okada, and A. Urano. 2006. Effects of insulin-like growth factor I on GnRH-induced gonadotropin subunit gene expressions in masu salmon pituitary cells at different stages of sexual maturation. Gen Comp Endocrinol **149**:21-29.

Arai Y, Kanda S, Karigo T, Hasebe M, Oka Y. 2015. Changes in GnRH sensitivity of LH cells play a key role in seasonal regulation of reproduction. 45rd Annual Meetings, Society for Neuroscience, Chicago, USA, 2015, Oct.W25

Baenziger, J. U., and E. D. Green. 1988. Pituitary Glycoprotein Hormone Oligosaccharides - Structure, Synthesis and Function of the Asparagine-Linked Oligosaccharides on Lutropin, Follitropin and Thyrotropin. Biochimica Et Biophysica Acta **947**:287-306.

Behrens, U., and H. J. Wagner. 2004. Terminal nerve and vision. Microsc Res Tech **65**:25-32.

Bosma, P. T., S. M. Kolk, F. E. Rebers, O. Lescroart, I. Roelants, P. H. Willems, and R. W. Schulz. 1997. Gonadotrophs but not somatotrophs carry gonadotrophin-releasing hormone receptors: receptor localisation, intracellular calcium, and gonadotrophin and GH release. J Endocrinol **152**:437-446.

Breton, B., M. Govoroun, and T. Mikolajczyk. 1998. GTH I and GTH II secretion profiles during the reproductive cycle in female rainbow trout: relationship with pituitary responsiveness to GnRH-A stimulation. Gen Comp Endocrinol **111**:38-50.

Broughton, R. E., R. R. Betancur, C. Li, G. Arratia, and G. Orti. 2013. Multi-locus phylogenetic analysis reveals the pattern and tempo of bony fish evolution. PLoS Curr **5**.

Canosa, L. F., N. Stacey, and R. E. Peter. 2008. Changes in brain mRNA levels of gonadotropin-releasing hormone, pituitary adenylate cyclase activating polypeptide, and somatostatin during ovulatory luteinizing hormone and growth hormone surges in goldfish. Am J Physiol Regul Integr Comp Physiol **295**:R1815-1821.

Cattanach, B. M., C. A. Iddon, H. M. Charlton, S. A. Chiappa, and G. Fink. 1977. Gonadotrophin-Releasing Hormone Deficiency in a Mutant Mouse with Hypogonadism. Nature **269**:338-340.

Chang, J. P., A. Mar, M. Wlasichuk, and A. O. Wong. 2012. Kisspeptin-1 directly stimulates LH and GH secretion from goldfish pituitary cells in a Ca(2+)-dependent manner. Gen Comp Endocrinol **179**:38-46.

Chang, J. P., R. E. Peter, and L. W. Crim. 1984a. Effects of dopamine and apomorphine on gonadotropin release from the transplanted pars distalis in goldfish. Gen Comp Endocrinol **55**:347-350.

Chang, J. P., R. E. Peter, C. S. Nahorniak, and M. Sokolowska. 1984b. Effects of catecholaminergic agonists and antagonists on serum gonadotropin concentrations and ovulation in goldfish: evidence for specificity of dopamine inhibition of gonadotropin secretion. Gen Comp Endocrinol **55**:351-360.

Charlton, H. 2008. Hypothalamic control of anterior pituitary function: a history. J Neuroendocrinol **20**:641-646.

Ching, M. 1982. Correlative surges of LHRH, LH and FSH in pituitary stalk plasma and systemic plasma of rat during proestrus. Effect of anesthetics. Neuroendocrinology **34**:279-285.

Clayton, R. N. 1985. Role of GnRH in the maturation of pituitary gonadotroph function. J Reprod Fertil **75**:307-315.

Couse, J. F., M. M. Yates, V. R. Walker, and K. S. Korach. 2003. Characterization of the hypothalamic-pituitary-gonadal axis in estrogen receptor (ER) Null mice reveals hypergonadism and endocrine sex reversal in females lacking ERalpha but not ERbeta. Mol Endocrinol **17**:1039-1053.

Cui, M., W. Li, W. Liu, K. Yang, Y. Pang, and L. Haoran. 2007. Production of recombinant orange-spotted grouper (*Epinephelus coioides*) luteinizing hormone in insect cells by the baculovirus expression system and its biological effect. Biol Reprod **76**:74-84.

Cummins, S. F., and J. H. Bowie. 2012. Pheromones, attractants and other chemical cues of aquatic organisms and amphibians. Nat Prod Rep **29**:642-658.

Daikoku-Ishido, H., Y. Okamura, N. Yanaihara, and S. Daikoku. 1990. Development of the hypothalamic luteinizing hormone-releasing hormone-containing neuron system in the rat: in vivo and in transplantation studies. Dev Biol **140**:374-387.

Daniels, E., and P. Licht. 1980. Effects of gonadotropin-releasing hormone on the levels of plasma gonadotropins (FSH and LH) in the bullfrog, Rana catesbeiana. Gen Comp Endocrinol **42**:455-463.

Deguchi, T., H. Suwa, M. Yoshimoto, H. Kondoh, and N. Yamamoto. 2005. Central connection of the optic, oculomotor, trochlear and abducens nerves in medaka, Oryzias latipes. Zoolog Sci **22**:321-332.

Dickey, J. T., and P. Swanson. 2000. Effects of salmon gonadotropin-releasing hormone on follicle stimulating hormone secretion and subunit gene expression in coho salmon (*Oncorhynchus kisutch*). Gen Comp Endocrinol **118**:436-449.

Donadeu, F. X., and M. Ascoli. 2005. The differential effects of the gonadotropin receptors on aromatase expression in primary cultures of immature rat granulosa cells are highly dependent on the density of receptors expressed and the activation of the inositol phosphate cascade. Endocrinology **146**:3907-3916.

Drager, U. C., and D. H. Hubel. 1975. Responses to visual stimulation and relationship between visual, auditory, and somatosensory inputs in mouse superior colliculus. J Neurophysiol **38**:690-713.

Duan, C., and L. Liu. 2015. It Takes Two Gonadotropins to Tango in Zebrafish But With a Mixed Tune. Endocrinology **156**:3490-3493.

Dubois, E. A., M. A. Zandbergen, J. Peute, J. Bogerd, and H. J. Goos. 2001. Development of three distinct GnRH neuron populations expressing two different GnRH forms in the brain of the African catfish (*Clarias gariepinus*). J Comp Neurol **437**:308-320.

Dubois, E. A., M. A. Zandbergen, J. Peute, I. Hassing, W. van Dijk, R. W. Schulz, and H. J. Goos. 2000. Gonadotropin-releasing hormone fibers innervate the pituitary of the male African catfish (*Clarias gariepinus*) during puberty. Neuroendocrinology **72**:252-262.

Eisthen, H. L., R. J. Delay, C. R. Wirsig-Wiechmann, and V. E. Dionne. 2000. Neuromodulatory effects of gonadotropin releasing hormone on olfactory receptor neurons. J Neurosci **20**:3947-3955.

Escobar, S., A. Servili, F. Espigares, M. M. Gueguen, I. Brocal, A. Felip, A. Gomez, M. Carrillo, S. Zanuy, and O. Kah. 2013. Expression of kisspeptins and kiss receptors suggests a large range of functions for kisspeptin systems in the brain of the European sea bass. PLoS One **8**:e70177.

Felip, A., S. Zanuy, R. Pineda, L. Pinilla, M. Carrillo, M. Tena-Sempere, and A. Gomez. 2009. Evidence for two distinct KiSS genes in non-placental vertebrates that encode kisspeptins with different gonadotropin-releasing activities in fish and mammals. Mol Cell Endocrinol **312**:61-71.

Forni, P. E., C. Taylor-Burds, V. S. Melvin, T. Williams, and S. Wray. 2011. Neural crest and ectodermal cells intermix in the nasal placode to give rise to GnRH-1 neurons, sensory neurons, and olfactory ensheathing cells. J Neurosci **31**:6915-6927.

Francis, R. C., H. N. Lee, and R. D. Fernald. 1994. Ontogeny of gonadotropin releasing hormone-containing neurons in the teleost brain. Brain Res Dev Brain Res **78**:151-160.

Ge, W. 2005. Intrafollicular paracrine communication in the zebrafish ovary: the state of the art of an emerging model for the study of vertebrate folliculogenesis. Mol Cell Endocrinol **237**:1-10.

Glidewell-Kenney, C., L. A. Hurley, L. Pfaff, J. Weiss, J. E. Levine, and J. L. Jameson. 2007. Nonclassical estrogen receptor alpha signaling mediates negative feedback in the female mouse reproductive axis. Proc Natl Acad Sci U S A **104**:8173-8177.

Grens, K. E., A. K. Greenwood, and R. D. Fernald. 2005. Two visual processing pathways are targeted by gonadotropin-releasing hormone in the retina. Brain Behav Evol **66**:1-9.

Grone, B. P., K. P. Maruska, W. J. Korzan, and R. D. Fernald. 2010. Social status regulates kisspeptin receptor mRNA in the brain of Astatotilapia burtoni. Gen Comp Endocrinol **169**:98-107.

Gur, G., D. Bonfil, H. Safarian, Z. Naor, and Z. Yaron. 2002. GnRH signaling pathways regulate differentially the tilapia gonadotropin subunit genes. Mol Cell Endocrinol **189**:125-134.

Hagiwara, A., K. Ogiwara, Y. Katsu, and T. Takahashi. 2014. Luteinizing Hormone-Induced Expression of Ptger4b, a Prostaglandin E-2 Receptor Indispensable for Ovulation of the Medaka Oryzias latipes, Is Regulated by a Genomic Mechanism Involving Nuclear Progestin Receptor. Biol Reprod **90**.

Han, S. K., M. L. Gottsch, K. J. Lee, S. M. Popa, J. T. Smith, S. K. Jakawich, D. K. Clifton, R. A. Steiner, and A. E. Herbison. 2005. Activation of gonadotropin-releasing hormone neurons by kisspeptin as a neuroendocrine switch for the onset of puberty. J Neurosci **25**:11349-11356.

Hanada, K., Y. Sawada, T. Kuromori, R. Klausnitzer, K. Saito, T. Toyoda, K. Shinozaki, W. H. Li, and M. Y. Hirai. 2011. Functional compensation of primary and secondary metabolites by duplicate genes in Arabidopsis thaliana. Mol Biol Evol **28**:377-382.

Hasebe, M., S. Kanda, H. Shimada, Y. Akazome, H. Abe, and Y. Oka. 2014. Kiss1 neurons drastically change their firing activity in accordance with the reproductive state: insights from a seasonal breeder. Endocrinology **155**:4868-4880.

Hassin, S., Y. Gothilf, O. Blaise, and Y. Zohar. 1998. Gonadotropin-I and -II subunit gene expression of male striped bass (*Morone saxatilis*) after gonadotropin-releasing hormone analogue injection: quantitation using an optimized ribonuclease protection assay. Biol Reprod **58**:1233-1240.

Hatanaka, F., and M. Wada. 1988. Mechanism controlling photostimulated luteinizing hormone secretion is different from preovulatory luteinizing hormone surge in Japanese quail (*Coturnix coturnix japonica*). Gen Comp Endocrinol **70**:101-108.

Herbison, A. E., and J. R. Pape. 2001. New evidence for estrogen receptors in gonadotropin-releasing hormone neurons. Front Neuroendocrinol **22**:292-308.

Hodne, K., F. A. Weltzien, Y. Oka, and K. Okubo. 2013. Expression and putative function of kisspeptins and their receptors during early development in medaka. Endocrinology **154**:3437-3446.

Hwang, W. Y., Y. Fu, D. Reyon, M. L. Maeder, S. Q. Tsai, J. D. Sander, R. T. Peterson, J. R. Yeh, and J. K. Joung. 2013. Efficient genome editing in zebrafish using a CRISPR-Cas system. Nat Biotechnol **31**:227-229.

Irwig, M. S., G. S. Fraley, J. T. Smith, B. V. Acohido, S. M. Popa, M. J. Cunningham, M. L. Gottsch, D. K. Clifton, and R. A. Steiner. 2004. Kisspeptin activation of gonadotropin releasing hormone neurons and regulation of KiSS-1 mRNA in the male rat. Neuroendocrinology **80**:264-272.

Ishizaki, M., and Y. Oka. 2001. Amperometric recording of gonadotropin-releasing hormone release activity in the pituitary of the dwarf gourami (teleost) [correction of (teleosat)] brain-pituitary slices. Neurosci Lett **299**:121-124.

Ito, H., and H. Vanegas. 1983. Cytoarchitecture and ultrastructure of nucleus prethalamicus, with special reference to degenerating afferents from optic tectum and telencephalon, in a teleost (*Holocentrus ascensionis*). J Comp Neurol **221**:401-415.

Ito, H., and H. Vanegas. 1984. Visual receptive thalamopetal neurons in the optic tectum of teleosts (*Holocentridae*). Brain Res **290**:201-210.

Iwamatsu, T. 1978a. Studies on oocyte maturation of the medaka, Oryzias latipes. V. On the structure of steroids that induce maturation in vitro. J Exp Zool **204**:401-408.

Iwamatsu, T. 1978b. Studies on oocyte maturation of the medaka, Oryzias latipes. VI. Relationship between the circadian cycle of oocyte maturation and activity of the pituitary gland. J Exp Zool **206**:355-363.

Iwamatsu, T., H. Nakamura, K. Ozato, and Y. Wakamatsu. 2003. Normal growth of the "see-through" medaka. Zoolog Sci **20**:607-615.

Jiang, Q., M. He, W. K. Ko, and A. O. Wong. 2014. Kisspeptin induction of somatolactin-alpha release in goldfish pituitary cells: functional role of cAMP/PKA-, PLC/PKC-, and Ca(2+)/calmodulin-dependent cascades. Am J Physiol Endocrinol Metab **307**:E872-884.

Kamei, H., T. Ohira, Y. Yoshiura, N. Uchida, H. Nagasawa, and K. Aida. 2003. Expression of a biologically active recombinant follicle stimulating hormone of Japanese Eel Anguilla japonica using methylotropic yeast, Pichia pastoris. Gen Comp Endocrinol **134**:244-254.

Kanda, S., Y. Akazome, T. Matsunaga, N. Yamamoto, S. Yamada, H. Tsukamura, K. Maeda, and Y. Oka. 2008. Identification of KiSS-1 product kisspeptin and steroid-sensitive sexually dimorphic kisspeptin neurons in medaka (*oryzias latipes*). Endocrinology **149**:2467-2476.

Kanda, S., Y. Akazome, Y. Mitani, K. Okubo, and Y. Oka. 2013. Neuroanatomical evidence that kisspeptin directly regulates isotocin and vasotocin neurons. PLoS One **8**:e62776.

Kanda, S., T. Karigo, and Y. Oka. 2012. Steroid sensitive kiss2 neurones in the goldfish: evolutionary insights into the duplicate kisspeptin gene-expressing neurones. J Neuroendocrinol **24**:897-906.

Kanda, S., K. Nishikawa, T. Karigo, K. Okubo, S. Isomae, H. Abe, D. Kobayashi, and Y. Oka. 2010. Regular pacemaker activity characterizes gonadotropin-releasing hormone 2 neurons recorded from green fluorescent protein-transgenic medaka. Endocrinology **151**:695-701.

Kanda, S., K. Okubo, and Y. Oka. 2011. Differential regulation of the luteinizing hormone genes in teleosts and tetrapods due to their distinct genomic environments--insights into gonadotropin beta subunit evolution. Gen Comp Endocrinol **173**:253-258.

Kandel-Kfir, M., G. Gur, P. Melamed, Y. Zilberstein, Y. Cohen, N. Zmora, M. Kobayashi, A. Elizur, and Z. Yaron. 2002. Gonadotropin response to GnRH during sexual ontogeny in the common carp, *Cyprinus carpio*. Comp Biochem Physiol B Biochem Mol Biol **132**:17-26.

Karigo, T., M. Aikawa, C. Kondo, H. Abe, S. Kanda, and Y. Oka. 2014. Whole brain-pituitary in vitro preparation of the transgenic medaka (*Oryzias latipes*) as a tool for analyzing the differential regulatory mechanisms of LH and FSH release. Endocrinology **155**:536-547.

Karigo, T., S. Kanda, A. Takahashi, H. Abe, K. Okubo, and Y. Oka. 2012a. Time-of-day-dependent changes in GnRH1 neuronal activities and gonadotropin mRNA expression in a daily spawning fish, medaka. Endocrinology **153**:3394-3404.

Karigo T, Uenoyama Y, Oishi S, Fujii N, Mitani Y, Kanda S, Oka Y. 2012b. Effects of Kisspeptins on LH Secretion and GnRH1 neuronal Activities in Goldfish and Medaka. 2nd world conference on kisspeptin signaling in the brain P-61

Karigo, T., and Y. Oka. 2013. Neurobiological study of fish brains gives insights into the nature of gonadotropin-releasing hormone 1-3 neurons. Front Endocrinol (Lausanne) **4**:177.

Karl, T., R. Pabst, and S. von Horsten. 2003. Behavioral phenotyping of mice in pharmacological and toxicological research. Exp Toxicol Pathol **55**:69-83.

Kauffman, A. S., D. K. Clifton, and R. A. Steiner. 2007. Emerging ideas about kisspeptin- GPR54 signaling in the neuroendocrine regulation of reproduction. Trends Neurosci **30**:504-511.

Kawai, T., H. Abe, Y. Akazome, and Y. Oka. 2010. Neuromodulatory effect of GnRH on the synaptic transmission of the olfactory bulbar neural circuit in goldfish, *Carassius auratus*. J Neurophysiol **104**:3540-3550.

Kazeto, Y., M. Kohara, T. Miura, C. Miura, S. Yamaguchi, J. M. Trant, S. Adachi, and K. Yamauchi. 2008. Japanese eel follicle-stimulating hormone (Fsh) and luteinizing hormone (Lh): production of biologically active recombinant Fsh and Lh by Drosophila S2 cells and their differential actions on the reproductive biology. Biol Reprod **79**:938-946.

Khakoo, S. I., A. J. Lobo, N. A. Shepherd, and S. P. Wilkinson. 1994. Histological assessment of the Sydney classification of endoscopic gastritis. Gut **35**:1172-1175.

Kinoshita, M., S. Kobayashi, A. Urano, and E. Ito. 2007. Neuromodulatory effects of gonadotropin-releasing hormone on retinotectal synaptic transmission in the optic tectum of rainbow trout. Eur J Neurosci **25**:480-484.

Kitano, J., S. C. Lema, J. A. Luckenbach, S. Mori, Y. Kawagishi, M. Kusakabe, P. Swanson, and C. L. Peichel. 2010. Adaptive divergence in the thyroid hormone signaling pathway in the stickleback radiation. Curr Biol **20**:2124-2130.

Knobil, E. 1980. The neuroendocrine control of the menstrual cycle. Recent Prog Horm Res **36**:53-88.

Ko, H., W. Park, D. J. Kim, M. Kobayashi, and Y. C. Sohn. 2007. Biological activities of recombinant Manchurian trout FSH and LH: their receptor specificity, steroidogenic and vitellogenic potencies. J Mol Endocrinol **38**:99-111.

Kok, F. O., M. Shin, C. W. Ni, A. Gupta, A. S. Grosse, A. van Impel, B. C. Kirchmaier, J. Peterson-Maduro, G. Kourkoulis, I. Male, D. F. DeSantis, S. Sheppard-Tindell, L. Ebarasi, C. Betsholtz, S. Schulte-Merker, S. A. Wolfe, and N. D. Lawson. 2015. Reverse genetic screening reveals poor correlation between morpholino-induced and mutant phenotypes in zebrafish. Dev Cell **32**:97-108.

Kudo, A., M. K. Park, and S. Kawashima. 1994. Effects of gonadotropin-releasing hormone (GnRH) on the cytodifferentiation of gonadotropes in rat adenohypophysial primordia in organ culture. Cell Tissue Res **276**:35-43.

Kumar, T. R., Y. Wang, N. Lu, and M. M. Matzuk. 1997. Follicle stimulating hormone is required for ovarian follicle maturation but not male fertility. Nature Genetics **15**:201-204.

Kwok, H. F., W. K. So, Y. Wang, and W. Ge. 2005. Zebrafish gonadotropins and their receptors: I. Cloning and characterization of zebrafish follicle-stimulating hormone and luteinizing hormone receptors--evidence for their distinct functions in follicle development. Biol Reprod **72**:1370-1381.

Lee, Y. R., K. Tsunekawa, M. J. Moon, H. N. Um, J. I. Hwang, T. Osugi, N. Otaki, Y. Sunakawa, K. Kim, H. Vaudry, H. B. Kwon, J. Y. Seong, and K. Tsutsui. 2009a. Molecular Evolution of Multiple Forms of Kisspeptins and GPR54 Receptors in Vertebrates. Endocrinology **150**:2837-2846.

Lee, Y. R., K. Tsunekawa, M. J. Moon, H. N. Um, J. I. Hwang, T. Osugi, N. Otaki, Y. Sunakawa, K. Kim, H. Vaudry, H. B. Kwon, J. Y. Seong, and K. Tsutsui. 2009b. Molecular evolution of multiple forms of kisspeptins and GPR54 receptors in vertebrates. Endocrinology **150**:2837-2846.

Ma, X., Y. Dong, M. M. Matzuk, and T. R. Kumar. 2004. Targeted disruption of luteinizing hormone beta-subunit leads to hypogonadism, defects in gonadal steroidogenesis, and infertility. Proc Natl Acad Sci U S A **101**:17294-17299.

Mananos, E. L., I. Anglade, J. Chyb, C. Saligaut, B. Breton, and O. Kah. 1999. Involvement of gamma-aminobutyric acid in the control of GTH-1 and GTH-2 secretion in male and female rainbow trout. Neuroendocrinology **69**:269-280.

Mateos, J., E. Mananos, M. Carrillo, and S. Zanuy. 2002. Regulation of follicle-stimulating hormone (FSH) and luteinizing hormone (LH) gene expression by gonadotropin-releasing hormone (GnRH) and sexual steroids in the Mediterranean Sea bass. Comp Biochem Physiol B Biochem Mol Biol **132**:75-86.

Matsumoto, M., and O. Hikosaka. 2007. Lateral habenula as a source of negative reward signals in dopamine neurons. Nature **447**:1111-1115.

Matsunaga, W., and E. Watanabe. 2010. Habituation of medaka (*Oryzias latipes*) demonstrated by open-field testing. Behav Processes **85**:142-150.

Mayer, C., M. Acosta-Martinez, S. L. Dubois, A. Wolfe, S. Radovick, U. Boehm, and J. E. Levine. 2010. Timing and completion of puberty in female mice depend on estrogen receptor alpha-signaling in kisspeptin neurons. Proc Natl Acad Sci U S A **107**:22693-22698.

Mayer, C., and U. Boehm. 2011. Female reproductive maturation in the absence of kisspeptin/GPR54 signaling. Nat Neurosci **14**:704-710.

Mitani, Y., S. Kanda, Y. Akazome, B. Zempo, and Y. Oka. 2010. Hypothalamic Kiss1 but not Kiss2 neurons are involved in estrogen feedback in medaka (*Oryzias latipes*). Endocrinology **151**:1751-1759.

Murakami, S., T. Seki, K. Wakabayashi, and Y. Arai. 1991. The ontogeny of luteinizing hormone-releasing hormone (LHRH) producing neurons in the chick embryo: possible evidence for migrating LHRH neurons from the olfactory epithelium expressing a highly polysialylated neural cell adhesion molecule. Neurosci Res **12**:421-431.

Murozumi, N., R. Nakashima, T. Hirai, Y. Kamei, T. Ishikawa-Fujiwara, T. Todo, and T. Kitano. 2014. Loss of follicle-stimulating hormone receptor function causes masculinization and suppression of ovarian development in genetically female medaka. Endocrinology **155**:3136-3145.

Ogawa, S., F. M. Nathan, and I. S. Parhar. 2014. Habenular kisspeptin modulates fear in the zebrafish. Proc Natl Acad Sci U S A **111**:3841-3846.

Ogawa, S., K. W. Ng, P. N. Ramadasan, F. M. Nathan, and I. S. Parhar. 2012. Habenular Kiss1 neurons modulate the serotonergic system in the brain of zebrafish. Endocrinology **153**:2398-2407.

Ogiwara, K., C. Fujimori, S. Rajapakse, and T. Takahashi. 2013. Characterization of luteinizing hormone and luteinizing hormone receptor and their indispensable role in the ovulatory process of the medaka. PLoS One **8**:e54482.

Ohga, H., S. Selvaraj, H. Adachi, Y. Imanaga, M. Nyuji, A. Yamaguchi, and M. Matsuyama. 2014. Functional analysis of kisspeptin peptides in adult immature chub mackerel (Scomber japonicus) using an intracerebroventricular administration method. Neurosci Lett **561**:203-207.

Ohkura, S., Y. Uenoyama, S. Yamada, T. Homma, K. Takase, N. Inoue, K. Maeda, and H. Tsukamura. 2009. Physiological role of metastin/kisspeptin in regulating gonadotropin-releasing hormone (GnRH) secretion in female rats. Peptides **30**:49-56.

Oka, Y., and M. Ichikawa. 1990. Gonadotropin-releasing hormone (GnRH) immunoreactive system in the brain of the dwarf gourami (*Colisa lalia*) as revealed by light microscopic immunocytochemistry using a monoclonal antibody to common amino acid sequence of GnRH. J Comp Neurol **300**:511-522.

Oka, Y., and T. Matsushima. 1993. Gonadotropin-releasing hormone (GnRH)-immunoreactive terminal nerve cells have intrinsic rhythmicity and project widely in the brain. J Neurosci **13**:2161-2176.

Okubo, K., and K. Aida. 2001. Gonadotropin-releasing hormones (GnRHs) in a primitive teleost, the arowana: phylogenetic evidence that three paralogous lineages of GnRH occurred prior to the emergence of teleosts. Gen Comp Endocrinol **124**:125-133.

Okubo, K., and Y. Nagahama. 2008. Structural and functional evolution of gonadotropin-releasing hormone in vertebrates. Acta Physiol (Oxf) **193**:3-15.

Okubo, K., F. Sakai, E. L. Lau, G. Yoshizaki, Y. Takeuchi, K. Naruse, K. Aida, and Y. Nagahama. 2006. Forebrain gonadotropin-releasing hormone neuronal development: insights from transgenic medaka and the relevance to X-linked Kallmann syndrome. Endocrinology **147**:1076-1084.

Okuyama, T., S. Yokoi, H. Abe, Y. Isoe, Y. Suehiro, H. Imada, M. Tanaka, T. Kawasaki, S. Yuba, Y. Taniguchi, Y. Kamei, K. Okubo, A. Shimada, K. Naruse, H. Takeda, Y. Oka, T. Kubo, and H. Takeuchi. 2014. A neural mechanism underlying mating preferences for familiar individuals in medaka fish. Science **343**:91-94.

Okuzawa, K., M. Amano, M. Kobayashi, K. Aida, I. Hanyu, Y. Hasegawa, and K. Miyamoto. 1990. Differences in salmon GnRH and chicken GnRH-II contents in discrete brain areas of male and female rainbow trout according to age and stage of maturity. Gen Comp Endocrinol **80**:116-126.

Ono, Y., and T. Uematsu. 1957. Mating ethogram in *Oryzias latipes*. J Fac Sc, Hokkaido Univ **13**:197–202.

Palevitch, O., K. Kight, E. Abraham, S. Wray, Y. Zohar, and Y. Gothilf. 2007. Ontogeny of the GnRH systems in zebrafish brain: in situ hybridization and promoter-reporter expression analyses in intact animals. Cell Tissue Res **327**:313-322.

Parhar, I. S., T. Soga, Y. Ishikawa, Y. Nagahama, and Y. Sakuma. 1998. Neurons synthesizing gonadotropin-releasing hormone mRNA subtypes have multiple developmental origins in the medaka. J Comp Neurol **401**:217-226.

Pinelli, C., M. Fiorentino, B. D'Aniello, S. Tanaka, and R. K. Rastogi. 1996. Immunohistochemical demonstration of FSH and LH in the pituitary of the developing frog, Rana esculenta. Gen Comp Endocrinol **104**:189-196.

Proudman, J. A., F. Vandesande, and L. R. Berghman. 1999. Immunohistochemical evidence that follicle-stimulating hormone and luteinizing hormone reside in separate cells in the chicken pituitary. Biol Reprod **60**:1324-1328.

Reynhout, J. K., C. Taddei, L. D. Smith, and M. J. LaMarca. 1975. Response of large oocytes of Xenopus laevis to progesterone in vitro in relation to oocyte size and time after previous HCG-induced ovulation. Dev Biol **44**:375-379.

Sander, J. D., L. Cade, C. Khayter, D. Reyon, R. T. Peterson, J. K. Joung, and J. R. Yeh. 2011. Targeted gene disruption in somatic zebrafish cells using engineered TALENs. Nat Biotechnol **29**:697-698.

Schindelin, J., I. Arganda-Carreras, E. Frise, V. Kaynig, M. Longair, T. Pietzsch, S. Preibisch, C. Rueden, S. Saalfeld, B. Schmid, J. Y. Tinevez, D. J. White, V. Hartenstein, K. Eliceiri, P. Tomancak, and A. Cardona. 2012. Fiji: an open-source platform for biological-image analysis. Nat Methods **9**:676-682.

Schwanzel-Fukuda, M., and D. W. Pfaff. 1989. Origin of luteinizing hormone-releasing hormone neurons. Nature **338**:161-164.

Senthilkumaran, B., K. Okuzawa, K. Gen, T. Ookura, and H. Kagawa. 1999. Distribution and seasonal variations in levels of three native GnRHs in the brain and pituitary of perciform fish. J Neuroendocrinol **11**:181-186.

Servili, A., Y. Le Page, J. Leprince, A. Caraty, S. Escobar, I. S. Parhar, J. Y. Seong, H. Vaudry, and O. Kah. 2011. Organization of two independent kisspeptin systems derived from evolutionary-ancient kiss genes in the brain of zebrafish. Endocrinology **152**:1527-1540.

Sisk, C. L., and D. L. Foster. 2004. The neural basis of puberty and adolescence. Nat Neurosci **7**:1040-1047.

Smith, J. T. 2013. Sex steroid regulation of kisspeptin circuits. Adv Exp Med Biol **784**:275-295.

Smith, J. T., M. J. Cunningham, E. F. Rissman, D. K. Clifton, and R. A. Steiner. 2005. Regulation of Kiss1 gene expression in the brain of the female mouse. Endocrinology **146**:3686-3692.

Sokolowska, M., R. E. Peter, C. S. Nahorniak, and J. P. Chang. 1985. Seasonal effects of pimozide and des Gly10 [D-Ala6] LH-RH ethylamide on gonadotrophin secretion in goldfish. Gen Comp Endocrinol **57**:472-479.

Tamamaki, N., K. Nakamura, T. Furuta, K. Asamoto, and T. Kaneko. 2000. Neurons in Golgi-stain-like images revealed by GFP-adenovirus infection in vivo. Neurosci Res **38**:231-236.

Tang, H., Y. Liu, D. Luo, S. Ogawa, Y. Yin, S. Li, Y. Zhang, W. Hu, I. S. Parhar, H. Lin, X. Liu, and C. H. Cheng. 2015. The kiss/kissr systems are dispensable for zebrafish reproduction: evidence from gene knockout studies. Endocrinology **156**:589-599.

Thermes, V., C. Grabher, F. Ristoratore, F. Bourrat, A. Choulika, J. Wittbrodt, and J. S. Joly. 2002. I-SceI meganuclease mediates highly efficient transgenesis in fish. Mech Dev **118**:91-98.

Tiong, J. D., J. G. Pakiam, and S. Wray. 2004. Gonadotropin releasing hormone-1 expression in incisors of mice. Endocrinology **145**:3608-3612.

Trudeau, V. L., B. D. Sloley, and R. E. Peter. 1993a. GABA stimulation of gonadotropin-II release in goldfish: involvement of GABAA receptors, dopamine, and sex steroids. Am J Physiol **265**:R348-355.

Trudeau, V. L., B. D. Sloley, A. O. Wong, and R. E. Peter. 1993b. Interactions of gonadal steroids with brain dopamine and gonadotropin-releasing hormone in the control of gonadotropin-II secretion in the goldfish. Gen Comp Endocrinol **89**:39-50.

Tsurudome, K., X. Li, and N. Matsumoto. 2005. Intracellular and current source density analyses of somatosensory input to the optic tectum of the frog. Brain Res **1064**:32-41.

Tsutsui, K., G. E. Bentley, G. Bedecarrats, T. Osugi, T. Ubuka, and L. J. Kriegsfeld. 2010. Gonadotropin-inhibitory hormone (GnIH) and its control of central and peripheral reproductive function. Front Neuroendocrinol **31**:284-295.

Uchida, K., S. Moriyama, S. A. Sower, and M. Nozaki. 2013. Glycoprotein hormone in the pituitary of hagfish and its evolutionary implications. Fish Physiol Biochem **39**:75-83.

Umino, O., and J. E. Dowling. 1991. Dopamine release from interplexiform cells in the retina: effects of GnRH, FMRFamide, bicuculline, and enkephalin on horizontal cell activity. J Neurosci **11**:3034-3046.

Wakabayashi, Y., T. Nakada, K. Murata, S. Ohkura, K. Mogi, V. M. Navarro, D. K. Clifton, Y. Mori, H. Tsukamura, K. Maeda, R. A. Steiner, and H. Okamura. 2010. Neurokinin B and dynorphin A in kisspeptin neurons of the arcuate nucleus participate in generation of periodic oscillation of neural activity driving pulsatile gonadotropin-releasing hormone secretion in the goat. J Neurosci **30**:3124-3132.

Wayne, N. L., K. Kuwahara, K. Aida, Y. Nagahama, and K. Okubo. 2005. Whole-cell electrophysiology of gonadotropin-releasing hormone neurons that express green fluorescent protein in the terminal nerve of transgenic medaka (*Oryzias latipes*). Biol Reprod **73**:1228-1234.

Weil, C. M., S. L. Wade, L. J. Bauman, H. Lynn, H. Mitchell, and J. Lavigne. 1999. The relationship between psychosocial factors and asthma morbidity in inner-city children with asthma. Pediatrics **104**:1274-1280.

White, R. B., and R. D. Fernald. 1998. Ontogeny of gonadotropin-releasing hormone (GnRH) gene expression reveals a distinct origin for GnRH-containing neurons in the midbrain. Gen Comp Endocrinol **112**:322-329.

Whitlock, K. E., N. Illing, N. J. Brideau, K. M. Smith, and S. Twomey. 2006. Development of GnRH cells: Setting the stage for puberty. Mol Cell Endocrinol **254-255**:39-50.

Whitlock, K. E., C. D. Wolf, and M. L. Boyce. 2003. Gonadotropin-releasing hormone (gnrh) cells arise from cranial neural crest and adenohypophyseal regions of the neural plate in the zebrafish, *danio rerio*. Developmental Biology **257**:140-152.

Wray, S. 2010. From nose to brain: development of gonadotrophin-releasing hormone-1 neurones. J Neuroendocrinol **22**:743-753.

Wray, S., A. Nieburgs, and S. Elkabes. 1989. Spatiotemporal cell expression of luteinizing hormone-releasing hormone in the prenatal mouse: evidence for an embryonic origin in the olfactory placode. Brain Res Dev Brain Res **46**:309-318.

Yamamoto, N., Y. Oka, M. Amano, K. Aida, Y. Hasegawa, and S. Kawashima. 1995. Multiple gonadotropin-releasing hormone (GnRH)-immunoreactive systems in the brain of the dwarf gourami, *Colisa lalia*: immunohistochemistry and radioimmunoassay. J Comp Neurol **355**:354-368.

Yamamoto, N., Y. Oka, and S. Kawashima. 1997. Lesions of gonadotropin-releasing hormone-immunoreactive terminal nerve cells: effects on the reproductive behavior of male dwarf gouramis. Neuroendocrinology **65**:403-412.

Yaron, Z., G. Gur, P. Melamed, H. Rosenfeld, A. Elizur, and B. Levavi-Sivan. 2003. Regulation of fish gonadotropins. Int Rev Cytol **225**:131-185.

Zhang, C., T. A. Roepke, M. J. Kelly, and O. K. Ronnekleiv. 2008. Kisspeptin depolarizes gonadotropin-releasing hormone neurons through activation of TRPC-like cationic channels. J Neurosci **28**:4423-4434.

Yoshimoto and Itoh. 2002. Neuroscience of Fish- forefront of fish neuroscience research.

Zhang, C., K. Shimada, N. Saito, and N. Kansaku. 1997. Expression of messenger ribonucleic acids of luteinizing hormone and follicle-stimulating hormone receptors in granulosa and theca layers of chicken preovulatory follicles. Gen Comp Endocrinol **105**:402-409.

Zhang, Z., S. W. Lau, L. Zhang, and W. Ge. 2015a. Disruption of Zebrafish Follicle-Stimulating Hormone Receptor (fshr) But Not Luteinizing Hormone Receptor (lhcgr) Gene by TALEN Leads to Failed Follicle Activation in Females Followed by Sexual Reversal to Males. Endocrinology **156**:3747-3762.

Zhang, Z., B. Zhu, and W. Ge. 2015b. Genetic analysis of zebrafish gonadotropin (FSH and LH) functions by TALEN-mediated gene disruption. Mol Endocrinol **29**:76-98.

Zhao, Y., M. C. Lin, M. Farajzadeh, and N. L. Wayne. 2013. Early development of the gonadotropin-releasing hormone neuronal network in transgenic zebrafish. Front Endocrinol (Lausanne) **4**:107.